STRESS-STRAIN MODELS
FOR SOILS
BASED ON PLASTICITY THEORY

by

MICHAEL KAVVADAS

DIPLOMA, N.T.U. Athens, Greece
(1977)

SUBMITTED IN PARTIAL FULFILLMENT
OF THE REQUIREMENTS FOR THE
DEGREE OF

MASTER OF SCIENCE IN
CIVIL ENGINEERING

at the

MASSACHUSETTS INSTITUTE OF TECHNOLOGY

June 1980

Signature of Author Signature redacted
Department of Civil Engineering
May 9, 1980

Certified by Signature redacted
Monsen M. Baligh
Thesis Supervisor

Accepted by Signature redacted
C. Allin Cornell
Chairman, Department Committee

STRESS-STRAIN MODELS

FOR SOILS

BASED ON PLASTICITY THEORY

by

MICHAEL KAVVADAS

Submitted to the Department of Civil Engineering on May 9, 1980 in partial fulfillment of the requirements for the Degree of Master of Science in Civil Engineering

ABSTRACT

Soils exhibit a non-linear and inelastic response even at low stress levels and hence require comprehensive modelling. An overview of Plasticity Theory is presented with emphasis on applications to soils.

Two incremental stress-strain constitutive laws are studied and evaluated by comparing their predictions with laboratory results on Normally Consolidated resedimented Boston Blue Clay.

The Cam-Clay Model is an Effective Stress model, appropriate for drained, undrained and partially drained (consolidation) loading. Comparisons with results of undrained tests show generally good predictions of trends. However the accuracy of predictions is limited especially for anisotropically consolidated soils.

The Mroz-Prevost Model is a Total Stress model, appropriate only for undrained loading conditions. The model provides good predictions but requires a large number of input soil parameters, which may limit its usefulness in practice.

Finally both models are used to predict the stress and pore pressure fields around an expanding cylindrical cavity.

Thesis Supervisor: Pr. M.M. Baligh

Title : Associate Professor of Civil Engineering

TO MY PARENTS

ACKNOWLEDGEMENTS

The author is grateful for the efforts of many who have assisted him in his graduate work and on his thesis.

Prof. M.M. Baligh, his advisor and thesis supervisor whose thought provoking comments made this work possible.

Prof. T.H.H. Pian for assisting him on the Mathematics of the Theory of Plasticity.

His friends and colleagues: Dr. Jean-Claude Hujeux, Dr. Jackques Levadoux and Mr. Spiro Pollalis for their useful comments and encouragement.

The National Science Foundation and INTEVEP provided financial support to the writer during his graduate studies at MIT.

TABLE OF CONTENTS

****

CHAPTER I

INTRODUCTION

The response of a soil mass to changes in loading conditions is of primary importance in Soil Mechanics. The geotechnical engineer evaluates the performance of a foundation (or an earth structure) by means of two criteria:

1. Adequacy against excessive deformations (i.e. settlement or lateral movement).
2. Adequacy against gross shear failure (i.e. instability).

The first criterion basically calls for the prediction of deformation fields. However, instability problems are also deformation-type problems. They simply occur when loading reaches a limiting state where the external energy supplied by the added loads can no longer be absorbed by the soil as strain energy and/or plastic deformation energy.

According to the Principles of Classical Mechanics, the prediction of deformations requires that the following conditions be satisfied everywhere in the soil mass:

1. Equilibrium of stresses.
2. Constitutive relations of the material (i.e. relations between stress and strain components).
3. Strain compatibility.

Due to the complexity of actual foundation problems and the need for predictions in designs, the above conditions are methodically violated. Three examples are presented:

1. In conventional slope stability analyses, (1) equilibrium is only satisfied globally and the shearing resistance of the soil is only needed along the assumed failure (shear) surface. Equilibrium and Constitutive relations at different points in the slope are neglected and strain compatibility cannot be (rigorously) considered, because deformations are basically neglected (except at the location of the shear surface). Consequently, stability considerations are usually limited to stress fields with little or no reference to kinematic restrictions (i.e. compatibility).

2. In estimating stress distributions in a soil mass Elasticity Theory is often used. In some cases results are satisfactory. (2) However, soils rarely exhibit the linear behavior assumed by the theory and hence constitutive relations are violated.

3. The Stress Path Method (3) (4) is another example where

---

(1) e.g circular arc analyses.

(2) when local yielding is not extensive.

(3)

strain compatibility is violated. The method basically consists of obtaining 'undisturbed' samples of the soil, subjecting them to stresses and stress changes (1) that are expected in the field and then computing deformations by appropriately integrating the measured strains. In applying the stress path method two different stress-strain relations are used. A simplified (usually linearly elastic) stress-strain law is used to estimate the stress changes in the field and a more rigorous one (obtained from the tests) is used to obtain the deformations resulting from the estimated stress changes.

The use of two different constitutive laws results in strain incompatibility. The effect is less pronounced in problems where the stresses are relatively independent of the material response. (2) In such problems (or cases approaching them) realistic stress changes can be calculated prior to the experimental evaluation of the stress strain characteristics of the soil. Unfortunately, few problems

---

T.W. Lambe (1967).'Stress Path Method'.JSMFD, ASCE, Vol.93, No.SM6, pp. 309-331.

(4) T.W. Lambe and W.A. Marr (1979) 'Stress Path Method: Second Edition'. JGED, ASCE, Vol.105, no.GT6 pp 727-738.

(1) as they are estimated by using simplified methods of analysis such as the Theory of Elasticity.

(2) such as the loading of a horizontal layer with constant thickness extending horizontally to infinity, by a constant load also extending to infinity.

result in stresses that are independent of the material properties.

In order to evaluate the effect of neglecting the strain compatibility in the stress path method, the settlement of a point lying under the centerline of a smooth flexible strip footing, resting on the surface of a uniform soil deposit which is loaded in an undrained mode, was evaluated by using two different integration paths for the strains.

(a) A vertical path.

(b) A horizontal path.

The analysis (described in Appendix V) shows that by neglecting strain compatibility the settlement computed from the second path is almost double than the settlement computed via the first path.

Furthermore the Stress Path Method has serious additional limitations. It requires an exceptionally high standard of sampling and testing and is therefore very expensive. Moreover, even given perfect sampling, it has been demonstrated (1) that the mere process of stress relief during sampling gives rise to behavior in the laboratory which may differ appreciably from the in-situ condition. A third difficulty is that in all but the simplest situations the stress changes that occur in the field are too complex to reproduce in routine laboratory tests, since they involve

---

(1) Skempton A.W and Sowa V.A (1963) 'The behavior of saturated clays during sampling and testing.' Geotechnique 13,4 pp 269-290.

rotations of principal stresses; it is often the region of complex stress changes that is of greatest interest to the engineer. Finally laboratory simulation of stress changes in zones of local yielding is very difficult to perform with existing laboratory tests.

Recent developments of large digital computers have rendered possible, in principle, the solution of a wide variety of problems without the need to violate equilibrium or compatibility (e.g. by using the Finite Element Method). In fact, by employing such techniques the fictitious distinction between stability and deformation problems can be eliminated by treating stability problems as problems of large uncontrollable deformations (i.e failure).
The major difficulties in implementing these powerful computational tools in practice are:

1. The complicated behavior of soils.
2. The difficulties associated with determining and describing the soil conditions in situ.

The complicated behavior of soil is caused by:

1. Soils exhibit non linear and inelastic behavior even at low stress levels and during unloading. (1)
2. The behavior of soils under stress (i.e.

---

(1) Hardin B.O. (1972) 'Effects of Strain Amplitude on the Shear Modulus of Soils'. Technical Report No. AFWL-TR-72-201 Air Force Base, NM. 63 p.

compressibility moduli and strength) is controlled by the effective stresses acting on the skeleton. Since soils are multiphase materials where water (and possibly gases) contribute in resisting the applied stresses , the response of soil masses can only be estimated rationally and systematically after the pore pressure distribution is determined. Pore pressures develop in soils due to isotropic (hydrostatic) and shear (as discussed later) loading and dissipate with time. Due to these complexities, analyses are usually performed for two limiting conditions:

(a) Undrained; where no fluid migration takes place during loading and

(b) Drained; where no excess pore pressures develop during loading.

3. Shearing causes a tendency of volume change. During drained shearing, dense sands and highly overconsolidated clays tend to dilate, whereas loose sands and normally consolidated clays contract. However, after significant shearing it is generally accepted that soils approach a condition of no volume change. (1) When drainage is prevented (i.e. in undrained cases), negative (decreased) pore

---

(1) Rowe P.W. (1971) 'Theoretical Meaning and Observed Values of Deformation Parameters for Soil'.Proc. Roscoe Memorial Symp., Cambridge U. Editor R.H.G. Parry, pp.143-194.

pressures develop during shearing of dilatant soils and positive (increased) pore pressures develop in contracting soils. This coupling between volume change and changes in shear stress cannot be explained or simulated by the Theory of (linear isotropic) Elasticity.

4. Many soils (undrained or drained) exhibit a significant reduction in shearing resistance after the peak strength is reached. Strain softening behavior poses existence and uniqueness problems in the derived solutions. (1)
5. Some soils exhibit significant anisotropy due to the method of deposition (inherent anisotropy) and/or subsequent straining (often called stress induced anisotropy).
6. Soil conditions in situ are difficult to estimate. Soils are natural materials and therefore have variable properties (non homogeneous). Undisturbed sampling poses serious problems especially in sands. On the other hand, in situ tests are usually hard to interpret, because of the complicated boundary conditions and/or the non uniform conditions they impose in the soil (e.g Field Vane, Cone etc.)

---

(1) Prevost J.-H. and Hoeg K.(1975) 'Soil Mechanics and Plasticity Analysis of Strain Softening' Geotechnique 25,2,pp 279-297

Numerous formulations have been proposed in the Soil Mechanics literature, in recent years, to describe soil behavior under stress. Some of these models are strictly one-dimensional and thus their use in practical problems which are usually two or three dimensional is subject to significant errors. On the other extreme, some very general models are not useful in practice because of the large number of parameters they require to predict performance. (1) (2)

The theory of Incremental Plasticity provides a powerful and versatile mathematical tool for modeling Soil Behavior. It was initially developed for metals but in the last two decades, considerable efforts were devoted to apply the basic concepts of plasticity theory to soils. In metals, inelastic deformations involve various dislocation processes which depend primarily on the level of shearing but are largely unaffected by the level of the hydrostatic stress. Therefore Plasticity Theory for soil applications requires significant modifications in the original Metal Plasticity Theory.

This study summarizes the state of the art of soil plasticity and evaluates the capabilities and limitations of a number of promising models.

---

(1) Cuellar V. et al (1977) 'Densification and Hysteresis of Sand under Cyclic Shear' JGED ,ASCE ,Vol.103,No GT5, pp399-416

(2) Bazant Z. and Krizek R. (1976) 'Endochronic Constitutive Law for Liquefaction of Sand' JEMD ASCE, Vol.102,No.EM2,pp 225-238

Chapter II reviews the basic concepts of the Theory of Incremental Plasticity for the Geotechnical Engineer.

Chapter III discusses various isotropic models and derives the incremental stress-strain equations.

Chapter IV applies some promising isotropic models in various laboratory loading conditions and discusses their limitations.

Chapter V decribes an anisotropic model developed by Mroz and studied extensively by Prevost. The model is evaluated by comparing predictions to test results performed on Boston Blue Clay.

In Chapter VI the expansion of a cylindrical cavity problem (pressuremeter) is interpreted by means of an isotropic model and the Mroz-Prevost model.

CHAPTER II

FUNDAMENTALS OF PLASTICITY THEORY IN SOIL APPLICATIONS

2.1. Incremental Formulations.

Non-linear behavior of materials can be described by constitutive laws formulated either in an integral or differential form.

Given a stress (or strain) history at an element of soil, integral laws relate the strains at any loading stage with the corresponding stresses, whereas differential (or flow) laws relate increments of strains to the corresponding increments of stresses.

Integral formulations are appropriate for non-linear but elastic materials (rubber-like materials) where no energy is dissipated by means of plastic deformation. These materials, when unloaded, follow the same curve, in a stress-strain diagram, that they followed when they were loaded. Unloading in soils is generally much stiffer than loading, and this makes integral laws have limited value in the solution of

boundary value problems by numerical procedures. On the contrary, differential relations follow different paths in loading (which induces irreversible strains) and unloading (where no irreversible strains occur) and so they are more appropriate for energy dissipating materials such as soils. In the following only differential laws will be studied. We will also restrict this study to rate independent constitutive relations i.e we will exclude creep and relaxation effects. Rate independency is a severe restriction to the constitutive relations, especially for modelling highly structured and/or highly plastic or organic clays. However for more typical clays the exclusion of rate-of-loading effects is a reasonable assumption.

2.2 Yield Function.

For convenience, the state of stress at any point of a soil mass is mapped onto a point in a nine-dimensional stress space with coordinates given by the stress components:

$$\sigma_{ij} \qquad j \quad i,j = 1,2,3$$

In fact, because of conservation of angular momentum, $\sigma_{ij} = \sigma_{ji}$ for all i,j and hence a six-dimensional space suffices. Any loading sequence is thus represented in the stress space by a stress path. About the origin of this space (zero stresses), an elastic zone is assumed to exist. Stress paths located within the elastic zone produce no change in permanent (i.e irreversible or plastic) strains. The rest of the space defines the totality of plastic states and the boundary between the two subspaces defines the Yield Surface.

It is a fundumental assumption that the total strain increments (in the plastic range) $d\varepsilon_{ij}$, may be decomposed into elastic components $d\varepsilon_{ij}^{e}$ and plastic components $d\varepsilon_{ij}^{p}$ i.e:

$$d\varepsilon_{ij} = d\varepsilon_{ij}^{e} + d\varepsilon_{ij}^{p} \qquad (II-1)$$

where the symbol 'd' denotes an increment of the quantity to which it is applied.

The sum (over the strain path) of the corresponding plastic strain increments, defines the components of the plastic strain tensor ε_{ij}^{p} .

In addition, we assume that the elastic strain increments are linearly related to the stress increments by the generalized Hooke's law:

$$d\sigma_{ij} = C^{e}_{ijkl}\ d\varepsilon^{e}_{kl} \qquad (II-2)$$

Einstein's summation convention of repeated indices is used in Eq. II-2 and the rest of this thesis unless otherwise stated. The matrix C^{e}_{ijkl} is the Elastic stiffness (rigidity) matrix which is assumed to be symmetric and positive definite.

For convenience eq. II-2 can be written in a matrix form:

$$\underset{\sim}{d\sigma} = \underset{\sim}{C}^{e}\ \underset{\sim}{d\varepsilon}^{e} \qquad (II-2a)$$

or inverted to determine the elastic strain increment $d\varepsilon^{e}$ in terms of the stress increment $\underset{\sim}{d\sigma}$:

$$\underset{\sim}{d\varepsilon}^{e} = \underset{\sim}{S}^{e}\ \underset{\sim}{d\sigma} \qquad (II-2b)$$

where $\underset{\sim}{C}^{e}$ is the rigidity matrix and $\underset{\sim}{S}^{e}$ is the flexibility matrix (inverse of $\underset{\sim}{C}^{e}$).

For isotropic materials the elastic stress-strain relations reduce to:

$$d\sigma_{ij} = 2G\, d\varepsilon^{e}_{ij} + \left(K - \frac{2G}{3}\right) d\varepsilon^{e}_{kk}\ \delta_{ij} \qquad (II-3)$$

where G and K are the shear and bulk modulus respectively, and δ_{ij} is the Kronecker delta (equal to one for i=j and equal to zero for i different than j).

The yield surface is often (1) written in the form:

$$f(\sigma_{ij}, \varepsilon^{p}_{ij}) = 0 \qquad (II-4)$$

and defined such that, for elastic states, the value of the function is negative (i.e the corresponding stress points lie inside the yield surface) and plastic states satisfy eq. II-4 (i.e stress points lie on the yield surface). States which make the function positive are inadmissible. Furthermore, when the soil is in a plastic state (i.e when f=0) any infinitesmal stress change which induces plastic strain increments, is referred to as a 'loading' condition and leads to a new plastic state. On the other hand 'unloading' refers to conditions resulting in no plastic strain increments. During loading, plastic strains accumulate and (since we require eq. II-4 to hold) the shape, size and location of the yield surface may change in the stress space, but the stress point always remains on it. During unloading, the yield surface does not change in shape, size and location and the stress point retreats from it. Further stress changes may lead to situations where the stress point again reaches the yield surface and starts to push it, i.e yielding restarts. However yielding is not synonymous with failure, (2) but only

---

(1) Hill R. (1950) 'The Mathematical Theory of Plasticity', Clarendon press, Oxford England.

(2) Failure (or critical state) is defined as the condition where the material undergoes significant shear strains with no further changes of the applied shear stress and no further volumetric strains.

means the onset of irreversible strains. As mentioned earlier, (Chapter I), plastic strains develop in soils at very low stress levels and even during unloading and therefore, the notions of elasticity and yielding are somewhat arbitrary and are only maintained herein for the sake of clarity and mathematical convenience. The effects of this simplification depend on the history and level of straining in the problem considered.

The parameters defining the functional form of the yield surface (typically functions of plastic strains) may vary in such a way that the yield surface expands during loading (i.e stresses increase) and then the soil is said to be strain-hardening. Inversely when the yield surface contracts during loading, stresses decrease and the soil strain-softens. Finally when the yield surface does not change during yielding, the onset of yielding and the critical state (failure) occur simultaneously and a soil model having such a yield surface is called perfectly plastic.

2.3. Hardening rules.

The form of the yield surface given by eq. II-4 is too general for practical purposes and simplifying assumptions are necessary. It is almost universally accepted that the shape of the yield surface is invariant during straining.

If only the size and location (but not the shape) of the yield surface is allowed to vary during loading, the effect of stresses and plastic strains on the yield surface can be decoupled and eq. II-4 can be written in the form:

$$f \equiv f'(\sigma_{ij}) - F(\varepsilon^p_{ij}) = 0 \qquad (II-5a)$$

Function f' describes the shape of the yield surface whereas function F determines its size based on the plastic strains undergone during loading, and thus describes the strain hardening or strain softening characteristics of the soil. This type of hardening or softening behavior is called Isotropic Hardening (or Softening).

Another type of hardening is the so-called 'kinematic hardening'. It refers to a shift (translation) of the yield surface in the stress space without (necessarily) a change in size during yielding. Mathematically a kinematic nardening model is described by:

$$f \equiv f'(\sigma_{ij} - \alpha_{ij}) - c = 0 \qquad (II-5b)$$

where α_{ij} are the coordinates of some characteristic point of the yield surface (e.g its center) and 'c' the size

(radius) of the yield surface.

Combining eq. II-5a and eq. II-5b , we can introduce an isotropic and kinematic hardening model which has the following functional form:

$$f \equiv f'(\sigma_{ij} - \alpha_{ij}) - F(\varepsilon^p_{ij}) = 0 \qquad (II-6)$$

A further simplification is introduced by assuming that the hardening characteristics of the soil depend on invariant measures of plastic strain, rather than the individual plastic strain components. This assumption is always done for isotropic models (as we will discuss in a subsequent section) but it is quite common in some anisotropic soil models like the Mroz-Prevost Model.

Defining the plastic deviatoric strain increments by:

$$de^p_{ij} = d\varepsilon^p_{ij} - \frac{1}{3}(d\varepsilon^p_{kk})\,\delta_{ij} \qquad (II-7)$$

then, two invariant strain quantities are given by:

$$\varepsilon^p_v = \int_{path} d\varepsilon^p_v \quad ; \quad d\varepsilon^p_v = d\varepsilon^p_{kk}$$

$$\bar{\varepsilon}^p = \int_{path} d\bar{\varepsilon}^p \quad ; \quad d\bar{\varepsilon}^p = \left\{ \frac{2}{3} de^p_{ij} de^p_{ij} \right\}^{1/2} \qquad (II-8)$$

The first, ε^p_v, is a measure of plastic volumetric strains

and the second , $\bar{\varepsilon}^p$, provides a measure of plastic shear distortions (deviatoric strains). Using these two invariants in the equation of the yield surface, eq. II-5a and eq. II-6 take the simpler form:

$$f \equiv f'(\sigma_{ij}) - H(\varepsilon_v^p, \bar{\varepsilon}^p) = 0 \qquad (II-9)$$

$$f \equiv f'(\sigma_{ij} - \alpha_{ij}) - H(\varepsilon_v^p, \bar{\varepsilon}^p) = 0 \qquad (II-9a)$$

2.4. Incremental stress-strain relations (Flow rule)

Elastic materials have no memory, i.e the strain increments depend only on the specified stress increments and do not depend on the current stress state nor the stress (or strain history). On the contrary Theory of Plasticity introduces such characteristics.

In order to relate the plastic strain increments to the current stress state, a so-called 'Flow Rule' is required. This functional dependence can be quite arbitrary and is usually chosen to simplify analyses rather than comply with physical requirements (such as laws of thermodynamics or the behavior of the material in the micro-scale).

We start from the intuitive remark that a stress path which remains on the yield surface without moving it, should not result in any plastic strain increments, i.e :

if df=0 then $d\epsilon_{ij}^{p}=0$.

Using eq. II-5a the last requirement results in:

$$\frac{\partial f}{\partial \sigma_{kl}} d\sigma_{kl} = 0 \qquad (II-10)$$

So a functional dependence of the form:

$$d\epsilon_{ij}^{p} = \xi_{ij}\left(\frac{\partial f}{\partial \sigma_{kl}} d\sigma_{kl}\right) \qquad (II-11)$$

is justified.

In addition, if we introduce a 'Plastic Potential Function' $g(\sigma_{ij})$, such that:

$$\xi_{ij} = \alpha \frac{\partial g}{\partial \sigma_{ij}} \qquad (II-12)$$

then, instead of nine unknown proportionality parameters (these are functions of the stress and the plastic strain components) in eq. II-11, we only have to specify the potential 'g' (which is only a function of stresses), and the scalar α (which includes some dependence on the strains). Then eq. II-11 reduces to:

$$d\varepsilon_{ij}^{P} = \alpha \left(\frac{\partial f}{\partial \sigma_{kl}} d\sigma_{kl} \right) \frac{\partial g}{\partial \sigma_{ij}} \qquad (II-13)$$

This implies that the plastic strain increment vector, is perpendicular to the plastic potential function (actually to the surfaces g=constant). Note that the relations between the plastic strain increments and the stress increments are linear, and for convenience we can write eq. II-13 in the following matrix form:

$$\underset{\sim}{d\varepsilon}^{P} = \underset{\sim}{S}^{P} \underset{\sim}{d\sigma} \qquad (II-13a)$$

where $\underset{\sim}{d\varepsilon}^{P}$ is the vector of plastic strain increments and $\underset{\sim}{d\sigma}$ the vector of the corresponding stress increments.

An interesting remark is that the matrix $\underset{\sim}{S}^{P}$ is singular (i.e it cannot be inverted) because if it was not singular, then given any arbitrary vector $\underset{\sim}{d\varepsilon}^{P}$, we could solve eq. II-13a for $\underset{\sim}{d\sigma}$. Then using these computed stress increments in eq. II-13 (which is equivalent to eq. II-13a), we will evidently get the same plastic strain increment vector (which was initially chosen arbitrarily). However

this vector is not arbitrary (since it is perpendicular to the plastic potential according to eq. II-13). This proves that $\underset{\sim}{S}^p$ is singular.

The final incremental stress-strain relations are then easily obtained by using eq. II-1 , II-2b , and II-13a :

$$d\underset{\sim}{\varepsilon} = d\underset{\sim}{\varepsilon}^e + d\underset{\sim}{\varepsilon}^p = \underset{\sim}{S}^e d\underset{\sim}{\sigma} + \underset{\sim}{S}^p d\underset{\sim}{\sigma}$$

or:

$$d\underset{\sim}{\varepsilon} = \left(\underset{\sim}{S}^e + \underset{\sim}{S}^p \right) d\underset{\sim}{\sigma} \qquad \text{(II-14)}$$

Usually the elastic strain increment $\underset{\sim}{S}^e d\underset{\sim}{\sigma}$ is small compared to the plastic strain increment $\underset{\sim}{S}^p d\underset{\sim}{\sigma}$. However, it cannot be neglected since $\underset{\sim}{S}^p$ is singular and consequently eq. II-14 cannot be inverted (inversion is usually required in numerical schemes). Consequently elastic strains although they do not contribute much in the total strains, allow us to invert the resulting equations.

Two important points require attention:

1. For simplicity the plastic potential function 'g' is often assumed to be identical to the yield function 'f', i.e we assume that they are given by the same functional form. In this case the flow rule eq. II-13 becomes:

$$d\varepsilon_{ij}^p = \alpha \left(\frac{\partial f}{\partial \sigma_{kl}} d\sigma_{kl} \right) \frac{\partial f}{\partial s_{ij}} \qquad \text{(II-15)}$$

which is usually called 'associated flow rule'.

2. The α parameter describing the magnitude of the plastic strain increments (eq. II-13), is evaluated from the so-called 'connectivity condition', which basically requires that the change in size of the yield surface (which depends on $d\epsilon_{ij}^{p}$) should be such that the new stress point $\sigma_{ij} + d\sigma_{ij}$ is always located on the yield surface. Detailled expressions for evaluating α will be given when the equations for the various models will be derived (see also Appendix I).

2.5. Convexity of the yield surface and normality.

In Section 2.4 the concept of an associated flow rule was introduced for simplicity of the mathematical formulation (elimination of the necessity to evaluate a plastic potential function). However there are somehow stronger indications that such an assumption should be done.

Let's assume that a plastic state has been reached and the stress point is currently located on the yield surface. A stress increment $d\sigma_{ij}$ is then applied and elastic strain increments $d\varepsilon^e_{ij}$ and plastic strain increments $d\varepsilon^p_{ij}$ are induced. The elastic strain increments are related to the corresponding stress increments through Hooke's law. Assuming isotropy, the elasticity matrix $\underset{\sim}{S}^e$ is positive definite and consequently:

$$d\varepsilon^e_{ij}\, d\sigma_{ij} = S^e_{ijkl}\, d\sigma_{kl}\, d\sigma_{ij} \geq 0 \qquad (II-16)$$

Under such an assumption the uniqueness of solution in linear elasticity can be proved. (1) Drucker (2) based on the arguments used to establish uniqueness in linear Elasticity assumed that the plastic flexibility matrix $\underset{\sim}{S}^p$ is also

---

(1) Timoshenko S.P. and Goodier J.N. (1970) 'Theory of Elasticity' McGraw-Hill , pp 269-271

(2) Drucker D.C. (1959) 'Definition of stable inelastic Material' J. of Applied Mechanics, 26, pp 101-186

positive definite, which directly results in:

$$d\varepsilon_{ij}^{P}\, d\sigma_{ij} = S_{ijkl}^{P}\, d\sigma_{kl}\, d\sigma_{ij} \geq 0 \qquad (II-17)$$

and based on that, proved the uniqueness of solutions in Incremental Plasticity using exactly the same arguments as for Linear Elasticity. Drucker's assumption is referred in the literature as Drucker's Postulate. For strain hardening materials $d\sigma_{ij}$ is required to point outside the current yield surface during loading and then eq. II-17 means that the plastic strain increment vector is orthogonal to the yield surface (Normality Rule).

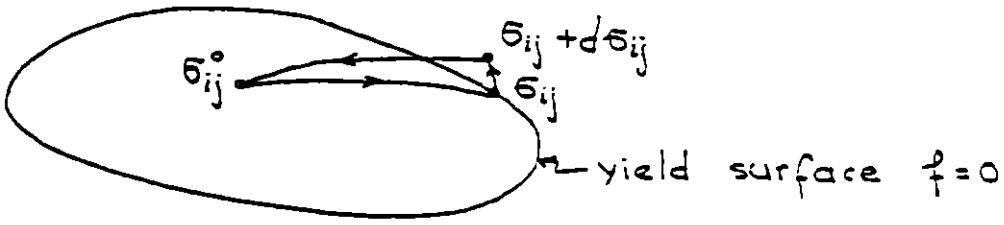

Based on the above postulate it can be proved (1) that the complementary work done during a cycle (see figure) which includes an infinitesmal plastic loading path, should be non-positive. Expressing the complementary work during such a cycle, it can be found that:

$$(\sigma_{ij} - \sigma_{ij}^{\circ})\, d\varepsilon_{ij}^{P} \geq 0 \qquad (II-18)$$

where σ_{ij}° is a stress point inside the yield surface,

---

(1) Martin J.B. (1975) "Plasticity: Fundamentals and General Results". MIT Press, Cambridge Mass. 931 p.

σ_{ij} a stress point on the yield surface and $d\varepsilon_{ij}^{p}$ the infinitesmal plastic strain increment, corresponding to the stress increment $d\sigma_{ij}$ (see previous figure).
Eq. II-18 again leads to the normality rule and it also requires that the yield surface is convex, since σ_{ij}^{o} is an arbitrary point inside the yield surface.

Assuming that normality holds, strain softening materials violate Drucker's Postulate (i.e eq. II-17) (1) and consequently there is no reason to obey the normality rule. However since most real materials include both a strain hardening (at low strains) and a strain softening region (at high strains) normality is often retained (even for strain softening materials) for the sake of convenience and simplicity.
As we discussed previously, assuming normality for a strain softening material means that:

$$d\varepsilon_{ij}^{p}\, d\sigma_{ij} < 0 \qquad (II-19)$$

Combining this with eq. II-15, we can immediately see that α is negative for a strain softening material and positive for strain hardening materials.
Eq. II-19 means that the plastic flexibility matrix $\underset{\sim}{S}^{p}$ is negative definite for strain softening materials. In fact using eq. II-13a and II-19 we get:

$$S_{ijkl}^{p}\, d\sigma_{ij}\, d\sigma_{kl} < 0$$

(1) since for such materials the stress increment points towards the interior of the yield surface

Prior to using such material laws, existence and uniqueness of solution has to be proved (because Drucker's proof is only valid for positive definite matrices). Prevost et al. (1) studied the conditions under which uniqueness of solution can be guaranteed, as well as the limit at which multiple solutions are possible (i.e when failure occurs). In fact a strain hardening material cannot fail theoretically. A strain softening material on the contrary, will fail when the strain softening zone extends spacially to a degree that the external work can no longer be absorbed by the material as elastic and/or plastic strain energy.

In the following Chapters Drucker's normality rule will be used unless otherwise stated. However it has to be understood that it does not result from thermodynamic requirements, nor it is necessary for uniqueness; it is just an assumption to simplify the mathematics. In addition using associated flow rules leads to symmetric flexibility matrices which greatly simplifies the numerical calculations.
In fact eq. II-15 can be rewritten:

$$d\epsilon_{ij}^{P} = \alpha \frac{\partial f}{\partial \sigma_{ij}} \frac{\partial f}{\partial \sigma_{kl}} d\sigma_{kl}$$

which means that the plastic flexibility matrix is given by:

$$S_{ijkl}^{P} = \alpha \frac{\partial f}{\partial \sigma_{ij}} \frac{\partial f}{\partial \sigma_{kl}} = S_{klij}^{P}$$

---

(1) Prevost J-H. and Hoeg K. (1975) 'Soil Mechanics and Plasticity Analysis of Strain Softening'. Geotechnique 25, No.2, pp.279-297.

which is symmetric. However $\underset{\sim}{S}^e$ is also symmetric, hence their sum (which is the flexibility matrix) is symmetric, too.

2.6 Isotropic yield functions.

A soil is isotropic when its stress-strain-strength behavior does not depend on the inclinations of the principal stress directions. In such a case the explicit dependence of the yield function on the stress components (eq. II-9), can be substituted by a dependence on merely three mutually independent invariant stress measures.

In choosing these measures it is convenient to separate the effect of hydrostatic pressure from the effect of shear stresses because of the different response of soils to hydrostatic versus shear (deviatoric) loading.

The first invariant I_1 of the stress tensor, provides a good measure of the hydrostatic confinement. It is defined as:

$$I_1 = \sigma_{kk} = \sigma_1 + \sigma_2 + \sigma_3 \qquad (II-20)$$

where $\sigma_1, \sigma_2, \sigma_3$ are the principal stresses. We further define the components of the deviatoric stress tensor, by just subtracting the effect of the hydrostatic part from the corresponding stress components as follows:

$$s_{ij} = \sigma_{ij} - \frac{1}{3}\sigma_{kk}\delta_{ij} \qquad (II-21)$$

The second and third invariants J_2 and J_3 of the deviatoric stress tensor are commonly used as invariant stress measures in the yield function. They are defined as follows:

$$J_2 = \frac{1}{2} s_{ij} s_{ij} = \frac{1}{6} \left\{ (\sigma_1 - \sigma_2)^2 + (\sigma_2 - \sigma_3)^2 + (\sigma_3 - \sigma_1)^2 \right\}$$

(II-22)

$$J_3 = \frac{1}{3} s_{ij} s_{jk} s_{ki}$$

For simplicity, the dependence of the yield function on the J_3 invariant, is often omitted because it is considered that only one shear measure is enough to express the dependence of actual behavior on shearing. (1) However Nayak et al. (2) and Lade and Duncan (3) suggest that inclusion of the third invariant may be a realistic improvement.

In the following we will only use dependence of the yield function on the I_1 and J_2 invariants.

A further improvement according to Roscoe and Burland (1) is to use these two measures, but multiplied with appropriate coefficients to make them energetically congugate with the invariant strain measures defined by eq. II-8.

Using:

---

(1) Roscoe K.H. and Burland J.B. (1968) 'On the Generalised Stress-Strain Behavior of Wet Clays'. Eng. Plasticity. Heyman and Leckie Eds. ,Cambridge U. Press, pp. 535-609

(2) Nayak G.C. and Zienkiewicz O.C. (1972) 'Convenient Form of Stress Invariants for Plasticity'. J. of the Str. D., ASCE Vol 98, No ST4 pp. 949-954

(3) Lade P.V. and Duncan J.M. (1973) 'Cubical Triaxial tests on Cohesionless Soil' JSMFD,ASCE Vol 99,SM10, pp. 793-812

$$p = \frac{1}{3} I_1$$

$$q = \sqrt{3 J_2} \qquad \text{(II-23)}$$

energetic conjugacy means that :

$$dW_p = \sigma_{ij} d\varepsilon_{ij}^p = p d\varepsilon_v^p + q d\bar{\varepsilon}^p$$

which is an expression of the increment of the plastic work. Using 'p' and 'q' , the equation for the yield surface II-9, for the simplified isotropic material becomes:

$$f \equiv f'(p,q) - H(\varepsilon_v^p, \bar{\varepsilon}^p) = 0 \qquad \text{(II-24)}$$

This last form is the basis for most isotropic models and will be discussed in detail in conjuction with the Cam-Clay model.

The incremental stress-strain relations (eq. II-15), can also be simplified for the case of isotropic models.
It can be proved (see Appendix I) that:

$$d\varepsilon_v^p = \alpha \left(\frac{\partial f}{\partial p} dp + \frac{\partial f}{\partial q} dq \right) \frac{\partial f}{\partial p}$$

$$d\bar{\varepsilon}^p = \alpha \left(\frac{\partial f}{\partial p} dp + \frac{\partial f}{\partial q} dq \right) \frac{\partial f}{\partial q} \qquad \text{(II-25)}$$

These equations express the normality rule in a two

dimensional invariant stress space 'p' and 'q', with appropriately chosen invariant strain measures 'ε_v^p' and

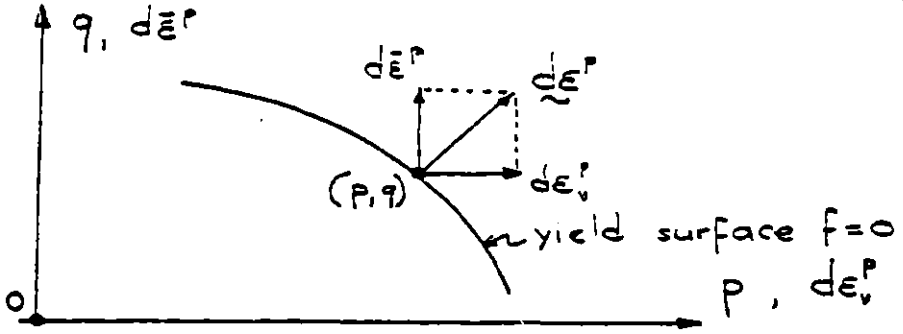

'$\bar{\varepsilon}^p$'. In fact if the yield surface is plotted in the p,q space (see figure) the plastic strain increment vector $d\underset{\sim}{\varepsilon}^p$ is perpendicular to the yield surface. The projections of this vector on the axes, are equal to the volumetric and distortional plastic strain increments.

2.7. Effective versus Total Stress Formulations.

The Effective Stress concept (1) is universally accepted in soil mechanics. It states that the total stress vector $\underset{\sim}{\sigma}$ acting on each soil element, is resisted by the pore water pressure components $u\,\underset{\sim}{m}$ (2) and by stresses on the soil skeleton $\underset{\sim}{\bar{\sigma}}$, according to the equation:

$$\underset{\sim}{\sigma} = \underset{\sim}{\bar{\sigma}} + u\,\underset{\sim}{m} \qquad \text{(II-27a)}$$

or in increments:

$$\Delta\underset{\sim}{\sigma} = \Delta\underset{\sim}{\bar{\sigma}} + \Delta u\,\underset{\sim}{m} \; . \qquad \text{(II-27b)}$$

Under fully drained loading conditions, no pore pressures are created in excess to the steady state (usually hydrostatic) conditions.

Under fully undrained conditions pore pressure increments are developed to reduce (or increase) the effective stresses to a degree that the no-volume-change condition holds.

It is widely accepted (3) (4) (5) that effective stresses

---

(1) Terzaghi K.V. (1925) 'Erd- mechanik auf bodenphysikalischer Grundlage' Vienna

(2) $\underset{\sim}{m}$ stores the Kronecker delta components.

(3) Bishop A.W. and Blight G.E. (1963) 'Some Aspects of Effective

govern the behavior of soil materials irrespective of drainage conditions. More specifically experiments indicate that strength and volume change of all soils, are controlled by the effective stresses for each mode of deformation.

The Effective Stress concept, however, does not mean that there is a unique relationship between effective stresses and the various strain measures (e.g. void ratio, moduli etc). Such unique relationship holds only in Theory of Elasticity.

The Effective stress concept means that:

> Loading (or unloading) paths which follow the same stress path in an EFFECTIVE stress space, will have the same strain measures (e.g. void ratio, moduli etc) regardless of the magnitude of the total stresses associated with this path.

On the contrary, a total stress concept, would imply that:

> Loading (or unloading) paths which follow the same stress path in a TOTAL stress space, will have the same strain measures, regardless of the magnitude of the effective stresses associated with this path.

Stress in Saturated and Partly Saturated Soils'. Geotechnique 13, p. 177

(4) Jennings J.E. (1961) 'A Revised Effective Stress Law for Use in the Prediction of Behavior of Unsaturated Soils'. Pore pressure and Suction in Soils, London (Butterworth)

(5) Skempton A.W. (1961) 'Effective Stress in Soils, Concrete and Rocks.' Pore Pressure and Suction in Soils, London (Butterworth).

According to the previous definitions, effective stresses do control soil behavior. However it needs to be clarified that when we say 'total' stresses we do not mean total DEVIATORIC stresses. Most formulations which are mentioned in the literature as 'total stress formulations' (e.g. the Mroz-Prevost model), involve deviatoric stresses. As we will prove later, this is necessary in order for the resulting matrices to be non-singular. At the same time, however, the use of deviatoric total stresses instead of total streses makes these formulations equivalent to an effective stress formulation (only for undrained loadind, though) as we will also prove at the end of this section.

Under drained loading (i.e slow enough so that no significant excess pore pressures to develop), only effective stress formulations are applicable.

Under undrained loading (i.e fast enough so that water does not have time to escape and consequently the assumption of no volume changes is generally acceptable), pore pressures develop and the externally applied loads are undertaken by both the soil skeleton and hydrostatic pressures in the liquid phase. In this case both total and effective stress formulations can be used (and they have been used in the Literature), and their comparative merits and limitations will be studied in the following:

A. Effective Stress Formulations.

An effective stress incremental Constitutive relation is of the form:

$$\underset{\sim}{d\bar{\sigma}} = \underset{\sim}{\bar{\bar{C}}}\, \underset{\sim}{d\varepsilon} \quad \text{or:} \quad \underset{\sim}{d\varepsilon} = \underset{\sim}{\bar{\bar{S}}}\, \underset{\sim}{d\bar{\sigma}} \qquad (II\text{-}26)$$

where $\underset{\sim}{d\bar{\sigma}}$ are the effective stress changes and $\underset{\sim}{\bar{\bar{C}}}$ and $\underset{\sim}{\bar{\bar{S}}}$ the incremental stiffness and flexibility matrices respectively.

Cam-Clay model is such a formulation.

During an undrained loading the following question arises:

> Given a total stress increment what is the corresponding pore pressure increment ?

Let's assume that we know the total stress increment $\underset{\sim}{\Delta\sigma}$ and we want to compute the corresponding pore pressure change Δu , resulting from this increment. If $\underset{\sim}{\Delta\bar{\sigma}}$ is the effective stress increment and $\underset{\sim}{m}$ the Kronecker delta vector (1) then:

$$\underset{\sim}{\Delta\bar{\sigma}} = \underset{\sim}{\Delta\sigma} - \underset{\sim}{m}\, \Delta u \qquad (II\text{-}27)$$

If B^w is the bulk modulus of water, B^s the bulk modulus of the solids (i.e grains), 'n' the porosity and I a 6x6 unit matrix, then Appendix III shows that the pore pressure increment will be given by:

---

(1) It contains 1 at the normal stress locations and 0 at the locations of the shear stresses.

$$\Delta u = \frac{\underset{\sim}{m}^T \left\{ \underset{\sim}{S} - \frac{1-n}{B^s} \underset{\sim}{I} \right\} \underset{\sim}{\Delta\sigma}}{\underset{\sim}{m}^T \underset{\sim}{S} \underset{\sim}{m} + \frac{n}{B^w} - \frac{3(1-n)}{B^s}} \qquad (II\text{-}28)$$

Eq. II-28 relates linearly the pore pressure increment with the components of the total stress increment, provided that the effective flexibility matrix $\underset{\sim}{S}$ is known. (i.e an effective stress model is used.)

For the more common case of incompressible grains and fluid ($B^w = B^s = \infty$) eq. II-28 simplifies to:

$$\Delta u = \frac{\underset{\sim}{m}^T \underset{\sim}{S} \underset{\sim}{\Delta\sigma}}{\underset{\sim}{m}^T \underset{\sim}{S} \underset{\sim}{m}} \qquad (II\text{-}28a)$$

The last equation may seem unfamiliar to the Geotechnical Engineers. A form like:

$$\Delta u = \Delta\sigma_{oct} + a \ \Delta\tau_{oct}$$

where the contributions of the octahedral and the deviatoric stress increments $\Delta\sigma_{oct}$ and $\Delta\tau_{oct}$ respectively (1) on the pore pressure increment are separated is more common. Appendix III shows that eq. II-28a can be put in the form of eq. II-28b. The parameter 'a' depends only on the

---

(1) Henkel D.J. and Wade N.H. (1966) 'Plane Strain Tests on a Saturated Remolded Clay' JSMFD, ASCE Vol 92, No SM6, Nov 1966, pp 67-80.

cross-coupling terms between shear stresses and nc
volumetric) strains of the matrix $\underset{\sim}{\underline{\underline{S}}}$. Conse
there is no such coupling (as in Theory of Linear
Elasticity) then a=0. This means that the por
increment is equal to the total octahedral stress
a result well known in Theory of Elasticity.

It is interesting to note that an effecti
formulation can lead to total stress i
relationships. Using Eqs. II-28 and II-26 we can w

$$\underset{\sim}{\Delta\varepsilon} = \underset{\sim}{\underline{\underline{S}}}\ \underset{\sim}{\Delta\bar{\sigma}} \quad \Rightarrow \quad \underset{\sim}{\Delta\varepsilon} = \underset{\sim}{\underline{\underline{S}}} \left(\underset{\sim}{\Delta\sigma} - \underset{\sim}{m}\,\Delta u \right)$$

or

$$\underset{\sim}{\Delta\varepsilon} = \underset{\sim}{\underline{\underline{S}}}\ \underset{\sim}{\Delta\sigma} - \underset{\sim}{\underline{\underline{S}}}\ \underset{\sim}{m} \cdot \frac{\underset{\sim}{m}^T \left\{ \underset{\sim}{\underline{\underline{S}}} - \frac{1-n}{B^g}\ \underset{\sim}{\underline{\underline{I}}} \right\} \underset{\sim}{\Delta\sigma}}{\underset{\sim}{m}^T\ \underset{\sim}{\underline{\underline{S}}}\ \underset{\sim}{m} + \frac{n}{B^w} - \frac{3(1-n)}{B^g}}$$

which is of the form:

$$\underset{\sim}{\Delta\varepsilon} = \underset{\sim}{\underline{\underline{S}}}\ \underset{\sim}{\Delta\sigma} \qquad (\text{II-29a})$$

Eq. II-29a provides the incremental strains in
the total stress increment.
For the common case of incompressible water and gr
total stress formulation derived above can be put i
deviatoric stresses (form similar to the Mroz-Prevc
In fact for this case eq. II-29 reduces to:

$$\underset{\sim}{\Delta\varepsilon} = \underset{\approx}{S}\,\underset{\sim}{\Delta\sigma} - \underset{\approx}{S}\,\underset{\sim}{m}\cdot\frac{\underset{\sim}{m}^T\,\underset{\approx}{S}\,\underset{\sim}{\Delta\sigma}}{\underset{\sim}{m}^T\,\underset{\approx}{S}\,\underset{\sim}{m}} \qquad (II-29b)$$

Substituting the total stress increment $\underset{\sim}{\Delta\sigma}$ in terms of the deviatoric stress increment $\underset{\sim}{\Delta s}$ and the octahedral stress increment $\Delta\sigma_{oct}$ from the equation:

$$\underset{\sim}{\Delta\sigma} = \underset{\sim}{\Delta s} + \Delta\sigma_{oct}\,\underset{\sim}{m}$$

the octahedral stress terms drop out and eq. II-29b reduces to:

$$\underset{\sim}{\Delta e} = \underset{\approx}{S}\,\underset{\sim}{\Delta s} - \underset{\approx}{S}\,\underset{\sim}{m}\,\frac{\underset{\sim}{m}^T\,\underset{\approx}{S}\,\underset{\sim}{\Delta s}}{\underset{\sim}{m}^T\,\underset{\approx}{S}\,\underset{\sim}{m}} \qquad (II-30)$$

Eq II-30 is of the form:

$$\underset{\sim}{\Delta e} = \underset{\approx}{S}\,\underset{\sim}{\Delta s} \qquad (II-30a)$$

and it relates linearly the deviatoric strain increments with the deviatoric total stress increments.

B. Total Stress Formulations.

Since there is no volume change, only the deviatoric components $\underset{\sim}{\Delta e}$ of the strain increment must be considered in the formulation. (1) On the other hand we cannot use the total stress increment $\underset{\sim}{\Delta\sigma}$ in the formulation, since an equation of the form:

$$\underset{\sim}{\Delta\sigma} = \underset{\approx}{C}\,\underset{\sim}{\Delta e} \qquad (II-32)$$

(1) The volumetric component is zero.

will necessarily have singular $\underset{\sim}{C}$ matrix.

In fact let's assume an arbitrary deviatoric strain increment $\underset{\sim}{\Delta\varepsilon}$ and applying eq. II-32, compute the corresponding total stress increment $\underset{\sim}{\Delta\sigma}$. The stress increment $\underset{\sim}{\Delta\sigma} - p\underset{\sim}{m}$, where p is an arbitrary parameter, will correspond to the same deviatoric strain increment $\underset{\sim}{\Delta\varepsilon}$ because hydrostatic pressures are completely resisted by the pore water and cause no deviatoric strains. Consequently:

$$\underset{\sim}{\Delta\sigma} - p\underset{\sim}{m} = \underset{\sim}{C}\,\underset{\sim}{\Delta\varepsilon} \qquad (II-33)$$

However if $\underset{\sim}{C}$ is non-singular, we can always find a vector $\underset{\sim}{x}$ (not identically zero) such that:

$$\underset{\sim}{C}\,\underset{\sim}{x} = \underset{\sim}{m} \qquad (II-34)$$

Then combining eq. II-33 and II-34 we get:

$$\underset{\sim}{\Delta\sigma} = \underset{\sim}{C}\left(\underset{\sim}{\Delta\varepsilon} + p\underset{\sim}{x}\right) \qquad (II-35)$$

Eq. II-32 and II-35 show that we have more than one solution (1) of the matrix equation II-32.

Hence matrix $\underset{\sim}{C}$ is singular.

The singularity of $\underset{\sim}{C}$ requires the use of a deviatoric stress incremental constitutive relation and hence, instead of an equation of the form II-32 we consider:

$$\underset{\sim}{\Delta s} = \underset{\sim}{C}\,\underset{\sim}{\Delta\varepsilon} \qquad (II-36)$$

---

(1) actually we have an infinity of solutions since parameter p is arbitrary

Matrix $\underset{\sim}{C}$ is no longer singular.

The Mroz-Prevost model to be discussed in Chapter V, is an example of a total stress model of the last form.

A disadvantage of the method is, that there is no way to compute the pore pressures developed, unless we make additional assumptions relating the magnitude of the pore pressure changes with the change of the total stresses.

Let's summarize what we have discussed so far on the effective and total stress formulations.

(1) An effective stress incremental model of the form:

$$\underset{\sim}{\Delta\bar{\sigma}} = \underset{\sim}{\bar{C}}\,\underset{\sim}{\Delta\varepsilon} \quad \text{or:} \quad \underset{\sim}{\Delta\varepsilon} = \underset{\sim}{\bar{S}}\,\underset{\sim}{\Delta\bar{\sigma}} \qquad (II\text{-}26)$$

is sufficient for the treatment of problems involving drained loading, partially drained loading (i.e soils undergoing consolidation) and loading of partially saturated soils.

For an undrained loading it is also sufficient, provided that an appropriate Variational Principle is used in the Finite Element scheme.

(2) A total stress formulation has to be of the form given by eq. II-36.

$$\underset{\sim}{\Delta s} = \underset{\sim}{C}\,\underset{\sim}{\Delta e} \quad \text{or} \quad \underset{\sim}{\Delta e} = \underset{\sim}{S}\,\underset{\sim}{\Delta s} \qquad (II\text{-}36)$$

i.e it has to involve the deviatoric stress increments and

not the total stress increments. Such a formulation can only be used for undrained loading conditions and fails to predict the pore pressure increment. A separate model has to be used for this purpose, which will associate the pore pressures generated due to shear stress increments.

We will further show that such a total stress formulation is equivalent to an effective stress formulation, in the following sense:

If a total stress increment $\underset{\sim}{\Delta\sigma}$, applied under undrained loading conditions, results in no strain increment according to either of the two formulations, then it will give no strains with the other formulation, too. In addition if it gives a non-zero incremental strain with one formulation then the same total stress increment will result in a unique and non-zero strain increment with the other.

In fact let $\underset{\sim}{\Delta\sigma}$ be a total stress increment such that the corresponding strain increment through a total stress formulation is zero. Then:

$$\underset{\sim}{0} = \underset{\sim}{\Delta\varepsilon} = \underset{\approx}{S}\,\underset{\sim}{\Delta s}$$

But since $\underset{\approx}{S}$ is non-singular, $\underset{\sim}{\Delta s} = \underset{\sim}{0}$.

This means that the total stress increment has to be of the form $\underset{\sim}{\Delta\sigma} = p\underset{\sim}{m}$ which is a hydrostatic stress increment. However a hydrostatic stress increment does not produce strains according to an effective stress formulation.

Similarly, if $\underset{\sim}{\Delta\varepsilon} \neq 0$ then: $\underset{\sim}{\Delta s} \neq 0$ which means that:

$$\underset{\sim}{\Delta\sigma} \neq p\underset{\sim}{m}$$

i.e the stress increment is not hydrostatic. But a non-hydrostatic total stress increment gives a unique and non-zero strain increment through an effective stress formulation, too.

Consequently the two formulations are equivalent in the sense that there is a one-to-one correspondence between stress paths in an effective stress space, and stress paths in a total deviatoric stress space. These stress paths may result in different strain paths (depending on the specific form of each formulation) (1) but there is no stress path in one stress space which corresponds to a null stress path in the other stress space.

(1) or the same strain path may result in different stress paths depending on which formulation is used.

2.8. Summary of results.

The Theory of Incremental Plasticity enables the increment of strains $\underset{\sim}{d\varepsilon}$ in a soil element to be determined in terms of the stress increment (1) $\underset{\sim}{d\sigma}$ from an equation of the form:

$$\underset{\sim}{d\varepsilon} = \left(\underset{\sim}{S}^{e} + \underset{\sim}{S}^{p} \right) \underset{\sim}{d\sigma} \qquad (II-14)$$

The term in parenthesis can thus be considered the 'incremental flexibility matrix'. $\underset{\sim}{S}^{e}$ is the contribution of the elastic strains which is usually insignificant in magnitude, but absolutely necessary in order for the flexibility matrix to be non-singular. $\underset{\sim}{S}^{p}$ is the contribution of the plastic strains; this matrix is singular but symmetric (provided that an associated flow rule is used; see Section 2.5). Inverting the last expression we get the incremental stiffness matrix:

$$\underset{\sim}{d\sigma} = \underset{\sim}{C}\, \underset{\sim}{d\varepsilon} \qquad (II-37)$$

In the special case of elastic behavior (e.g during unloading) no plastic strain changes occur and consequently:

$$\underset{\sim}{d\varepsilon} = \underset{\sim}{S}^{e}\, \underset{\sim}{d\sigma} \quad \text{or} \quad \underset{\sim}{d\sigma} = \underset{\sim}{C}^{e}\, \underset{\sim}{d\varepsilon}$$

---

(1) Total or Effective stress increment depending on if a total stress or an effective stress formulation is used.

The elastic flexibility matrix depends on the elastic shear and bulk moduli.

The plastic flexibility matrix depends on the following quantities provided that normality rule is used:

1. The current stress state σ_{ij} .
2. The functional form of the yield surface (and the plastic potential if a non-associated flow rule is used).
3. The strain hardening function $H(\varepsilon_v^p, \bar{\varepsilon}^p)$ describing the size of the yield surface during plastic flow. 'H' is usually assumed to depend only on the two invariant strain measures (eq.II-8).
4. The cummulative invariant plastic strains which depend on the loading history (eq. II-8).

Provided that normality rule is used, the incremental stress-plastic strain equations are given by eq. II-13. If an associated flow rule is also used they are given by eq. II-15. For the case of an isotropic model eq. II-24 and II-25 can be used.

CHAPTER III

ISOTROPIC SOIL MODELS

3.1 THE CAM-CLAY MODEL

The Cam-Clay Model, developed by the Cambridge University group, will be studied in this Chapter. The following presentation is largely based on the paper by Roscoe and Burland. (1)

The Cam-Clay model is an isotropic model and consequently the general form of the yield function is given by (see eq. II-24 in Chapter II):

$$f \equiv f'(p,q) - H(\varepsilon_v^p, \bar{\varepsilon}^p) = 0 \qquad (II-24)$$

where p is the mean effective stress, q is related to the second invariant of the stress deviator, and ε_v^p, $\bar{\varepsilon}^p$ are their associated invariant strain measures (for exact

(1) Roscoe K.H and Burland J.B (1968) 'On the Generalized Stress-Strain Behavior of Wet Clays' Eng. Plasticity. Heyman and Leckie Eds. Cambridge U. Press, pp. 535-609

definitions see eq. II-8 and II-23).

By assuming a specific form for the function f' (e.g ellipse) and the hardening function H, and applying the procedure described in Appendix I, (1) the incremental stress-strain relations can be obtained. However such a mathematical presentation does not provide the necessary insight to the physical principles of the model.

A further assumption (in addition to the assumption of isotropic behavior implied in eq. II-24), is that the effect of the plastic shear strains $\bar{\varepsilon}^p$ on the size of the yield surface is neglected. So plastic volumetric strains ε_v^p, solely determine the size of the yield surface, and eq. II-24 now simplifies to:

$$f \equiv f'(p,q) - H(\varepsilon_v^p) = 0 \qquad (II-24a)$$

The plastic volumetric strain increments $d\varepsilon_v^p$, are directly related to the plastic void ratio increments de^p by the equation:

$$de^p = -(1+e)\, d\varepsilon_v^p \qquad (III-1)$$

where 'e' is the void ratio. (2) Similarly for the elastic components:

$$de^e = -(1+e)\, d\varepsilon_v^e \qquad (III-2)$$

---

(1) also assuming normality and associated flow rule

(2) The void ratio is defined as the ratio of the volume of voids to the volume of solids in an element of soil.

According to eq II-24a, the state of soil can be represented in a three-dimensional space of 'p','q', and the plastic void ratio 'e^p' (or just the void ratio 'e'). This space is familiar to the soil engineers because its subspaces are used extensively. The e-p subspace is used for the representation of results of isotropic (and K_o) consolidation tests (e.g the oedometer test). The p-q subspace is used for the representation of shear tests. In fact in a triaxial test $\sigma_2 = \sigma_3$, and eq. II-23 reduces to:

$$p = \frac{1}{3}(\sigma_1 + 2\sigma_3) \quad ; \quad q = |\sigma_1 - \sigma_3| \qquad (III-3)$$

which are similar to the:

$$s = \frac{1}{2}(\sigma_1 + \sigma_3)$$

$$t = \frac{1}{2}(\sigma_1 - \sigma_3)$$

commonly (1) used in the representation of triaxial tests.

Fig. 2 represents various stress paths in the e-p-q space. During virgin isotropic consolidation the point representing the state of the soil moves along curve DE. During isotropic rebound from points like D or E, the stress point moves along curves DH or EJ'' respectively, which lie on the e-p plane. (i.e the q=0 plane) Note that points (on the e-p plane) lying outside the region between the virgin

---

(1) T.W.Lambe (1967) 'Stress Path Method' JSMFD,ASCE, Vol 93, No SM6, pp. 309-331.

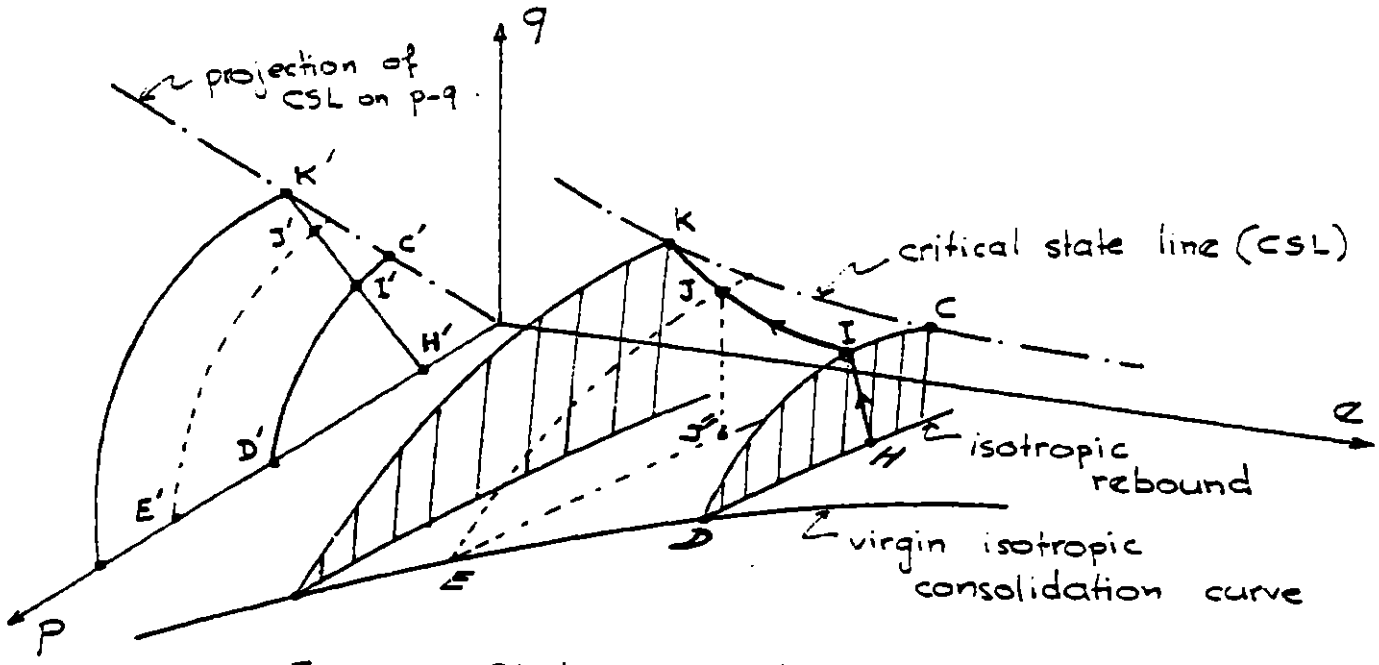

Fig 2 : State Boundary Surface

isotropic consolidation curve and the e-axis cannot be reached by any loading path. Points inside this region can be reached by unloading from an appropriate position (e.g point H can be reached by unloading from point D, lying on the virgin isotropic consolidation curve). All such points correspond to overconsolidated states. We can easily extend the idea of a boundary curve (like DE), separating accessible from inaccessible states on the e-p plane, to a boundary surface separating accessible from inaccessible states in the e-p-q space. The so-called 'State Boundary Surface' (SBS), is represented by the surface EDICJ in Fig. 2.

Points inside the SBS correspond to overconsolidated states, and it is assumed that Elasticity Theory is appropriate in describing stress paths in this region. Linear Elasticity could be used, but it was prefered to stick to the results of

tests which show that isotropic (and K_o) rebound, relates the void ratio linearly with the logarithm of the octahedral (or 'p') stress. Expressing this mathematically:

$$de^e = -k\frac{dp}{p} \qquad (III-4)$$

where 'k' is an elastic (rebound) volumetric flexibility measure. (1) However linear elasticity will be used for the deviatoric components:

$$ds_{ij} = 2G\, de_{ij} \qquad (III-6)$$

where ds_{ij} are the deviatoric stress increments, de_{ij} are the deviatoric strain increments and 'G' an elastic shear modulus.

Parametric studies performed for this thesis on the effect of the specific value assumed for the elastic shear modulus have shown that the value of 'G' has a negligible effect on the resulting stress paths, and only a minor effect on the stress-strain curves (because elastic strains are anyway

---

(1) Using eq. III-2 and eq. III-4 we can compute the bulk modulus 'K' as a function of 'k':

$$K \equiv \frac{dp}{d\varepsilon_v^e} = \frac{p(1+e)}{k} \qquad (III-5)$$

Note that the bulk modulus 'K' is not a constant (as in linear elasticity), but it depends on the stress level 'p' and the current void ratio. On the contrary, 'k' is assumed to be constant.

small compared to the plastic ones). (1) However 'G' has to be finite because, otherwise, the flexibility matrix will be singular (as it was proved in Chapter II).

From equations III-4, III-5 and III-6, the elastic flexibility matrix can be computed:

$$\underset{\sim}{d\varepsilon}^e = \underset{\sim}{\overline{S}}^e \, \underset{\sim}{d\sigma} \qquad (III-7)$$

where for a principal stress space:

$$\underset{\sim}{S}^e = \frac{1}{3}\begin{bmatrix} \left\{\frac{k}{3p(1+e)} + \frac{1}{G}\right\} & \left\{\frac{k}{3p(1+e)} - \frac{1}{2G}\right\} & \left\{\frac{k}{3p(1+e)} - \frac{1}{2G}\right\} \\ & \left\{\frac{k}{3p(1+e)} + \frac{1}{G}\right\} & \left\{\frac{k}{3p(1+e)} - \frac{1}{2G}\right\} \\ \text{symmetric} & & \left\{\frac{k}{3p(1+e)} + \frac{1}{G}\right\} \end{bmatrix} \qquad (III-8)$$

Points on the SBS correspond to normally consolidated states. The curve DIC, (Fig. 2), is the intersection of the SBS with a vertical 'wall' passing through an isotropic rebound curve.

A Yield Surface, (as it was studied in Chapter II), is represented in a space of stress components only, which is

---

(1) For undrained loading the effect of the specific value of 'G' is significant because the elastic volumetric strain is equal in magnitude to the plastic one, which enforces the elastic strain components to have the same order of magnitude with the plastic ones.

evidently different than the e-p-q space shown in Fig. 2. It would be nice however, instead of defining the yield surface independently, to somehow relate it with the SBS, because they do have something in common: they both separate accessible from inaccessible states. (1) This is the major contribution of the Cambridge University group. By relating the yield surface to the State Boundary Surface they linked an otherwise purely Mathematical Model to the mechanics of actual Soil Behavior.

The Yield Surface will be represented in the p-q subspace of the e-p-q space and specifically it will be assumed to be identical to the projection D'I'C' of the curve DIC (lying on the SBS) on the p-q plane. Consequently a movement of the stress point from the location ,say, I (on the SBS), to a new location J (also on the SBS), will correspond to a change of the yield surface from the positicn D'I'C' to the new position E'J'. (the projection of the stress point stays on the yield surface). An ellipse (see also Fig. 3), having its major axis located along the p-axis (with length p_c) and passing through the origin was chosen as a yield function (i.e it was assumed that the projection of the curves DIC on the p-q plane are such ellipses). The ratio of the major to the minor axes (denoted by 'M') was kept constant during the deformation process and consequently the only degree of

---

(1) The only difference is that the yield surface is represented in a stress space, and the SBS is represented in a space which also includes one strain component, namely the void ratio).

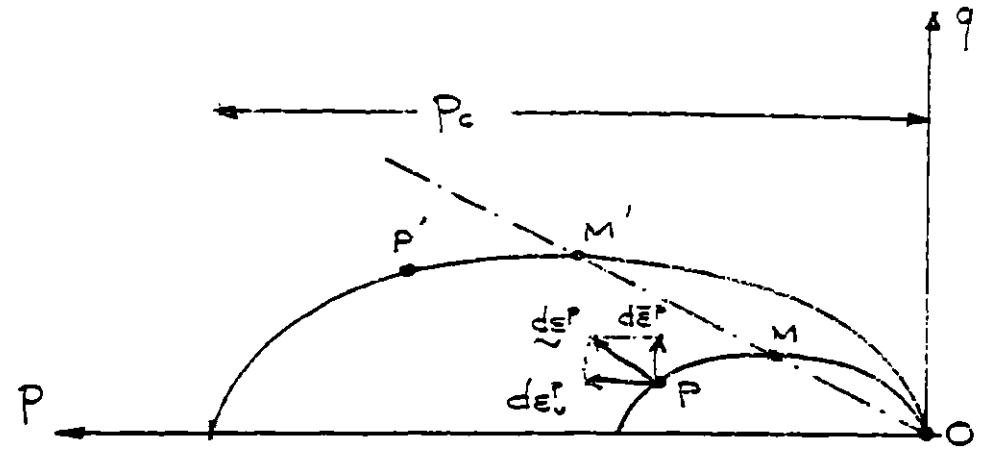

Fig. 3 : Cam-Clay yield function.

freedom of the ellipse is the size of the p-axis, p_c, which (as mentioned in the beginning of the chapter) was assumed to depend only on the plastic void ratio. (Hardening rule)

So:

$$p_c = p_c(e^p) \qquad (\text{III}-9)$$

As loading proceeds, the yield surface is pushed by the stress point and moves homothetically with pole the origin O, as it is shown schematically in Fig 3.

There is a characteristic behavior associated with the peak M of the ellipse. At this point (using normality) the plastic strain increment vector $d\underset{\sim}{\varepsilon}^p$ has no component along the p-axis, which means that:

$$d\varepsilon_v^p = 0 \qquad (\text{III}-10)$$

or using eq. III-1, that the plastic void ratio remains constant during subsequent shearing. Furthermore the size of the yield surface depends on e^p (eq. III-9), and hence it does not change. Consequently the stress point once it has

reached point M (the peak), it stays there provided that the sample is monotonically loaded. At this level only plastic deviatoric strains occur (eq. III-10), with no further changes of the stresses (because the stress point does not move). This condition is defined as 'failure'. The locus of points M (i.e line OM in Fig 3) is the projection of a curve on the SBS (curve KC in Fig 2) which is called the Critical State Line. (CSL) (1) The projection of the Critical State Line (or Failure line), on the e-p plane is assumed to be a curve parallel (in an e-lnp plot) to the isotropic consolidation line.

Undrained Stress Paths.

During undrained loading of a soil, the void ratio does not change. Hence the stress path for a normally consolidated sample under undrained loading, will be the intersection of the SBS with a plane e=constant (i.e a plane parallel to the p-q plane in Fig 2). Such a curve lies close to, but it is not identical, to a curve like DIC. (2) They are identical, only if the rebound flexibility 'k' is equal to zero. In

---

(1) Schofield A.N. and Wroth C.P. (1968) 'Critical State Soil Mechanics' McGraw-Hill, New York.

(2) Consequently the projection of the undrained stress path on the p-q plane is not identical with the curve D'I'C', but it lies very close to it (there is a small translation of the yield surface associated with small changes of the plastic void ratio which are compensated with equal changes of the elastic void ratio, so that their sum is zero as it is required for an undrained loading path.

this case the isotropic rebound curves are parallel to the p-axis (in the e-p-q plot).

Appendix II uses the equations developed in Appendix I in conjunction with the specific form chosen for the yield function (an ellipse), to evaluate the incremental stress-strain relations in the plastic region (i.e the plastic flexibility matrix $\underset{\sim}{S}^{P}$ is formulated in a principal stress space).

Input parameters.

The input parameters to the model are:

(1) The position of a consolidation curve under isotropic stresses, i.e its slope (λ) and the location of one point on it to specify the curve in a e-lnp plot. Since isotropic and K_o-consolidation curves are usually parallel in an e-lnp plot, the position of a K_o-consolidation curve can be used alternatively.

(2) The slope (k) of an isotropic rebound curve.

(3) The friction angle in one (arbitrary) mode of failure. This is expressed through the 'M' parameter which is the ratio of 'q' versus 'p' at failure for this specific mode of failure. If the triaxial compression mode of failure is chosen then:

$$M = \frac{3(N_\phi - 1)}{N_\phi + 2} \qquad (III-11)$$

where

$$N_\phi = \tan^2\left(45 + \frac{\bar{\phi}_{TC}}{2}\right) \qquad (III\text{-}12)$$

and $\bar{\phi}_{TC}$ is the friction angle at failure in the triaxial compression mode. (1)

For other modes of failure, a failure criterion (like the Mohr-Coulomb) should be employed to artificially cause failure to occur at a reasonable value of the friction angle. This is because (as we show in Chapter IV) the model itself will cause failure (i.e large shear strains with no further changes of the effective stresses) at unrealistically high values of the friction angle. With no additional failure criterion the model will cause failure only when the Critical State Line is reached.

For each water content (i.e for each e=constant plane in Fig 2) there is one corresponding point on the CSL. Hence the model predicts a unique relation between 'q' at failure (designated as 'q_f') and water content (or equivalently the

---

(1) Note that the Cam-Clay Model predicts different friction angle for compression and extension tests. Also note that the model is always strain hardening for normally consolidated samples. However actual undrained K_o-TC and K_o-PSA tests exhibit strain softening characteristics. Therefore the friction angle that will be used as an input to the model should be chosen with these in mind.

void ratio). (2) For a specific mode of failure, 'q_f' corresponds to a value of the 'undrained shear strength'. The undrained shear strength is defined as follows:

$$s_u = \frac{|\bar{\sigma}_{1f} - \bar{\sigma}_{3f}|}{2} \qquad (III-13)$$

where $\bar{\sigma}_{1f}, \bar{\sigma}_{3f}$ are the maximum and minimum principal stresses. Using this definition for the undrained shear strength, relations between 'q_f' and 's_u' can be established for the various modes of loading. For example for the triaxial test:

$$(s_u)_T = \frac{q_f}{2} \qquad (III-14)$$

For the plane strain test assuming that:

$$\bar{\sigma}_{2f} = \frac{1}{2}(\bar{\sigma}_{1f} + \bar{\sigma}_{3f})$$

we have: (1)

$$(s_u)_{PS} = \frac{1}{\sqrt{3}} q_f \qquad (III-14a)$$

So the model predicts a unique relation between the undrained shear strength and the corresponding void ratio for each mode

---

(2) irregardless of the mode of failure.

(1) Note that by dividing eq. III-14a and III-14 we get that the ratio of the undrained shear strengths of the plane strain versus the triaxial mode of failure is 1.155 .

of failure. (irrespective of the Overconsolidation Ratio) This agrees with the results obtained by Hvorslev. (1)

(1) Hvorslev M.J. (1960) 'Physical Components of the Shear Strength of Saturated Clays' ASCE,RCSSCS pp. 169-273

3.2 OTHER ISOTROPIC MODELS

3.2.1 Total Stress Models.

As we have mentioned in Chapter II Section 2.7, the total stress models are only useful for undrained loading of saturated soils, and they relate a total deviatoric stress increment $\underset{\sim}{\Delta s}$ with the corresponding deviatoric strain increment in the form:

$$\underset{\sim}{\Delta s} = \underset{\sim}{\subset}\, \underset{\sim}{\Delta e} \qquad \text{or:} \qquad \underset{\sim}{\Delta e} = \underset{\sim}{S}\, \underset{\sim}{\Delta s} \qquad (II-36)$$

3.2.1.1 Mises-Hencky Hardening Model.

Mises and Hencky (1) independently assumed the following form for the yield function (eq. II-24):

$$f \equiv q - H(\bar{\varepsilon}^p) = 0 \qquad (III-15)$$

and hence, the plastic incremental stress-strain relationships (eq. II-15) become:

$$d\varepsilon_{ij}^p = \alpha \left(\frac{3}{2q}\right)^2 s_{ij}\, s_{kl}\, ds_{kl} \qquad (III-16)$$

Evaluation of the hardening parameter α from the

---

(1) Hencky H. (1923) 'Uber einige statisch bestimmte Falle des Gleichwichts in plastichen Korpern' Z. Angew Math. Mech. Vol 3. pp 241-251.

consistency condition (see Appendix II), gives:

$$\alpha = \left(\frac{dH}{d\bar{\varepsilon}^p} \right)^{-1}$$

By including the elastic strain components, eq. III-16 rewrites:

$$de_{ij} = \frac{ds_{ij}}{2G} + \frac{1}{\left(\frac{dH}{d\bar{\varepsilon}^p}\right)} \left(\frac{3}{2q}\right)^2 s_{ij}\, s_{kl}\, ds_{kl} \qquad \text{(III-16a)}$$

which is the flexibility form of the incremental stress-strain relations.

Inverting eq. III-16a we get:

$$ds_{ij} = 2G \left\{ de_{ij} - \frac{2G}{3G + \frac{dH}{d\bar{\varepsilon}^p}} \left(\frac{3}{2q}\right)^2 s_{ij}\, s_{kl}\, de_{kl} \right\} \qquad \text{(III-17)}$$

which is the conjugate stiffness form of the incremental relations. Various forms of the hardening function $H(\bar{\varepsilon}^p)$ have been used in the literature. Hyperbolic relations, (1) or functional forms including softening (H decreases with increasing $\bar{\varepsilon}^p$ for large values of $\bar{\varepsilon}^p$) have been used (1).

3.2.1.2 Von Mises Perfectly Plastic Model

---

(1) Prevost J-H. and Hoeg K.(1975) 'Soil Mechanics and Plasticity Analysis of Strain Softening' Geotechnique 25,2 pp. 279-297

It can be obtained from the previous formulation by just setting H=0.

Then eq. III-17 rewrites:

$$ds_{ij} = 2G\left\{de_{ij} - \frac{3}{2q^2} s_{ij} s_{kl} de_{kl}\right\} \qquad (III-18)$$

which is the stiffness form of the incremental relations. Note that the stiffness matrix is singular. This is the case for ALL perfectly plastic models.

In fact there is no flexibility form as we can easily see from eq. III-16a because for H=0, the denominator vanishes.

3.2.2 Effective Stress Models.

3.2.2.1 Extended Von Mises Model. (1)

For an effective stress model, dependence on the 'p' stress invariant is necessary to model the behavior appropriately, since soils are pressure sensitive materials. Eq. III-15 generalizes in the following form:

$$f \equiv -Ap + q - H(\bar{\varepsilon}^p) = 0 \qquad (III-19)$$

where A>0.

Using the method described in Appendix I, (Eq. A-I-5, A-I-6 and A-I-7) the incremental stress-strain relations can be

---

(1) Drucker D.C. and Prager W. (1952) 'Soil Mechanics and Plastic Analysis of limit design' Q. Appl. Math. Vol 10 pp 157-165.

written in the form:

$$\begin{Bmatrix} d\varepsilon_v^p \\ d\bar{\varepsilon}^p \end{Bmatrix} = \frac{1}{\left(\frac{dH}{d\bar{\varepsilon}^p}\right)} \begin{bmatrix} A^2 & -A \\ -A & 1 \end{bmatrix} \begin{Bmatrix} dp \\ dq \end{Bmatrix} \qquad (III-20)$$

Eq. III-20 is similar to eq. A-II-7 which was derived for the Cam-Clay model. Consequently a procedure similar to the one described in Appendix II can be used to go from the invariant form of eq. III-20, to an incremental stress-strain relation in the principal space.

The major disadvantage of this model is that it predicts a dilatant behavior during shearing, (since A>0), as eq. III-20 shows. This contradicts experimental results from normally consolidated clays, (which contract during drained shear) and results from heavily overconsolidated clays which initially dilate but at large strains reach a condition where no further volume changes occur.

The Cam-Clay model is undoubtedly superior to the rest isotropic models and consequently it will be the only one evaluated by comparing its predictions with results of tests.

CHAPTER IV

EVALUATION OF PREDICTIONS OF THE CAM-CLAY MODEL

This chapter evaluates predictions of the Cam-Clay model by means of laboratory tests on resedimented samples of Boston Blue Clay. (1) (2) (3)

The following tests were simulated by using the Cam-Clay model.

[1] Consolidation Tests.

(1.1) Isotropic Consolidation

(1.2) K_o-Consolidation (no latteral strains are allowed)

---

(1) Ladd C.C and Varallyay J. (1966). 'The influence of stress system on the behavior of saturated clays during undrained shear'.Research in Earth Physics. Phase Report No.1, Part II, MIT Department of Civil Engineering, RR65-11.

(2) Kinner E.B and Ladd C.C (1970) 'Load deformation behavior of saturated clays during undrained shear'. Research in Earth Physics, Phase Report No.13, MIT Department of Civil Engineering,RR70-27.

(3) Ladd C.C, Bovee R.B, Edgers L., and Rixner J.J (1971) 'Consolidated Undrained Tests on Boston Blue Clay.' Research in Earth Physics, Phase Report No.15 MIT, Department of Civil Engineering RR71-13.

[2] Undrained Triaxial Tests

(2.1) Consolidated Isotropically Triaxial Compression (CIUC)

(2.2) Consolidated Isotropically Triaxial Extension (CIUE)

(2.3) K_o-Consolidated Triaxial Compression (CK_oUC)

(2.4) K_o-Consolidated Triaxial Extension (CK_oUE)

[3] Undrained Plane Strain Tests

(3.1) K_o-Consolidated Plane Strain Compression (CK_oUPSC)

(3.2) K_o-Consolidated Plane Strain Extension (CK_oUPSE)

(3.3) Pressuremeter type of loading (CK_oUPM)

1. INPUT PARAMETERS

For the isotropically consolidated tests the initial conditions were assumed to be:

$$\bar{\sigma}_c = 8.0 \text{ psi} \quad ; \quad e = 1.130$$

For the K_o-Consolidated tests the initial conditions were assumed to be:

$$\bar{\sigma}_{vo} = 10 \text{ psi} \quad ; \quad \bar{\sigma}_{ho} = 5.5 \text{ psi} \quad ; \quad e = 1.130$$

According to data from the previously mentioned reports, a value of: $C_c = 0.345$ (Consolidation Index from isotropic consolidation tests) was used, which corresponds to: $\lambda = 0.15$ since: (1)

$$\lambda = C_c \log_{10}(2.7183)$$

(1) 2.7183 is the base of the physical logarithms (number 'e').

A value for the Recompression Index of C_r=0.092 was also used which corresponds to k=0.04 .
Finally: M=1.20 was used which is equivalent to $\bar{\Phi}$=30° for the triaxial compression tests.

2. RESULTS

Fig IV-1 shows an s-t plot (1) for K_o-consolidation test (oedometer test). The straight line corresponds to K_o=0.55 (the starting value). Clearly K_o predicted by the model increases from K_o=0.55 to stabilize at K_o=0.662.
Fig IV-2 through IV-15 show results of various undrained modes of failure. The continuous line is the Cam-Clay model prediction. Open Circles represent results of experiments on resedimented samples of Boston Blue Clay.
Figures with even numbers show the stress-strain curves for the various modes of loading and these with odd numbers show the associated effective stress paths.
Generally Cam-Clay prediction curves are softer than the measured ones and the best predictions are for isotropically consolidated samples, sheared in a triaxial compression mode. On the other hand, strength predictions in extension tests are too high and for K_o-consolidated compression tests, the

---

(1)

$$s = \frac{\bar{\sigma}_1 + \bar{\sigma}_3}{2\bar{\sigma}_{vc}} \quad ; \quad t = \frac{\bar{\sigma}_1 - \bar{\sigma}_3}{2\bar{\sigma}_{vc}}$$

model fails to account for the pronounced strain softening of the clay.

Fig IV-14 and IV-15 give model predictions for the pressuremeter mode of loading. (1)

The Cam-Clay predicts the same value of undrained shear strength for all plane strain modes of loading. It also predicts a unique value of shear strength for the two, (TC and TE), K_o-consolidated Triaxial modes. As it was proved in Chapter III, the ratio of these two values of undrained shear strength is predicted equal to $2/\sqrt{3}=1.155$.

Finally the friction angle for all modes of failure, (except for triaxial compression where it was forced to be equal to 30° by selecting M=1.2) is much higher than 30°. However experimental results also show a wide range of values for the friction angle ranging from $\bar{\Phi}=24.7^\circ$ for CK_oUC, to $\bar{\Phi}=51.2^\circ$ for CK_oUE.

Fig IV-16 summarizes test data and Cam-Clay predictions. For the test data, values are given at both the peak and critical condition (i.e after strain softening). Cam-Clay does not show strain softening, and so only the value at the peak is given (the peak coincides with the critical condition).

---

(1) Plane strain pressuremeter type of loading involves plane strain in the vertical direction, with the radial stress increased till the critical state is reached. Major and minor principal stresses are the two horizontal stresses. No rotation of principal planes takes place.

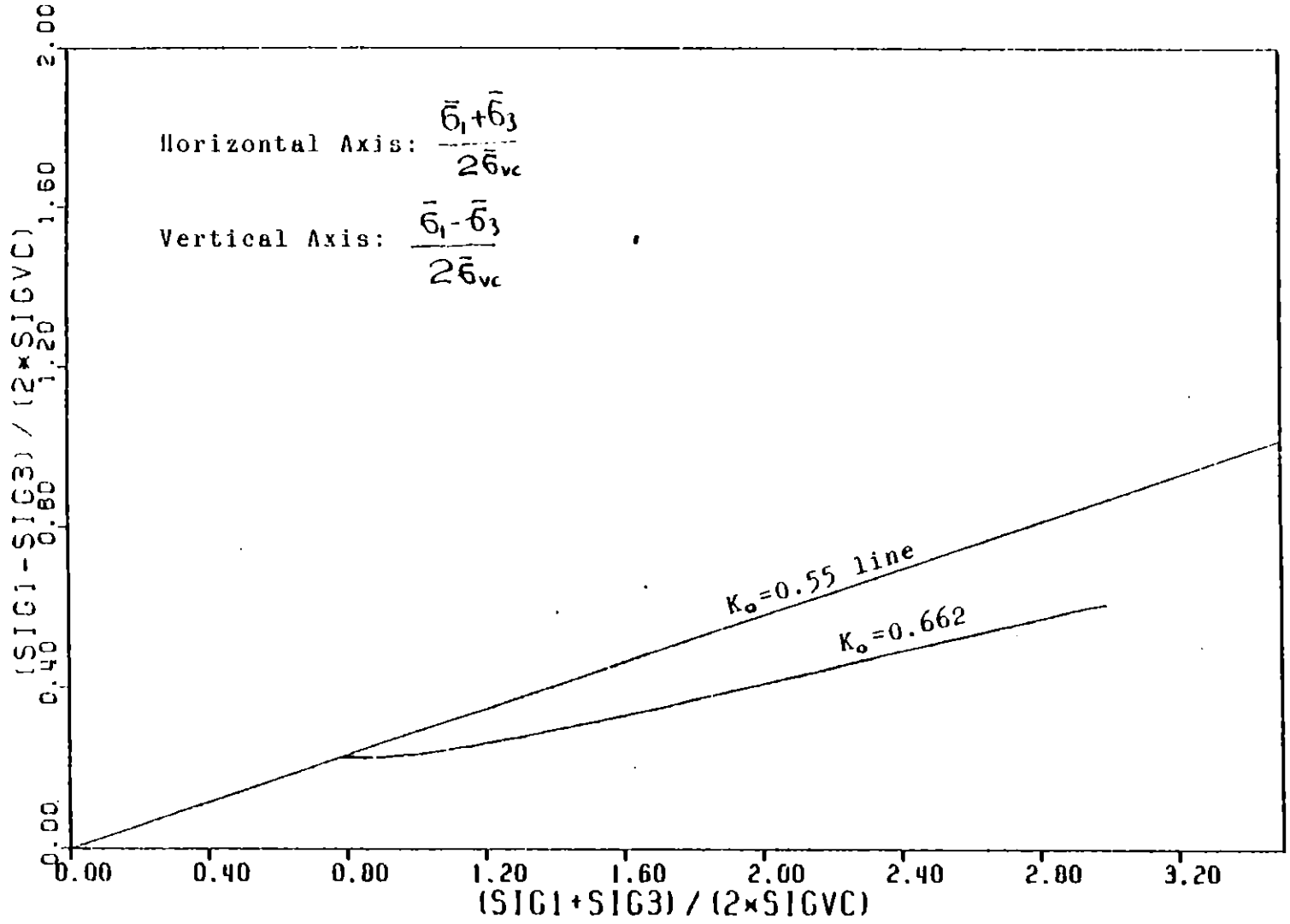
Horizontal Axis: $\frac{\bar{\sigma}_1+\bar{\sigma}_3}{2\bar{\sigma}_{vc}}$
Vertical Axis: $\frac{\bar{\sigma}_1-\bar{\sigma}_3}{2\bar{\sigma}_{vc}}$
K_o=0.55 line
K_o=0.662
(SIG1-SIG3) / (2×SIGVC)
(SIG1+SIG3) / (2×SIGVC)
0.00
0.40
0.80
1.20
1.60
2.00
2.40
2.80
3.20

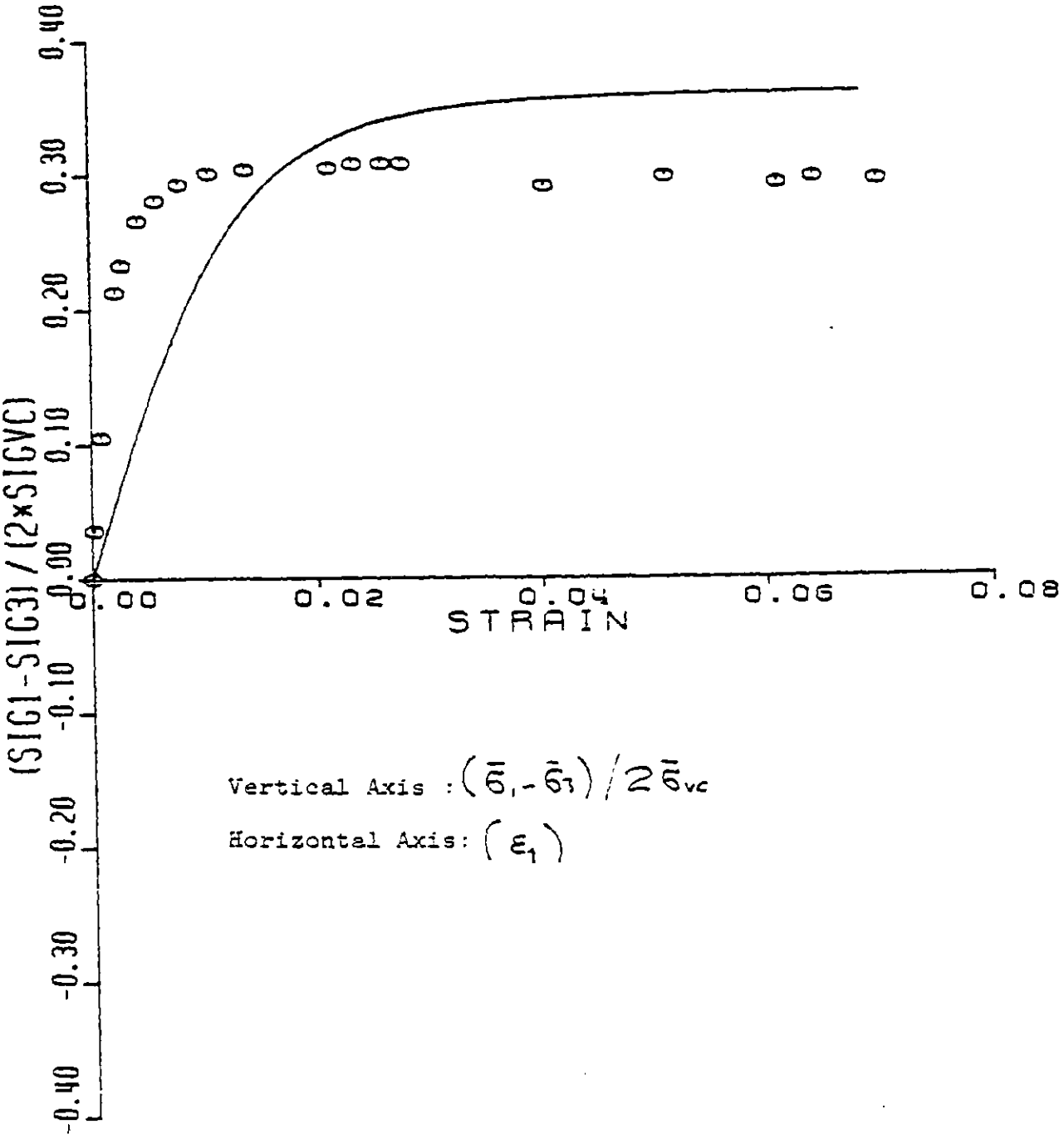

Fig IV-2 : Stress-Strain curve for Isotropically Consolidated Undrained Triaxial Compression (CIUC) test. Circles show experimental test results. Maximum shear strength = 0.361

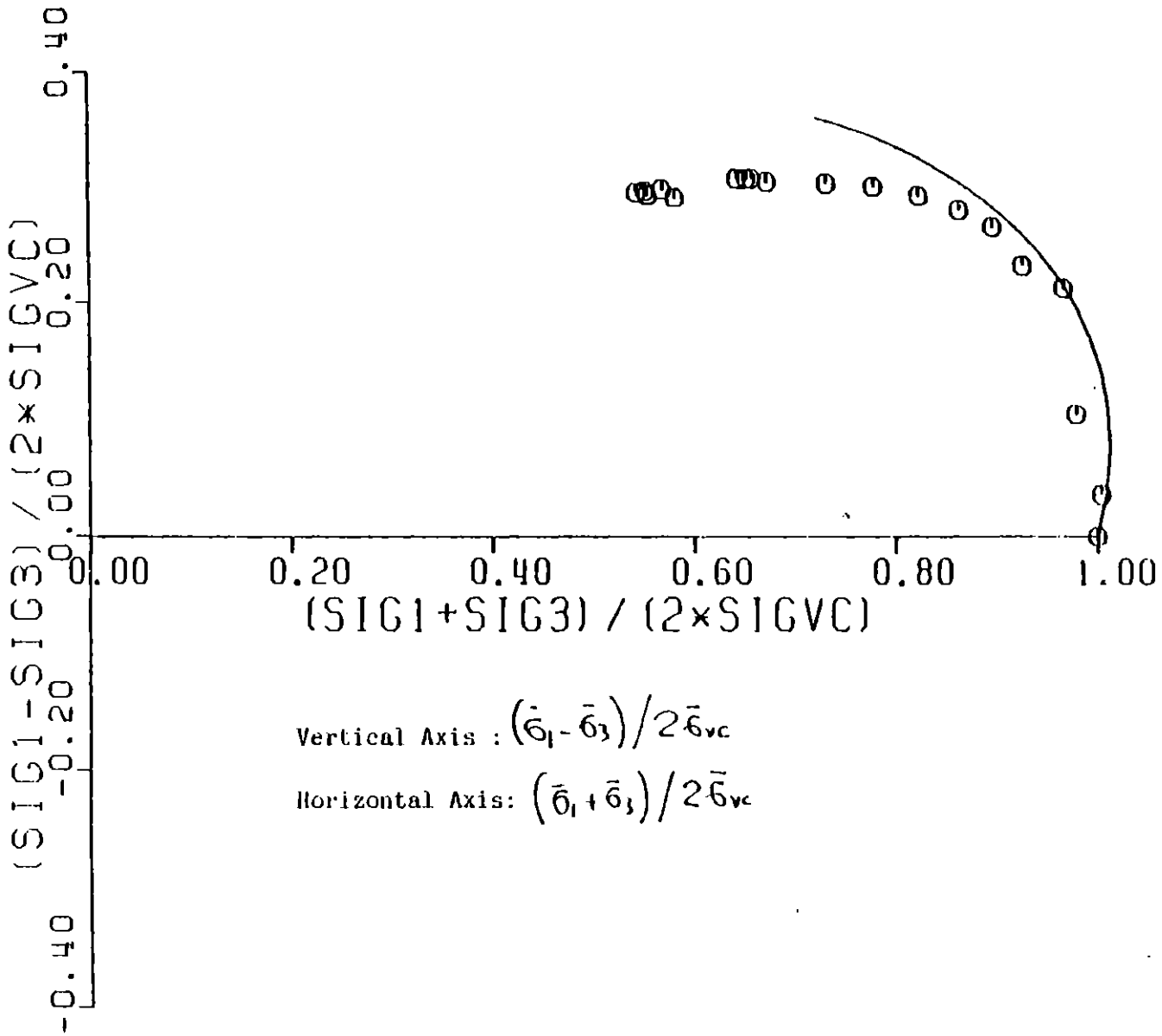

Fig. IV-3: s-t curve for Consolidated Isotropically Undrained Triaxial Compression (CIUC) test. Circles show experimental results.

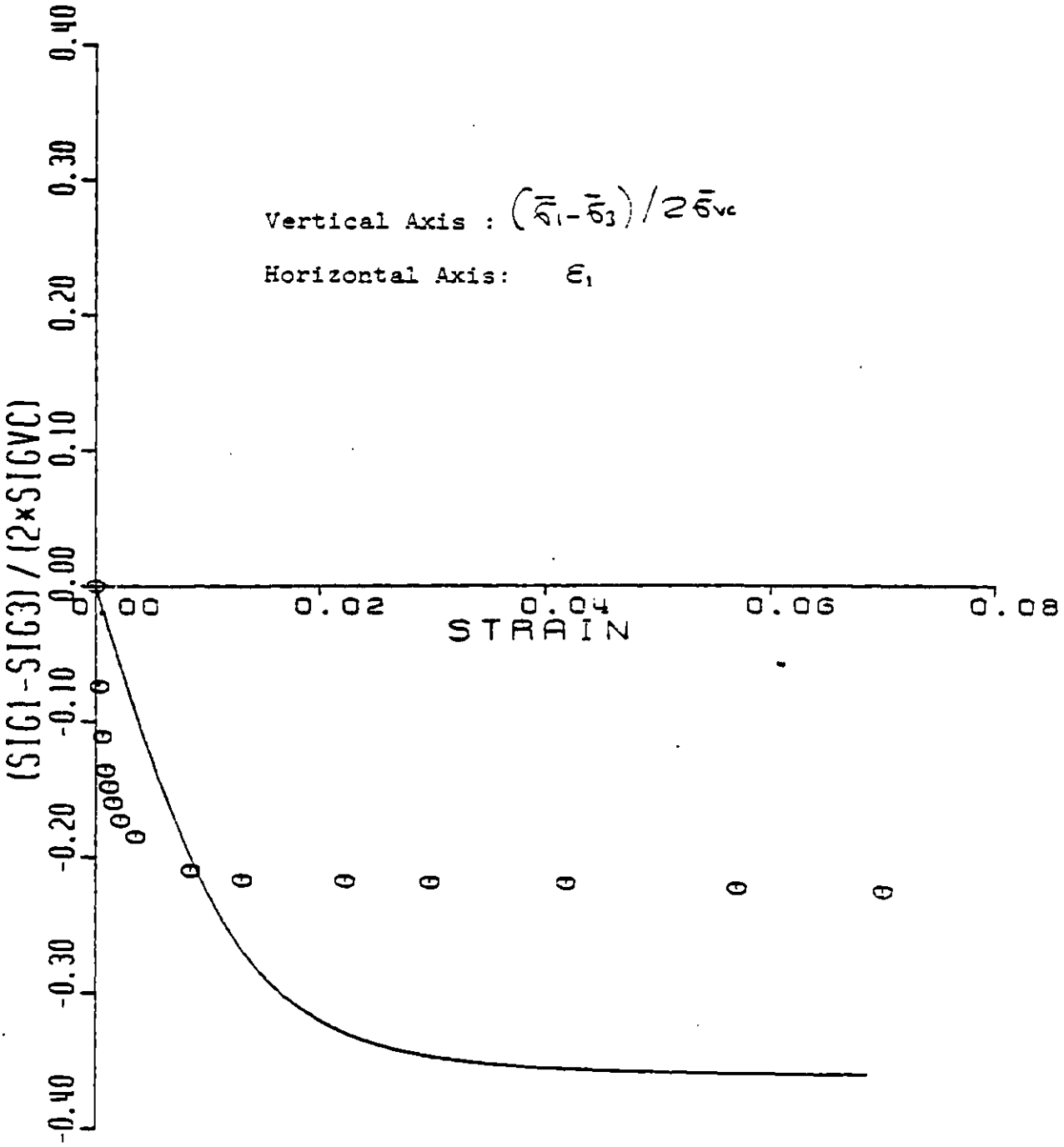

Fig. IV-4: Stress-Strain curve for Isotropically Consolidated Undrained Triaxial Extension test. Peak shear stregth =0.361 (Cam-Clay prediction). Circles show results of test.

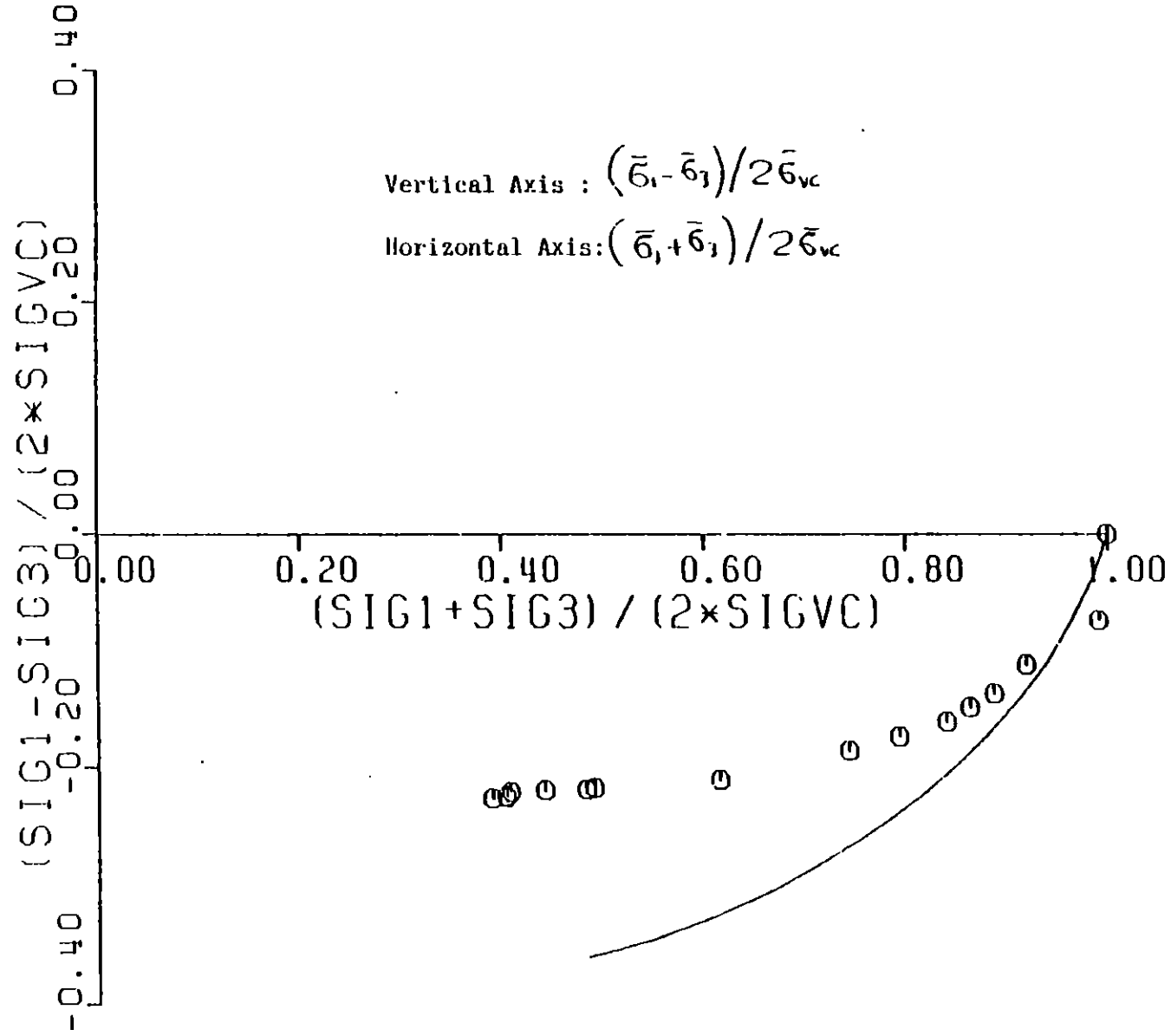

Fig. IV-5: s-t curve for Consolidated Isotropically Undrained Triaxial Extension Test (Cam-Clay prediction) Circles show experimental results.

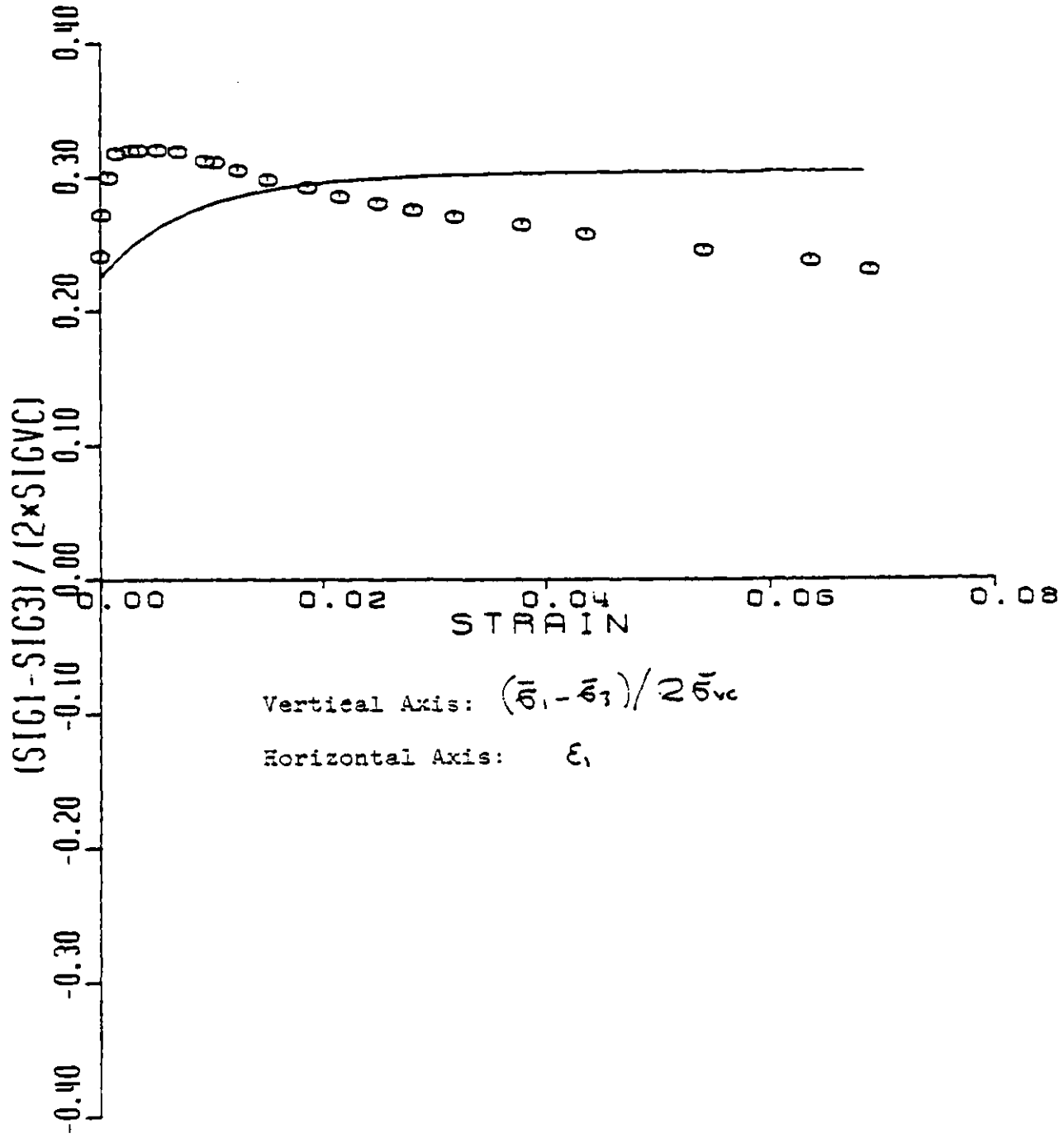

Fig. IV-6: Stress-Strain curve for K_o-Consolidated Undrained Triaxial Compression (Cam-Clay prediction). Peak strength= 0.304 Circles show experimental test results on BBC.

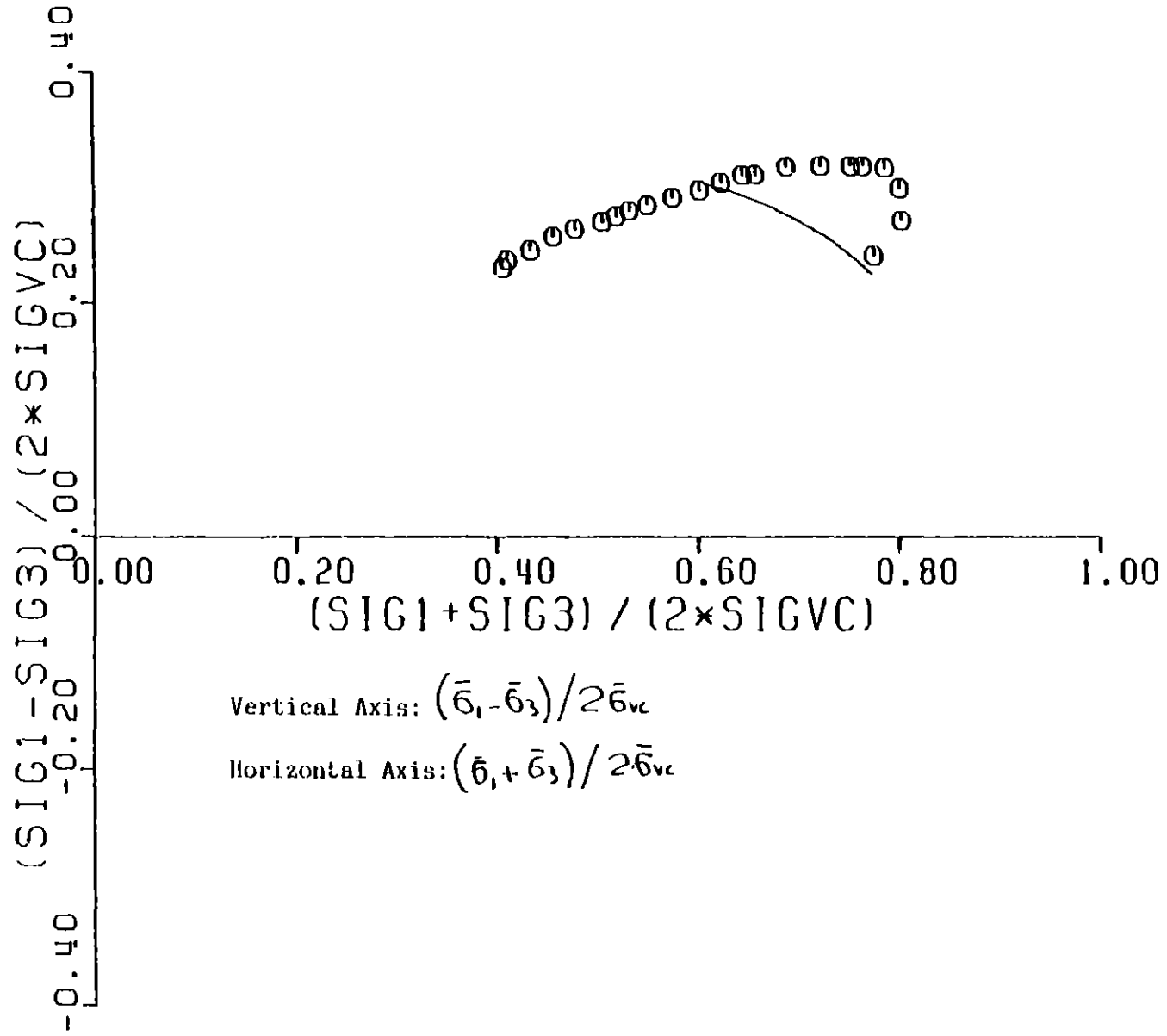

Fig. IV-7: s-t curve for K_o-Consolidated Undrained Triaxial Compression (CK_oUC) test (Cam-Clay prediction) Circles show experimental test results on BBC.

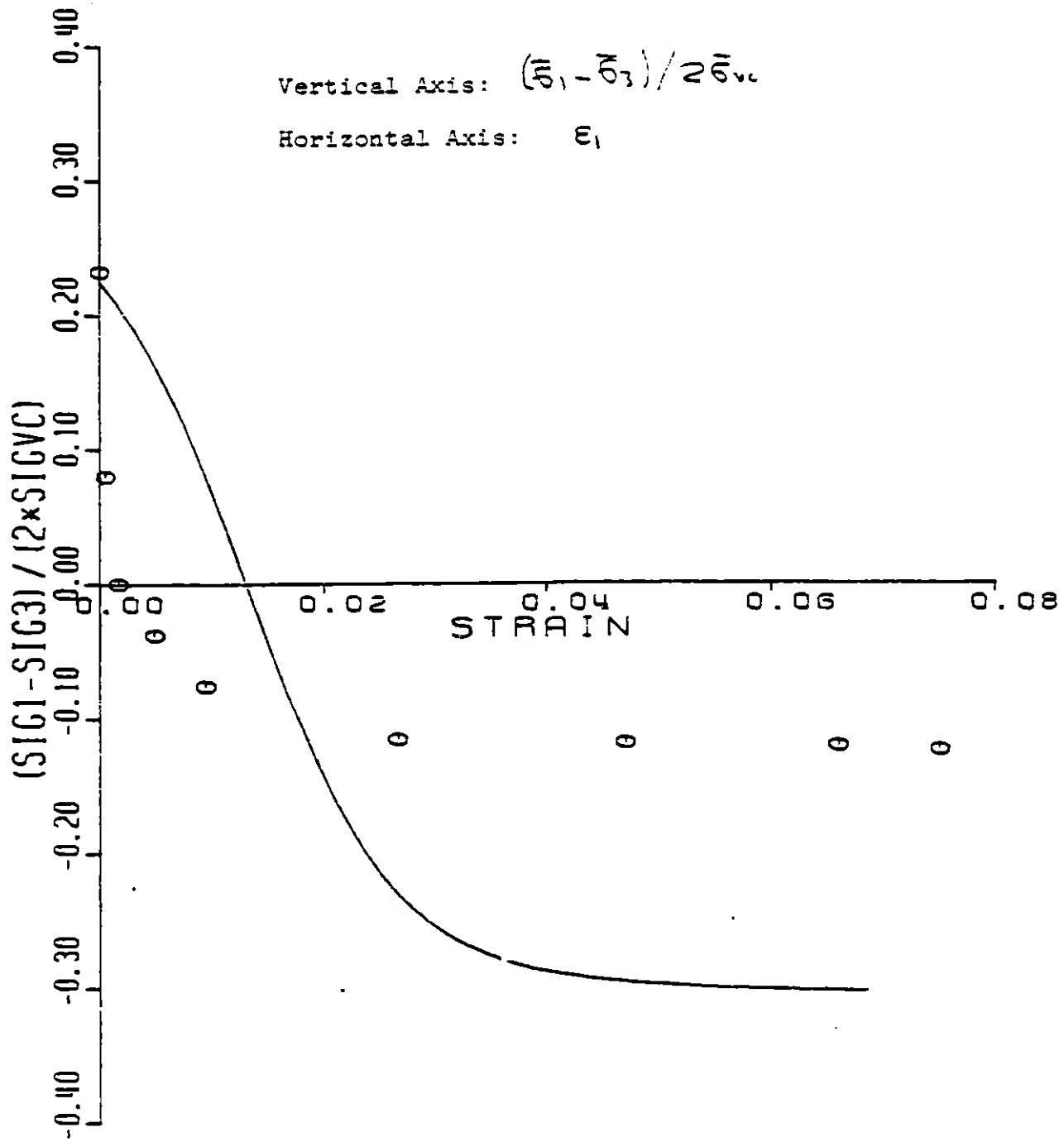

Fig IV-8: Stress-Strain Curve for K_o-consolidated Undrained Triaxial Extension test (CAM-CLAY prediction). Peak strength=0.303
Circles show experimental test results.

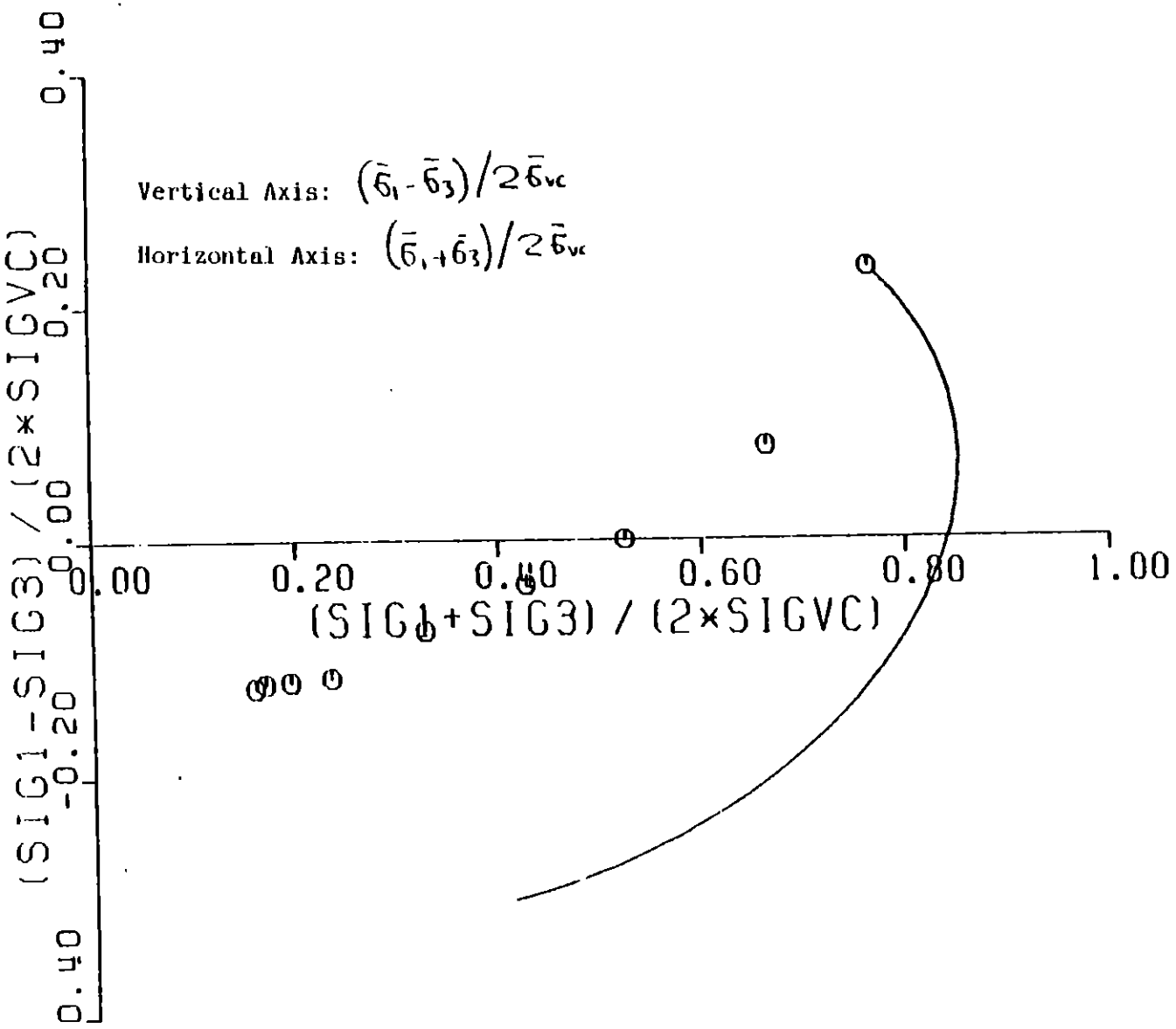

Fig. IV-9: s-t curve for K_o-consolidated Undrained Triaxial Extension test (Cam-Clay prediction). Circles show experimental test results.

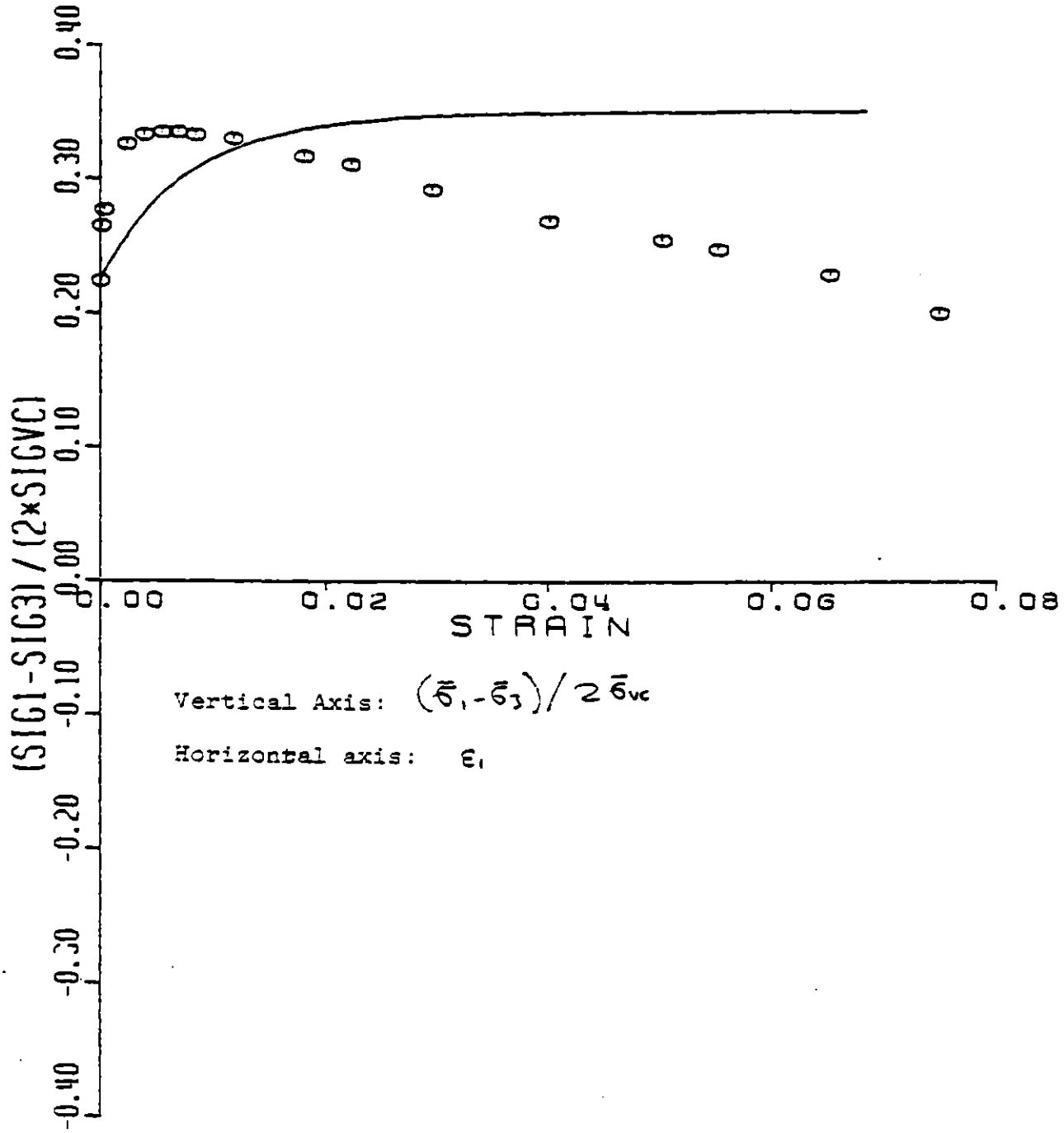

FIG. IV-10: Stress-Strain curve for K_o-consolidated Undrained Plane Strain test. Peak strength=0.351 (Cam-Clay prediction)
Circles show experimental test results.

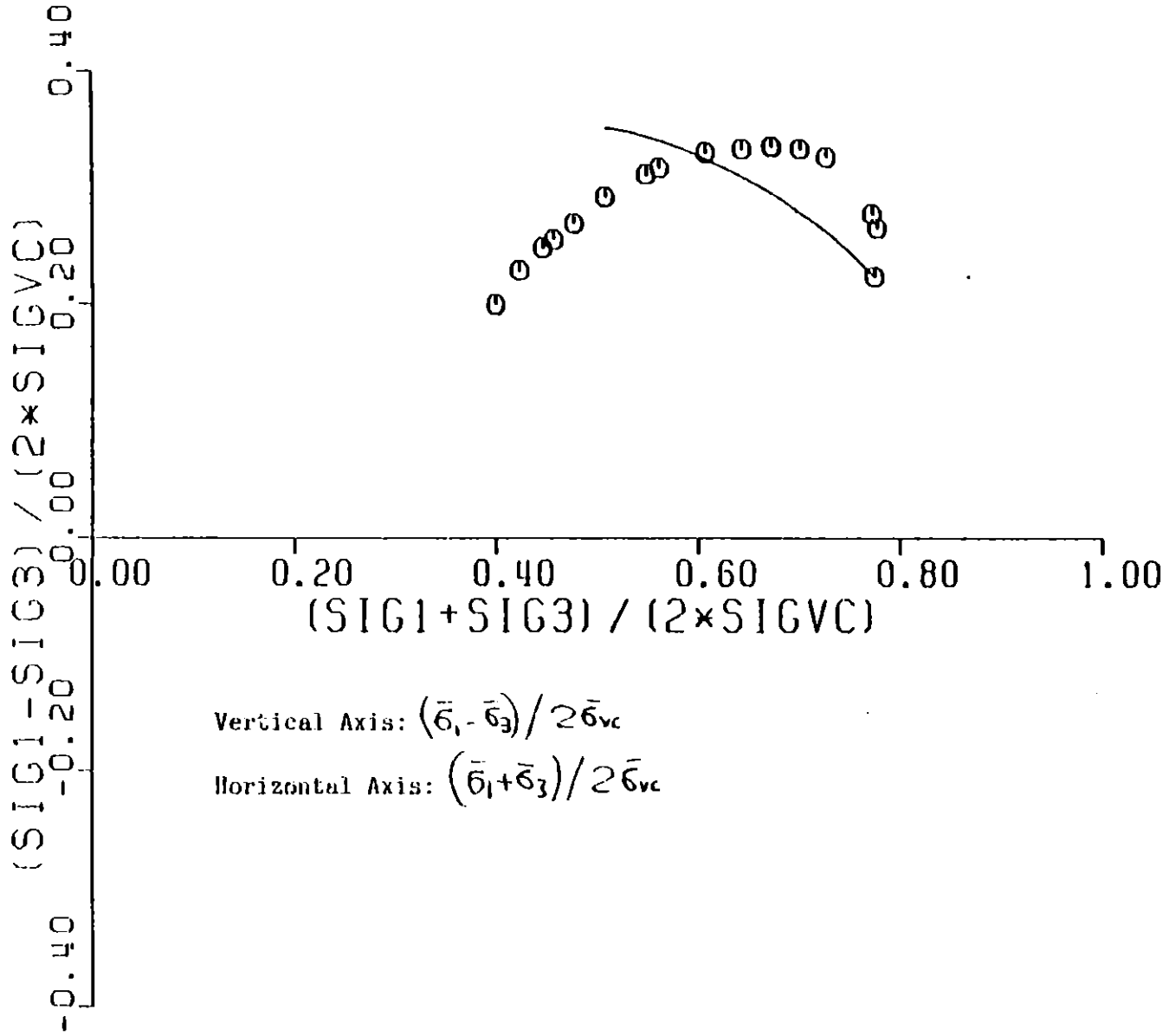

Fig. IV-11 : s-t curve for K_o-consolidated Undrained Plane strain Compression test.(Cam-Clay prediction)
Circles show experimental test results.

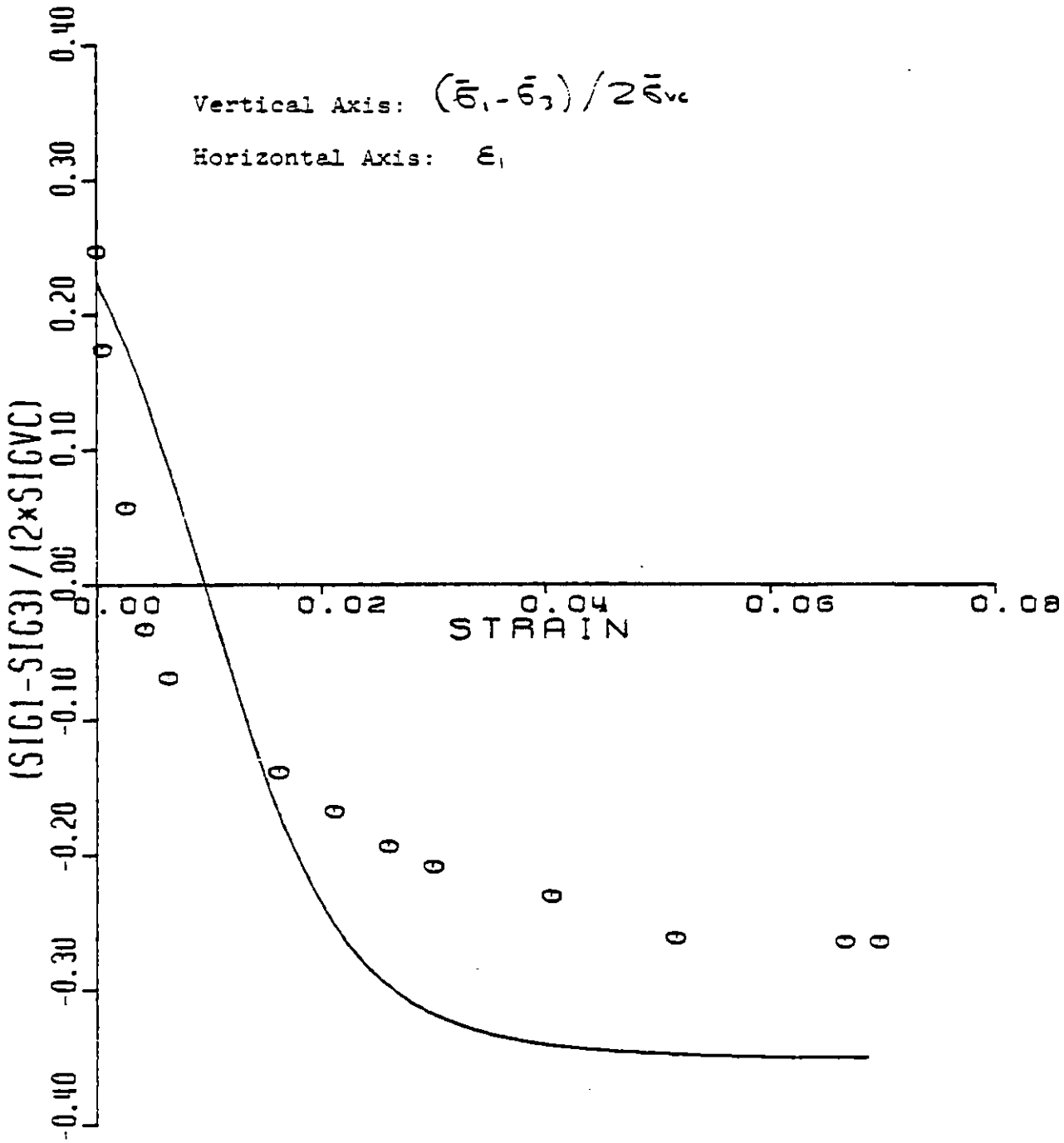

Fig. IV-12: Stress-Strain curve for K_o-consolidated Undrained Plane Strain Extension test. (Cam-Clay prediction). Peak strength=0.351 Circles show experimental test results on BBC.

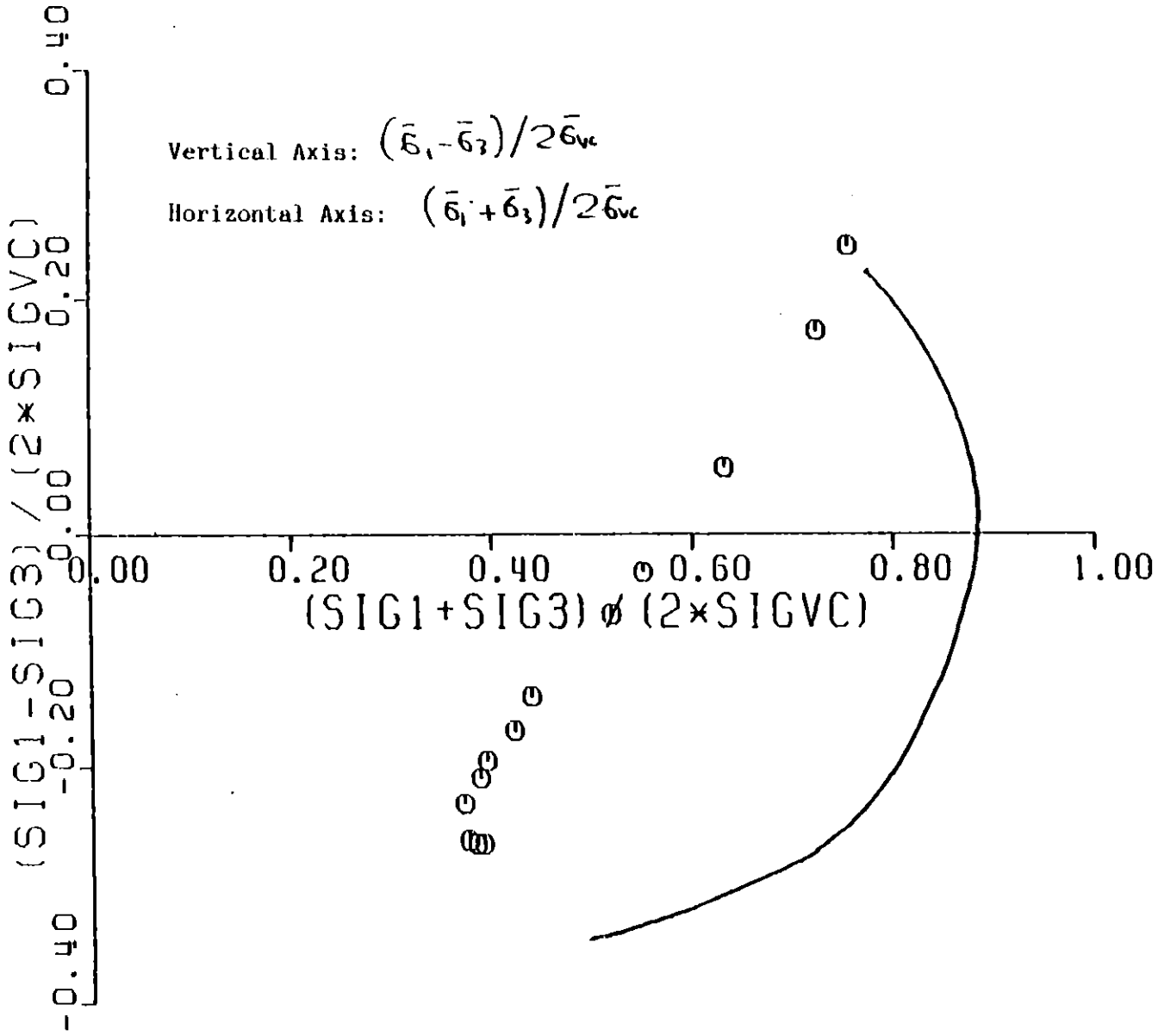

Fig. IV-13 : s-t curve for K_o-consolidated Undrained Plane Strain Extension test (Cam-Clay prediction) Circles show results of tests.

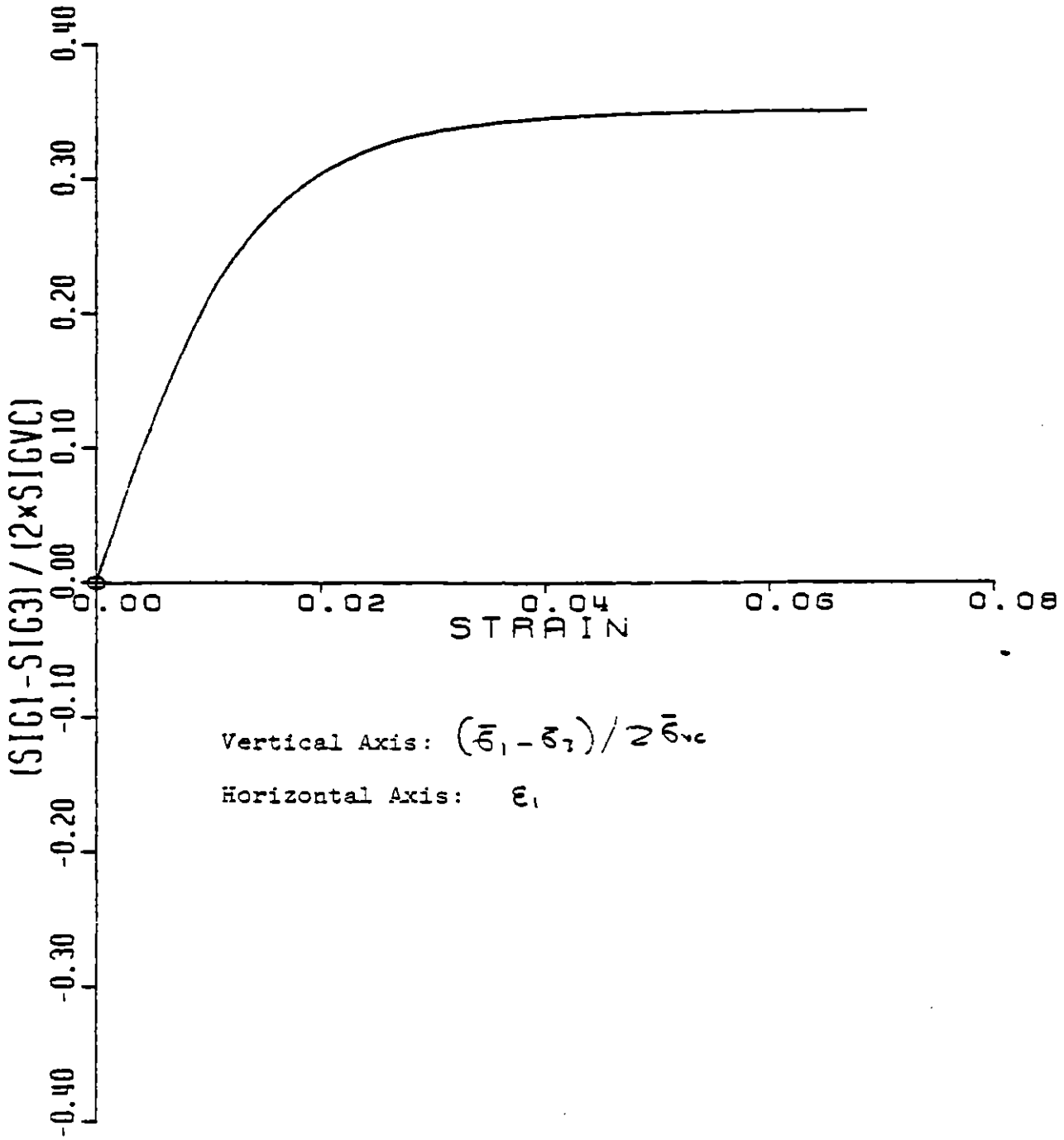

Fig. IV-14: Stress-Strain curve for K_o-consolidated Undrained Plane Strain Pressuremeter test (Cam-Clay prediction)
Peak Strength =0.351

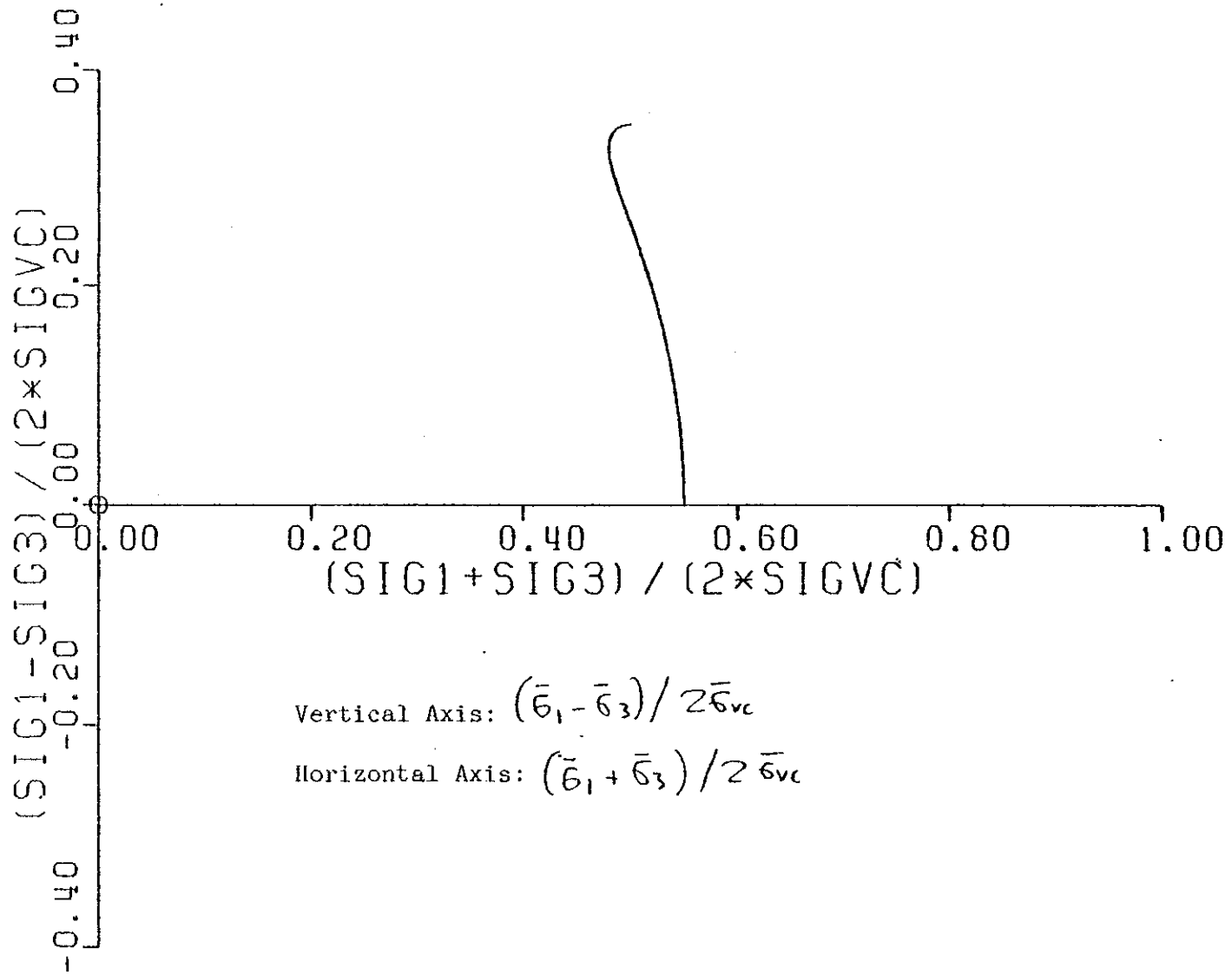

Fig. IV-15: s-t curve for K_o-consolidated Plane Strain Pressuremeter test (Cam-Clay prediction)

Loading Mode	TEST RESULTS: At peak condition $s_u/\bar{\sigma}_{vo}$	ε (%)	$\bar{\Phi}$	Ultimate condition $s_u/\bar{\sigma}_{vo}$	ε (%)	$\bar{\Phi}$	Cam-Clay simulation $s_u/\bar{\sigma}_{vo}$	ε (%)	$\bar{\Phi}$
CIUC	0.308	2.7	28.0	0.297	7.0	32.8	0.361	7.0	30.0
CIUE	-0.226	7.0	35.4	-0.226	7.0	35.4	-0.361	7.0	48.3
CK_oUC	0.320	0.3	24.7	0.230	7.0	34.4	0.304	7.0	30.0
CK_oUE	-0.124	7.0	51.2	-0.124	7.0	51.2	-0.303	7.0	48.3
CK_oUPSC	0.335	0.6	29.8	0.200	7.0	30.0	0.351	7.0	43.6
CK_oUPSE	-0.265	7.0	42.8	-0.265	7.0	42.8	-0.351	7.0	43.6
CK_oUPM	-	-	-	-	-	-	0.351	7.0	44.5

Fig. IV-16 : Data from experiments and comparisons with Cam-Clay predictions.

CHAPTER V

THE MROZ-PREVOST MODEL

The constitutive relations discussed so far, modelled the soil as an isotropic material. However since most soils occur in anisotropic conditions due to both the method of deposition and subsequent stressing, it seems that an anisotropic model would predict soil behavior more accurately.

Parameters useful in a quantitative estimate of the degree of anisotropy in a soil are:

(a) The latteral stress ratio under geostatic conditions, defined as:

$$K_o = \frac{\bar{\sigma}_h}{\bar{\sigma}_v}$$

It measures the stress induced anisotropy at the initial condition.

(b) The ratio of the undrained shear strengths in plane strain, i.e the undrained shear strengths measured in CK_oUPSC and CK_oUPSE modes of loading. This ratio is usually defined in the literature as:

$$K_s = \frac{S_u(PSC)}{S_u(PSE)}$$

It measures the combined effect of inherent and stress induced anisotropy.

Lean (i.e low Plasticity Index) Clays and/or highly precompressed (i.e with high Overconsolidation Ratio), are expected to exhibit less anisotropy and consequently an isotropic model can probably model their stress-strain behavior satisfactorily. For other clays an anisotropic model may be necessary.

The model to be discussed is a general mathematical model, based on the Theory of Incremental Plasticity and describes the anisotropic, elastoplastic, path-dependent stress-strain-strength properties of saturated inviscid (i.e time effects are neglected) clays under undrained conditions. The common assumption of incompressibility is made for undrained loading. The initial ideas of the model were stated by Iwan (1) and at the same time independently by Mroz (2) Prevost (3) (4) applied it in soils and studied the

---

(1) Iwan W.D(1967) 'On a Class of Models for the Yielding Behavior of Continuous and Composite Systems' Journal of Applied Mechanics Vol 34, pp 612-617

(2) Mroz Z.(1967) 'On the Description of Anisotropic Workhardening' Journal of the Mechanics and Physics of Solids. Vol 15 pp 163-175

(3)

mathematics of the incremental formulation for the loading conditions, common in Soil Engineering. The following presentation is based on the papers by Mroz and Prevost mentioned above.

The general formulation of a total stress model was studied in Chapter II and it was found that deviatoric stress increments have to be used in the formulation. The present model follows this principle. However a representation in a principal stress space (as it was done for Cam-Clay) is no longer possible. The model is anisotropic and consequently a full stress space representation has to be employed.
A modification of the Von Mises type Yield Function

$$f(\sigma_{ij}, \bar{\varepsilon}^p) \equiv \left\{ \frac{3}{2} s_{ij} s_{ij} \right\}^{1/2} - k(\bar{\varepsilon}^p) = 0$$

was used.
The Von Mises cylinder (represented by the previous equation) is isotropic with respect to rotations of the principal axes and centered at the origin. By removing the center of the cylinder from the origin, anisotropy is introduced.
A second order symmetric tensor a_{ij} was introduced to

Prevost J-H(1977) 'Mathematical Modeling of Monotonic and Cyclic Undrained Clay Behavior' International Journal for Numerical and Analytical Methods in Geomechanics. Vol 1,no 2, pp 195-216

(4) Prevost J-H. (1978) 'Anisotropic Undrained Stress-Strain Behavior of Clays'. JGED, ASCE Vol 104, No GT8 pp 1075-1090.

describe the coordinates of the center of the yield surface. Then the yield surface takes the form:

$$f(\sigma_{ij}, \bar{\varepsilon}^p) \equiv \left\{ \frac{3}{2} (s_{ij} - a_{ij})(s_{ij} - a_{ij}) \right\}^{1/2} - k(\bar{\varepsilon}^p) = 0 \; ; \; (V\text{-}1)$$

Since a_{ij} is not necessarily proportional to the isotropic δ_{ij} tensor (Kronecker delta), the material exhibits anisotropy (kinematic hardening).

The k parameter on the other hand, is a measure of the size of the yield surface, as it was used in the previous Chapters, and it is a function of the plastic strain increments. (Isotropic hardening)

If the physical coordinate axes x,y,z coincide with the principal axes of the material anisotropy, then

$$a_{xy} = a_{yz} = a_{zx} = 0$$

Due to the way of deposition, clays usually exhibit rotational anisotropy about the vertical axis (y), (i.e transverse isotropy in the horizontal plane) before shearing. This means that initially:

$$a_{xy} = a_{yz} = a_{zx} = 0 \qquad \text{and} \qquad a_x = a_z$$

However the original anisotropy of the soil is not preserved during subsequent shearing. If the principal axes of stress rotate during shearing, the principal axes of anisotropy will also rotate (1) and hence a_{ij} will no longer

---

(1)

be zero for $i \neq j$. This means that further stress induced anisotropy takes place.

In addition, due to the anisotropy caused by plastic flow, the strain tensor does not remain coaxial with the stress tensor (i.e their principal directions do not coincide), and the structure of the clay is altered. This means that application of shear stresses tends to erase the clay's memory of its previous history (1) and create a new state of anisotropy.

The concept of a field of plastic moduli is introduced to increase the flexibility of the model by increasing the number of its parameters. This field is defined in the deviatoric stress space, by a set $f_1, f_2, \ldots f_p$ of nested yield surfaces with respective sizes

$$k^{(1)} < k^{(2)} < \ldots < k^{(p)}$$

which delimit the regions of constant plastic moduli. (2) Each of the yield surfaces is represented by an equation of the form of eq. V-1:

$$f_m(\sigma_{ij}, \bar{\varepsilon}^p) \equiv \left\{ \frac{3}{2} (s_{ij} - a_{ij}^{(m)})(s_{ij} - a_{ij}^{(m)}) \right\}^{1/2} - k^{(m)}(\bar{\varepsilon}^p) = 0$$

Since $da_{ij} \neq 0$ as it is shown in Appendix IV.

(1) Expressed mainly through the parameters a_{ij} and k.

(2) Usually there is a finite number of yield surfaces and the resulting stress strain relations of the model are piecewise linear. If a continuous field is used then a non-linear behavior will result.

for m=1,2,...p

A shear modulus H'_m is associated with each of the yield surfaces and the associative flow rule (i.e normality rule with an associated potential function) is used to compute the plastic strain increments. Note that since the model only studies undrained loading, only deviatoric plastic flow occurs.

The outermost yield surface f_p plays the role of a failure surface, and it is the geometrical boundary in the stress space outside which the stress point and the inner yield surfaces cannot go. At any stage in the loading history of the material, stress points inside this yield surface represent stress states that can always be reached along stable paths. (1)

The Hardening rule which was used by Mroz and later by Prevost, specifies that the yield surfaces may be translated in the stress space by the stress point, without changing in form or orientation and they consecutively touch and push each other without intersecting. When the stress point reaches the yield surface f_m, all the prior yield surfaces $f_o, f_1, \ldots f_{m-1}$ have been translated and they are tangent to each other and to f_m at the contact point M as it is shown in fig V-1.

Complete specification of the model parameters requires

---

(1) i.e H'_m is allowed to be less or equal to zero only on the outermost yield surface f_p.

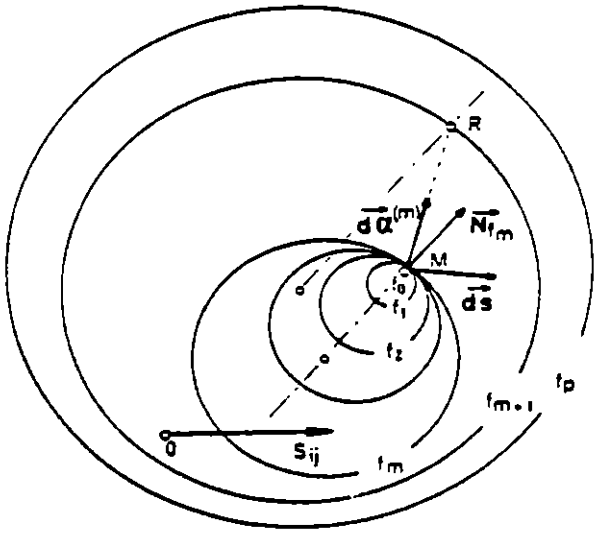

Fig V-1 : Nested yield surfaces

the determination of (1) the initial positions and sizes of the yield surfaces and their associated shear moduli and (2) The law which defines how the sizes of the yield surfaces change during plastic flow.

Appendix IV discusses the method of determination of the initial locations of the yield surfaces and the incremental stress-strain relations.

Model parameters can be evaluated by using solely the results from triaxial compression and extension tests. A computer program was written that automatically generates these parameters if data points from triaxial tests are given. The CK_oUC and CK_oUE test data presented in Chapter IV were used to evaluate the model parameters. In order to smooth the test results a hyperbolic function was fitted and

was subsequently used to locate the initial positions of the yield surfaces and the initial Hardening moduli. The program created 14 yield surfaces, which means that 71 parameters need to be saved and updated during shearing. Compared with the number of parameters of the Cam-Clay Model, the Mroz-Prevost model requires a lot more storage.

Fig V-1 and V-2 show the stress-strain curves for CK_oUC and CK_oUE tests backfigured by using input parameters from the same tests. As it is expected the predictions (continuous line) fits the data points (discrete dots) exactly.

Fig V-3 and V-4 show the predictions for CK_oU(PSC) and CK_oU(PSE) tests and data points from the tests described in Chapter IV. The model predictions are generally stiffer than the test data. In Plane strain compression it overpredicts the undrained peak shear strength by 8 per cent (0.355 versus 0.335 of the test) but in Plane strain extension it underpredicts by about 40 per cent (0.157 versus 0.265 of the test) Finally Fig V-5 gives the stress-strain curve for the pressuremeter mode of loading.

The values of the peak undrained shear strength:

$$S_u = \frac{\sigma_1 - \sigma_3}{2}$$

predicted by the model for the various modes of failure, depend only on the initial location and size of the outermost yield surface and can be predicted in closed form expressions.

Due to initial rotational anisotropy in the Horizontal plane

the outermost yield surface is centered on the S1 axis (i.e $a_2^{(p)}=a_3^{(p)}=0$). If $a_1^{(p)}$ and $k^{(p)}$ are the initial location and size of this surface, then using eq. V-1 and the kinematic restrictions of each mode of loading, it can be shown that:

$$S_u(TC) = \frac{1}{2}\left\{ a_1^{(p)} + k^{(p)} \right\}$$

$$S_u(TE) = \frac{1}{2}\left\{ a_1^{(p)} - k^{(p)} \right\}$$

$$S_u(PSC) = \frac{1}{2}\left\{ a_1^{(p)} + \frac{2}{\sqrt{3}} k^{(p)} \right\}$$

$$S_u(PSE) = \frac{1}{2}\left\{ a_1^{(p)} - \frac{2}{\sqrt{3}} k^{(p)} \right\}$$

$$\frac{S_u(TC)}{S_u(TE)} = \frac{a_1^{(p)} + k^{(p)}}{a_1^{(p)} - k^{(p)}}$$

The ratio of the peak undrained shear strength for PSC and TC is:

$$\frac{S_u(PSC)}{S_u(TC)} = \frac{a_1^{(p)} + \frac{2}{\sqrt{3}} k^{(p)}}{a_1^{(p)} + k^{(p)}}$$

If the material is initially isotropic, then the yield surfaces are initially centered at the origin; hence $a_1^{(p)}=0$ and the last expression reduces to:

$$\frac{S_u(PSC)}{S_u(TC)} = \frac{2}{\sqrt{3}}$$

Note that the same value of this ratio is predicted by

the Cam-Clay model as it was discussed in Chapter III. This is because both models use normality rule and for initially isotropic behavior the yield surfaces of the Mroz-Prevost model depend only on the second stress invariant J_2.

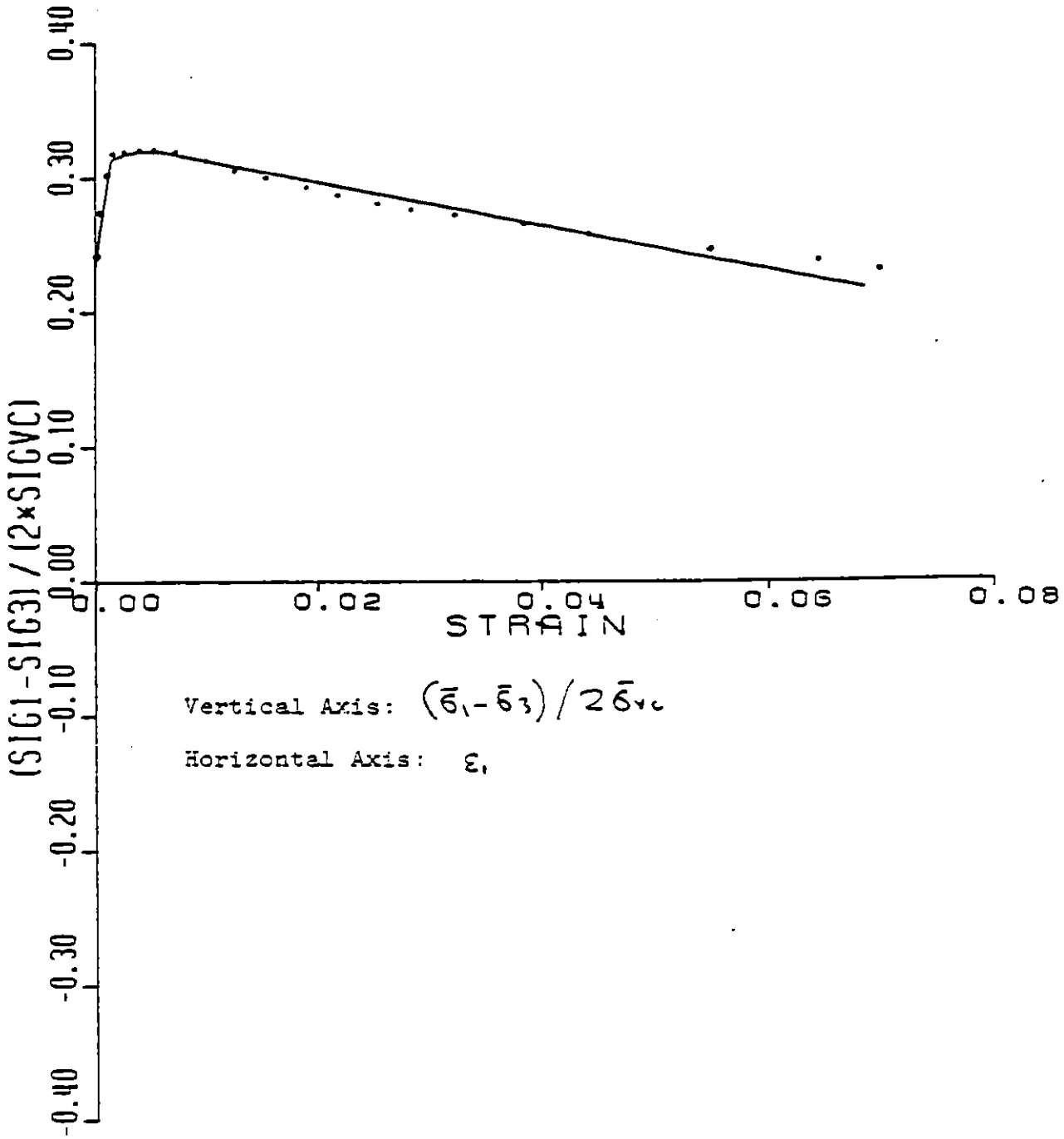

Fig. V-1: Stress-Strain curve for K_o-consolidated Undrained Triaxial Compression (Mroz-Prevost model prediction)
Peak strength =0.317 Dots show experimental test results

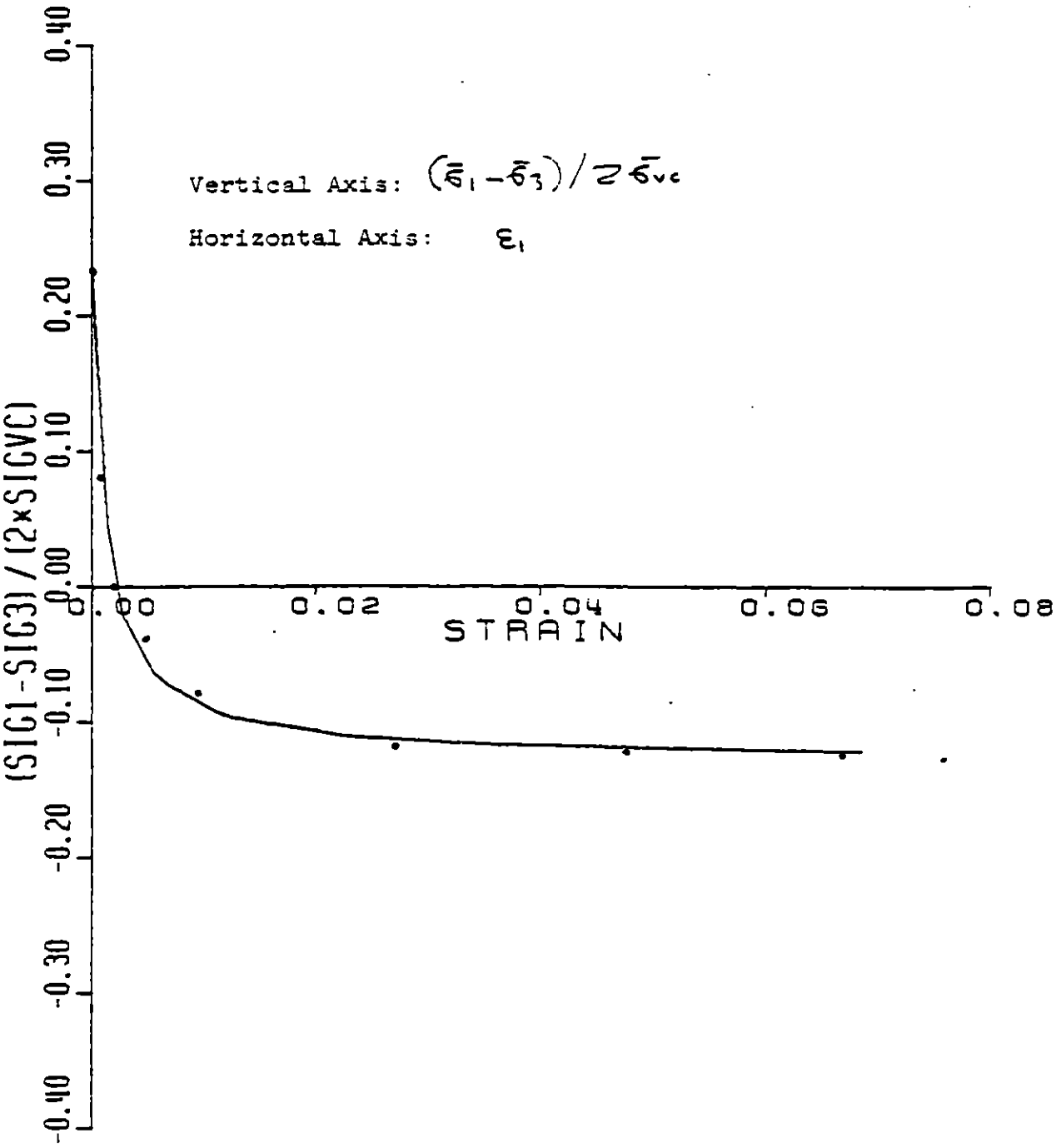

Fig. V-2: Stress-Strain curve for K_o-consolidated Undrained Triaxial Extension test (Mroz-Prevost model prediction)
Peak strength=0.140 Circles show experimental test results.

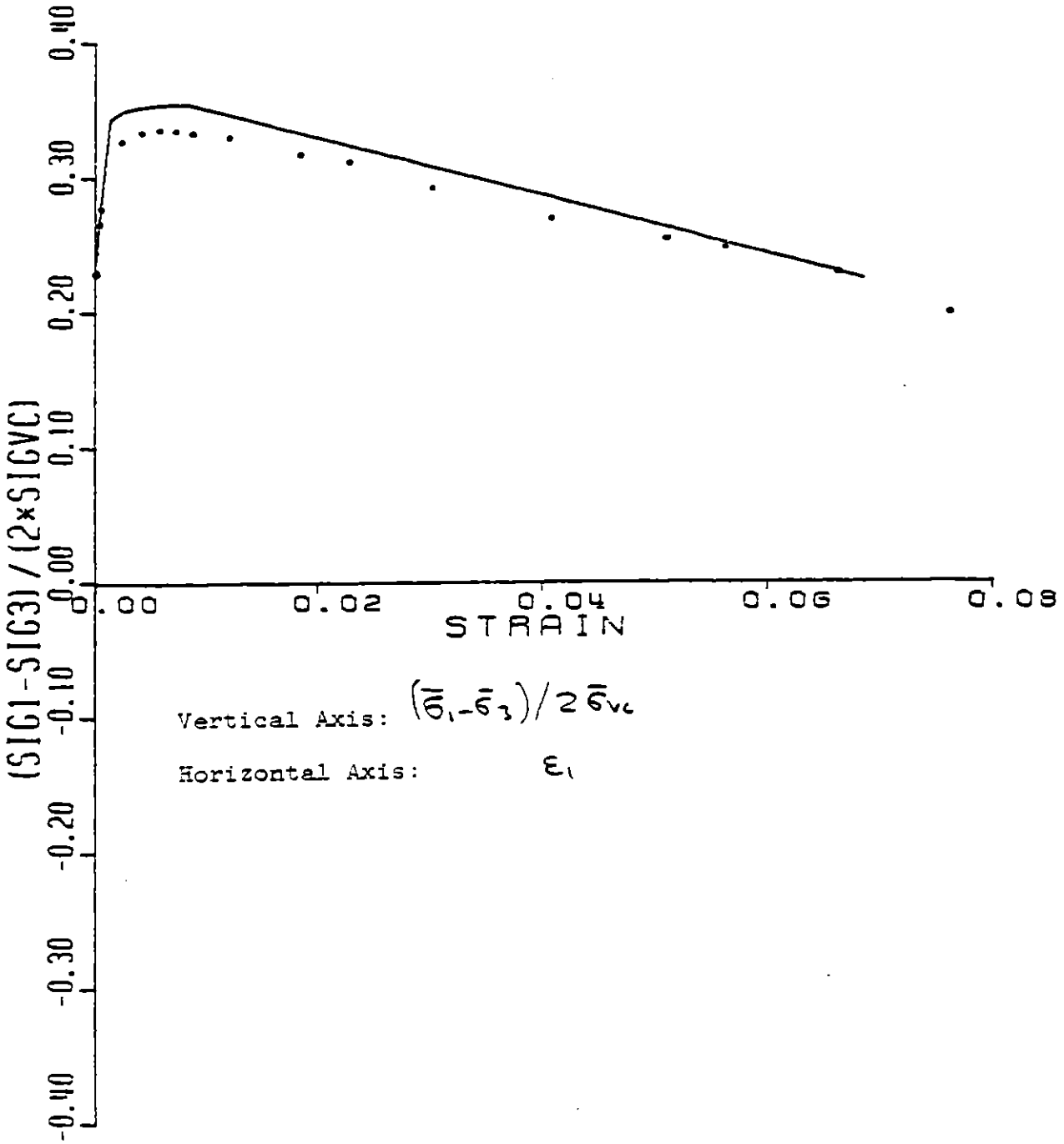

Vertical Axis: $(\bar{\sigma}_1 - \bar{\sigma}_3)/2\bar{\sigma}_{vc}$

Horizontal Axis: ε_1

Fig. V-3: Stress-Strain Curve for K_o-consolidated Undrained Plane Strain Compression Test (Mroz-Prevost model Prediction. Peak strength=0.355 Dots show experimental test results.

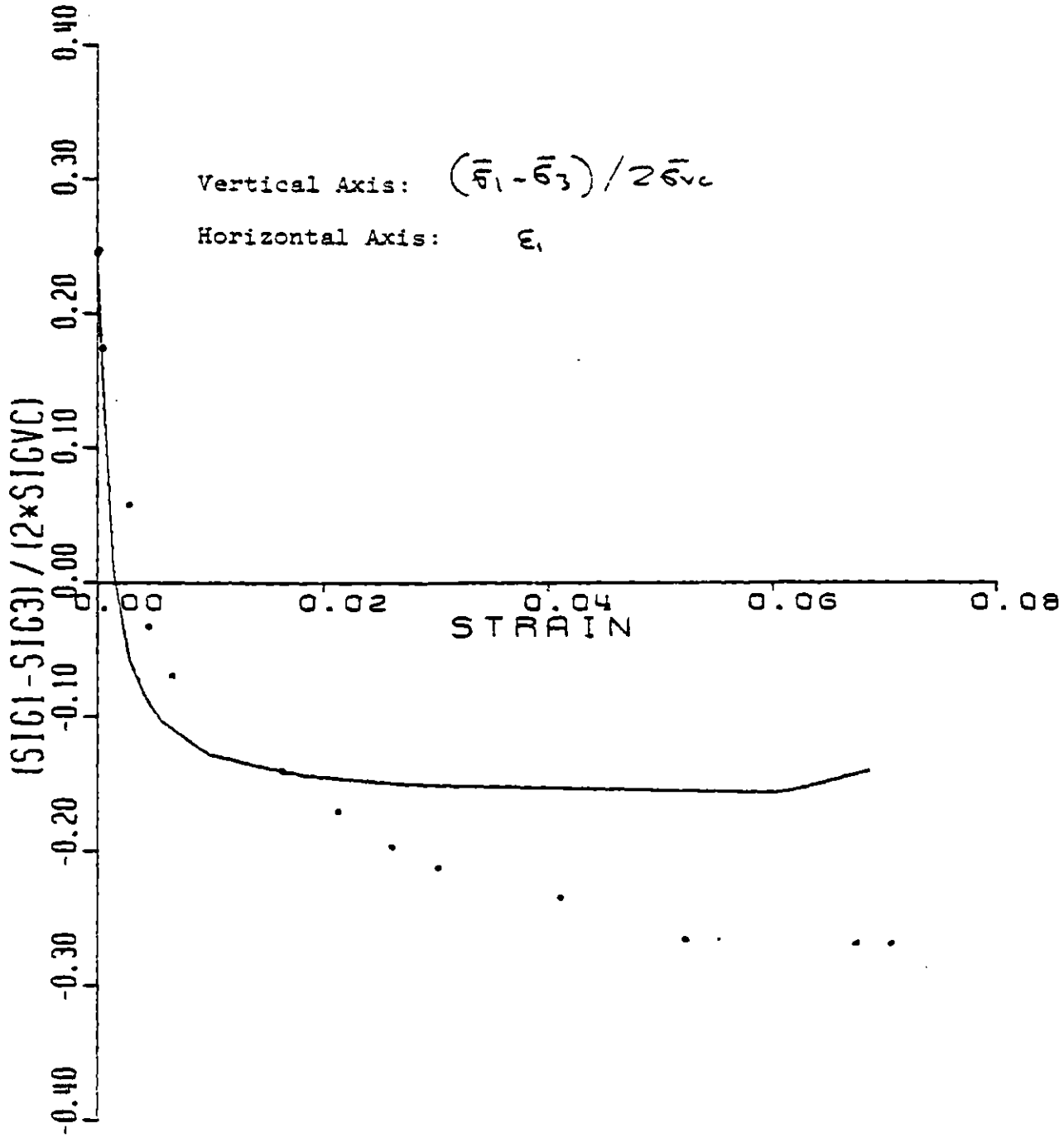

Fig. V-4: Stress-Strain curve for K_o-consolidated Plane Strain Extension test. (Mroz-Prevost model prediction).
Peak strength=0.157 Dots show results of tests on BBC.

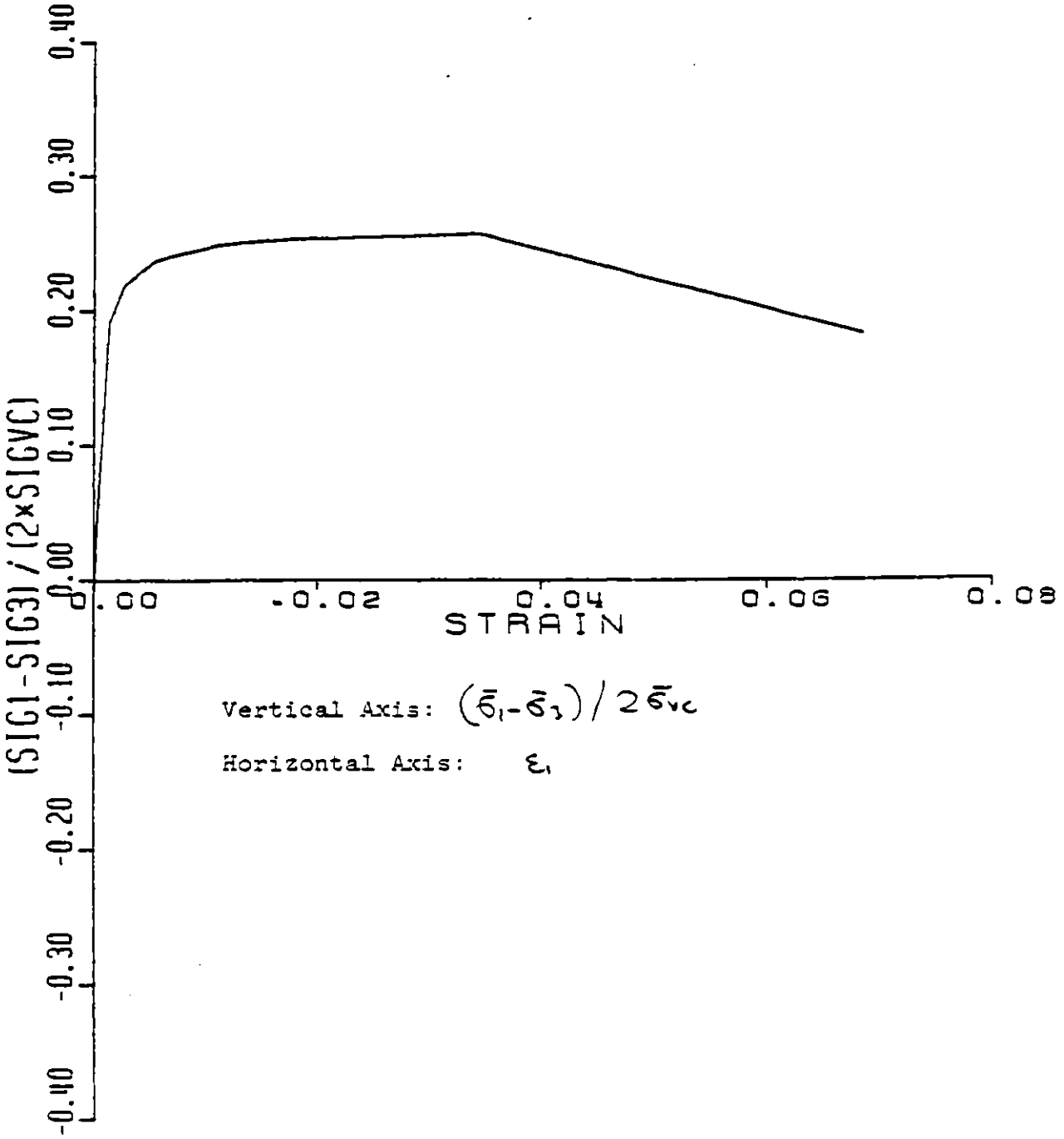

Fig. V-5: Stress-Strain curve for K_o-consolidated Undrained Pressuremeter test. Peak strength =0.26

CHAPTER VI

MODELLING OF THE UNDRAINED EXPANSION OF A CYLINDRICAL CAVITY

The undrained expansion of a long cylindrical cavity is a problem which can be easily analysed even for non-linear soil constitutive law. It has been used to model the in-situ pressuremeter test and the installation of a cylindrical pile into the ground.

In the case of modelling the pressuremeter test there are two major deviations from the in-situ conditions:

(a) The pressuremeter probe is not infinetely long, (it usually has an aspect ratio equal to 2).

(b) During the installation of the probe, stresses are relaxed (i.e some initial unloading takes place).

In the case of the pile driving, there are shear stresses along the pile shaft which are neglected in the analysis.

Due to kinematic constraints, the strains are independent of the material law. In fact loading is axisymmetric around the z-axis, and in plane strain in the z-direction. In addition the no volume change condition, (undrained loading)

allows the calculation of the displacement field around the cavity, as a function of the size of the hole, and the r-coordinate at any point.

Previous analyses of the expansion of a cylindrical cavity have been developed for the interpretation of the pressuremeter test by Gibson et al, Ladanyi, Baguelin et al, Palmer et al, and Randolph et al.

In the following, the total and effective stress changes around an expanding cylindrical cavity are studied for the case of a non-linear material law.

Two soil models are applied:

(a) The Mroz-Prevost Model (see Chapter V)

(b) The Cam-Clay Model (see Chapter III and IV)

The Mroz-Prevost Model, which is a total stress model, does not allow the estimation of the effective stresses and pore water pressures around the cavity. On the other hand, the Cam-Clay model will be used to estimate the total and effective stresses as well as the pore pressures .

The stress-strain curves used are those calculated in the previous Chapters for the pressuremeter mode of failure (Fig. IV-14 for the Cam-Clay and Fig. V-5 for the Mroz-Prevost).

The predicted values of the normalized shear strength are:

0.351 from the Cam-Clay.

0.258 from the Mroz-Prevost.

Note also that although the Cam-Clay does not show strain softening, the Mroz-Prevost strain-softens for strains larger than about 3.5%.

During expansion of the cavity, large strains develop especially in the immediate vicinity of the cavity. For this reason, large strain theory is used in this analysis.

Distribution of stresses and strains along the radial direction were calculated for four values of the expansion ratio $\Delta V/V_o$. (1) The curves in the subsequent figures, corresponding to these ratios, are labeled [1],[2],[3],[4] as shown in Table VI-1.

TABLE VI-1

Label	V/V (%)
[1]	4
[2]	10
[3]	40
[4]	100

Fig. VI-1 through VI-4 were produced by using the Mroz-Prevost Model. The radial coordinate in all figures is normalized with the initial radius of the hole.

Fig VI-1 shows the radial strain plotted versus the normalized radial coordinate, for the four values of the expansion ratio. Note that radial strains equal to 42.5% develop at the hole boundary for the largest expansion ratio.

Fig VI-2 shows the normalized shear stress $(\sigma_r - \sigma_\theta)/\bar{\sigma}_{vc}$, plotted versus the normalized radial coordinate. Even for the

(1) The expansion ratio is defined as the volume change due to the expansion divided by the initial volume.

smallest expansion ratio of 4.0%, the peak strength is reached at the cavity boundary and for the larger expansion ratios, the yielded zone extends quite significantly.

Fig. VI-3 shows the normalized radial stress $\sigma_r/\bar{\sigma}_{vc}$ plotted versus the normalized radial coordinate. Although the strain softening zone around the hole is quite extended, the radial stress at the cavity boundary continues to increase with increasing expansion ratio $\Delta V/V_o$. This is because the radial stress at the cavity boundary is not affected only by the local values of the shear stress $(\sigma_r-\sigma_\theta)/\bar{\sigma}_{vc}$, but it is a result of an integration of the shear stress from infinity to the boundary of the hole. (1) The same effect is also shown in Fig. VI-4 where the normalized radial stress at the boundary is plotted against the expansion ratios. The curve is monotonically increasing. It starts from an ordinate value of 0.55 (equal to K_o) for $\Delta V/V_o = 0.0$ and reaches an ultimate value of normalized boundary pressure equal to 1.734. This is the type of curve measured in the pressuremeter test.

Fig. VI-5 through VI-8 were produced by using the Cam-Clay model.

Fig VI-5 shows the shear stress $(\sigma_r-\sigma_\theta)/\bar{\sigma}_{vc}$ vs the normalized radial coordinate r/a_o . Since the Cam-Clay model does not strain soften, the curves are monotonically

---

(1) From equilibrium: $\frac{d\sigma_r}{dr} = -\frac{\sigma_r-\sigma_\theta}{r}$

increasing till the critical condition (reached for $(\sigma_r - \sigma_\theta)/\bar{\sigma}_{vc} = 0.702$)

Fig VI-6 shows the normalized total radial stress $\sigma_r/\bar{\sigma}_{vc}$ vs the normalized radial coordinate.

Fig VI-7 shows the normalized radial stress at the cavity boundary $(\sigma_r)_{r=r_0}/\bar{\sigma}_{vc}$ plotted vs the expansion ratio. The curve is again monotonically increasing and it approaches roughly the same limit pressure as the Mroz-Prevost curve, but it is much softer.

Finally Fig VI-8 shows the distribution of the pore pressure increment $\Delta u/\bar{\sigma}_{vc}$ vs r/a_0 . Table VI-2 shows the value of the normalized excess pore presures at the cavity boundary, for the 4 values of the expansion ratio.

TABLE VI-2

Label	$\Delta V/V_0$ (%)	$(\Delta u/\bar{\sigma}_{vc})_{r=r_0}$
[1]	4	0.168
[2]	10	0.402
[3]	40	0.776
[4]	100	0.973

An elastic perfectly plastic model gives the following relation for the pore pressure increment during an undrained expansion of a cylindrical cavity:

$$\frac{\Delta u}{\bar{\sigma}_{vc}} = \frac{s_u}{\bar{\sigma}_{vc}} \ln\left(\frac{G}{s_u}\right)$$

For tha Cam-Clay $s_u/\bar{\sigma}_{vc} = 0.351$

Also the following relation was used for the Cam-Clay prediction:

$$\frac{G}{K^e} = \frac{3(1-2\bar{\nu})}{2(1+\bar{\nu})} \quad ; \qquad \bar{\nu} = 0.35$$

and since

$$K^e = \frac{(1+e)}{k} p$$

we have:

$$\frac{G}{S_u} = \frac{3(1-2\bar{\nu})}{2(1+\bar{\nu})} \cdot \frac{(1+e)\left(\frac{1+2k_o}{3}\right)}{k \frac{S_u}{\bar{\sigma}_{vc}}} =$$

$$= 0.333 \times \frac{2.16 \times 0.70}{0.15 \times 0.351} \approx 10.0$$

So:

$$\frac{\Delta u}{\bar{\sigma}_{vc}} = 0.351 \times \ln(10.0) = 0.8$$

Comparing with the previous Table, this corresponds to an expansion ratio of about 50%.

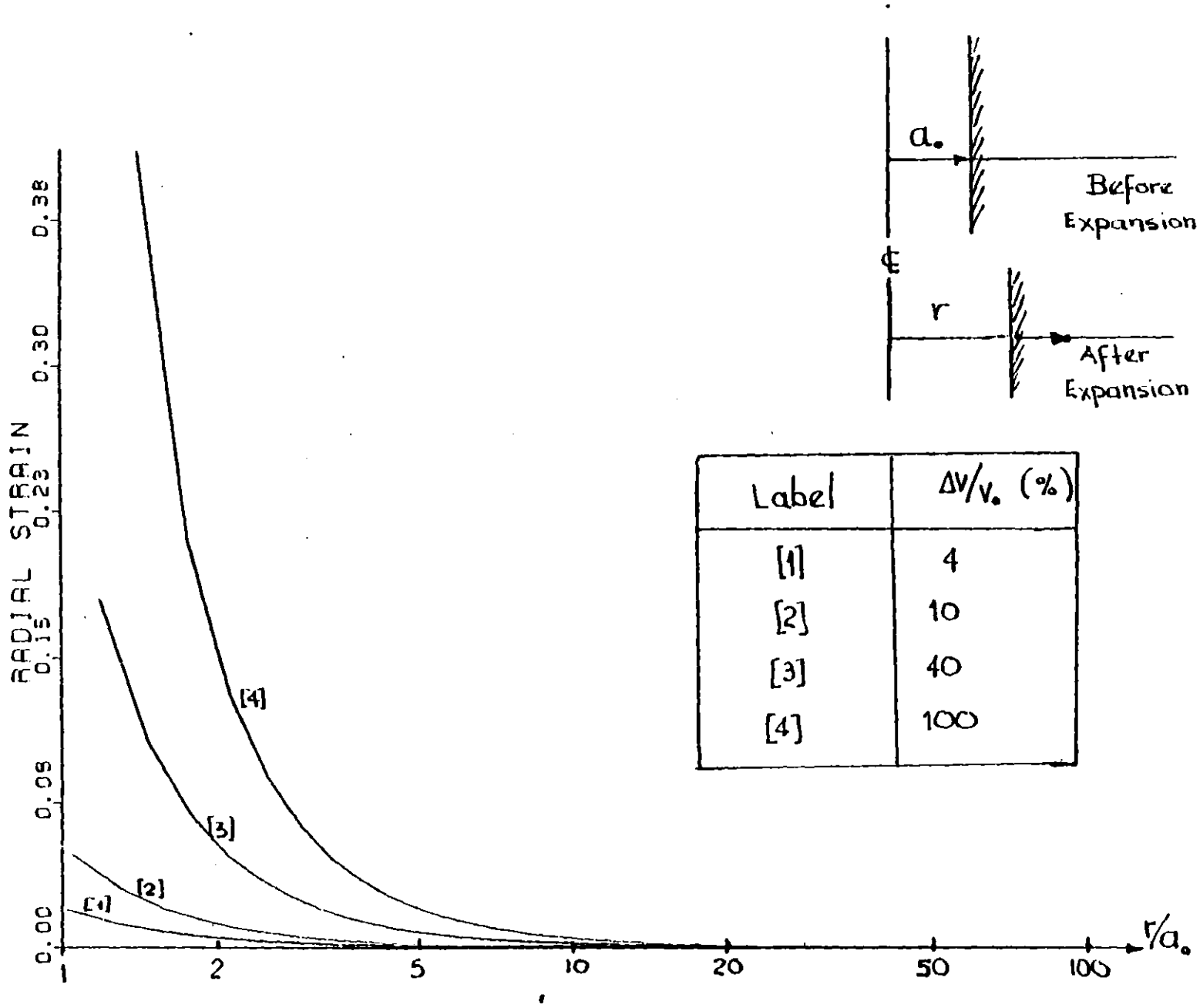

Label	$\Delta V/V_o$ (%)
[1]	4
[2]	10
[3]	40
[4]	100

Fig. VI-1: Radial Strain vs radial coordinate during the undrained expansion of a cylindrical cavity.

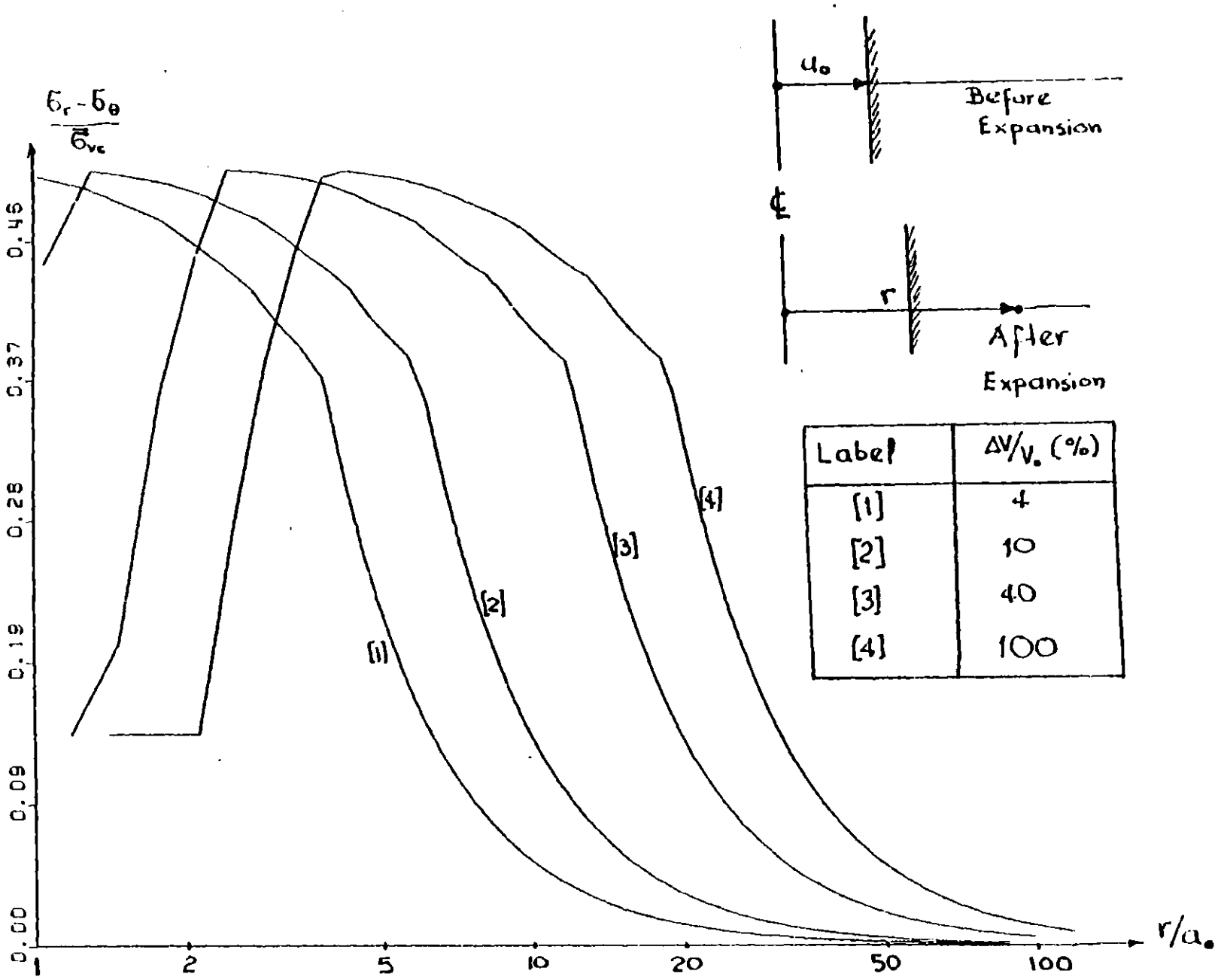

Fig. VI-2: Normalized shear stress versus radial coordinate during the undrained expansion of a cylindrical cavity (Mroz-Prevost model prediction)

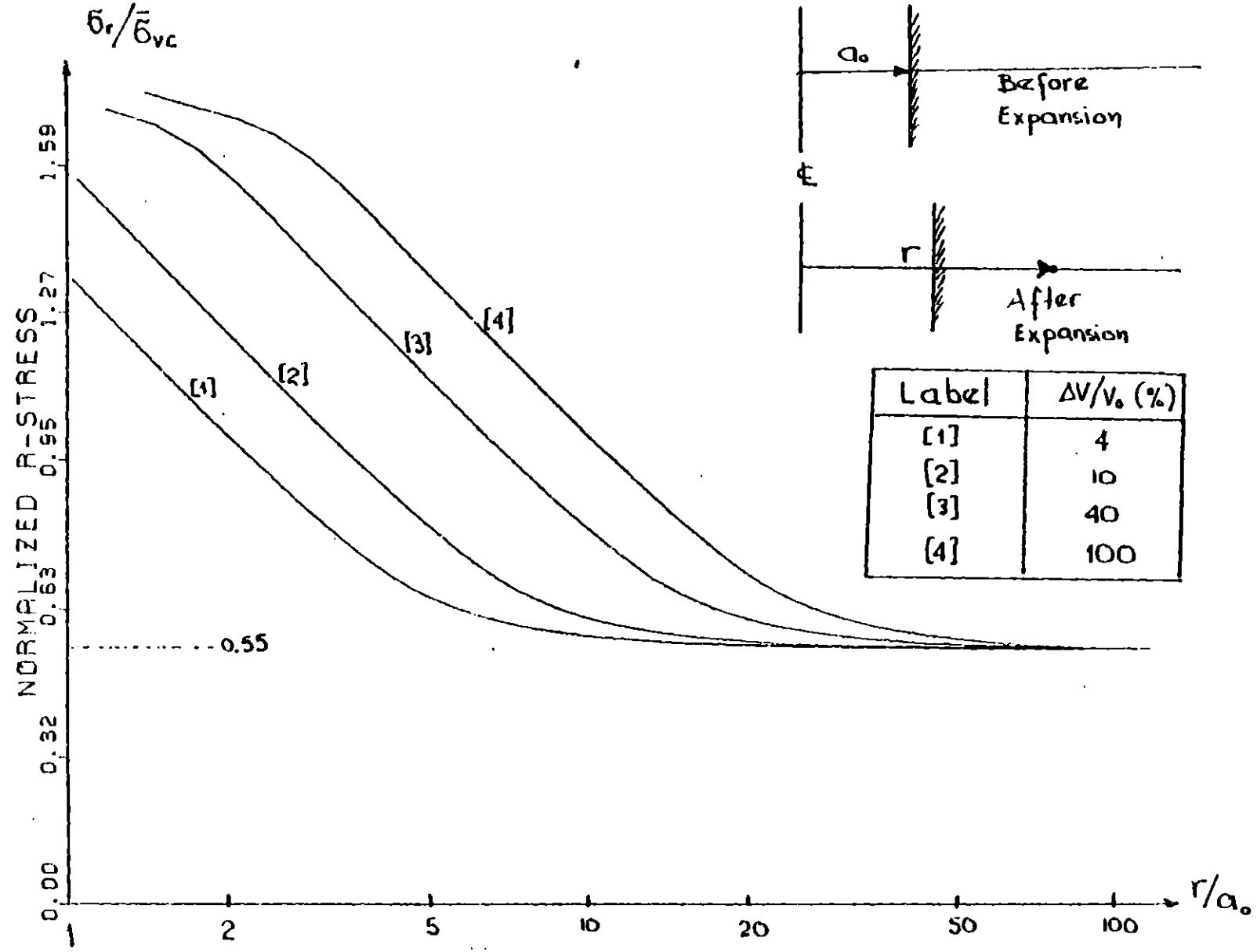

Fig. VI-3: Total radial stress vs radial coordinate during the undrained expansion of a cylindrical cavity. (Mroz-Prevost model prediction)

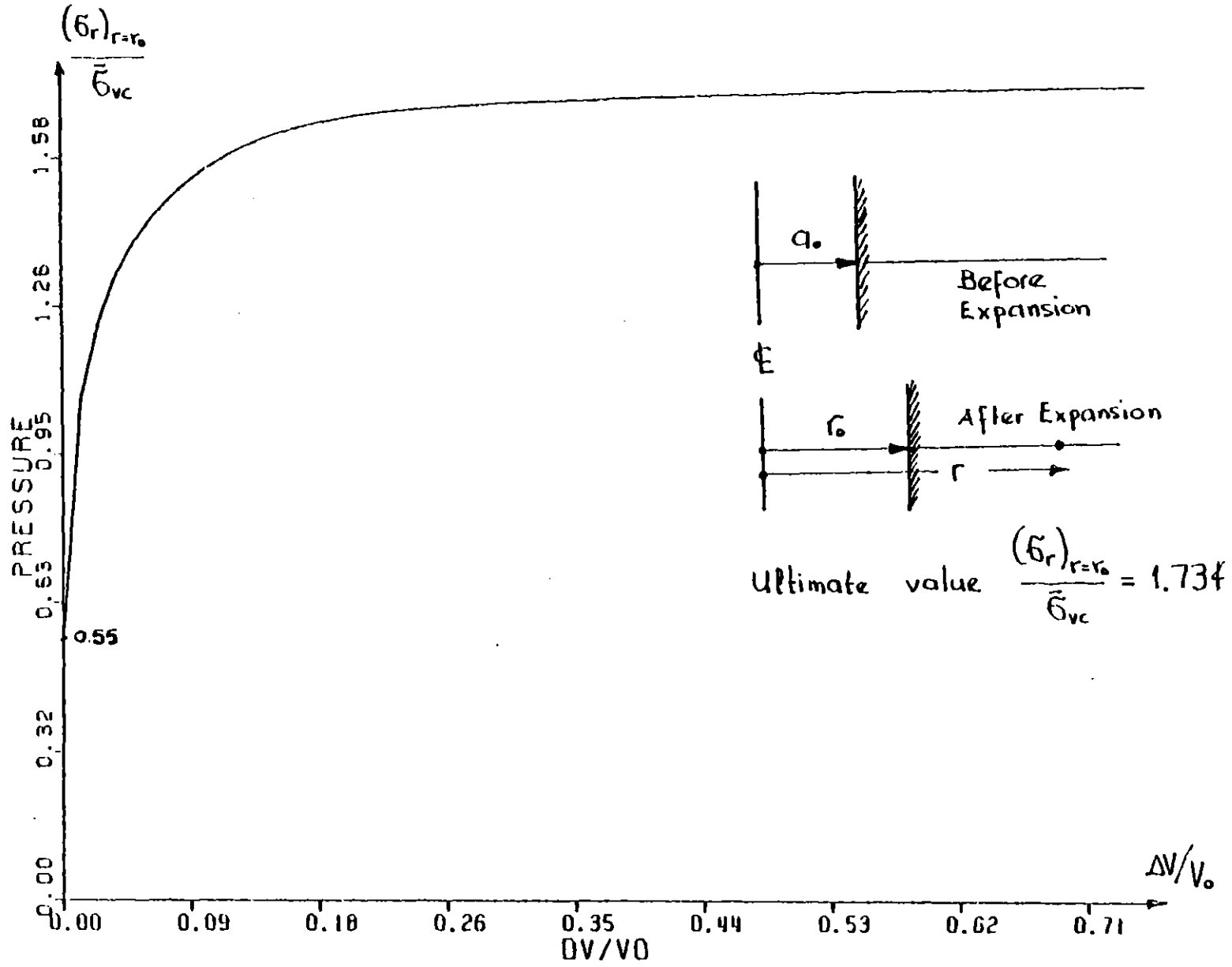

Fig. VI-4: Total radial stress at the hole boundary, vs the expansion ratio during the undrained expansion of a cylindrical cavity (Mroz-Prevost model prediction)

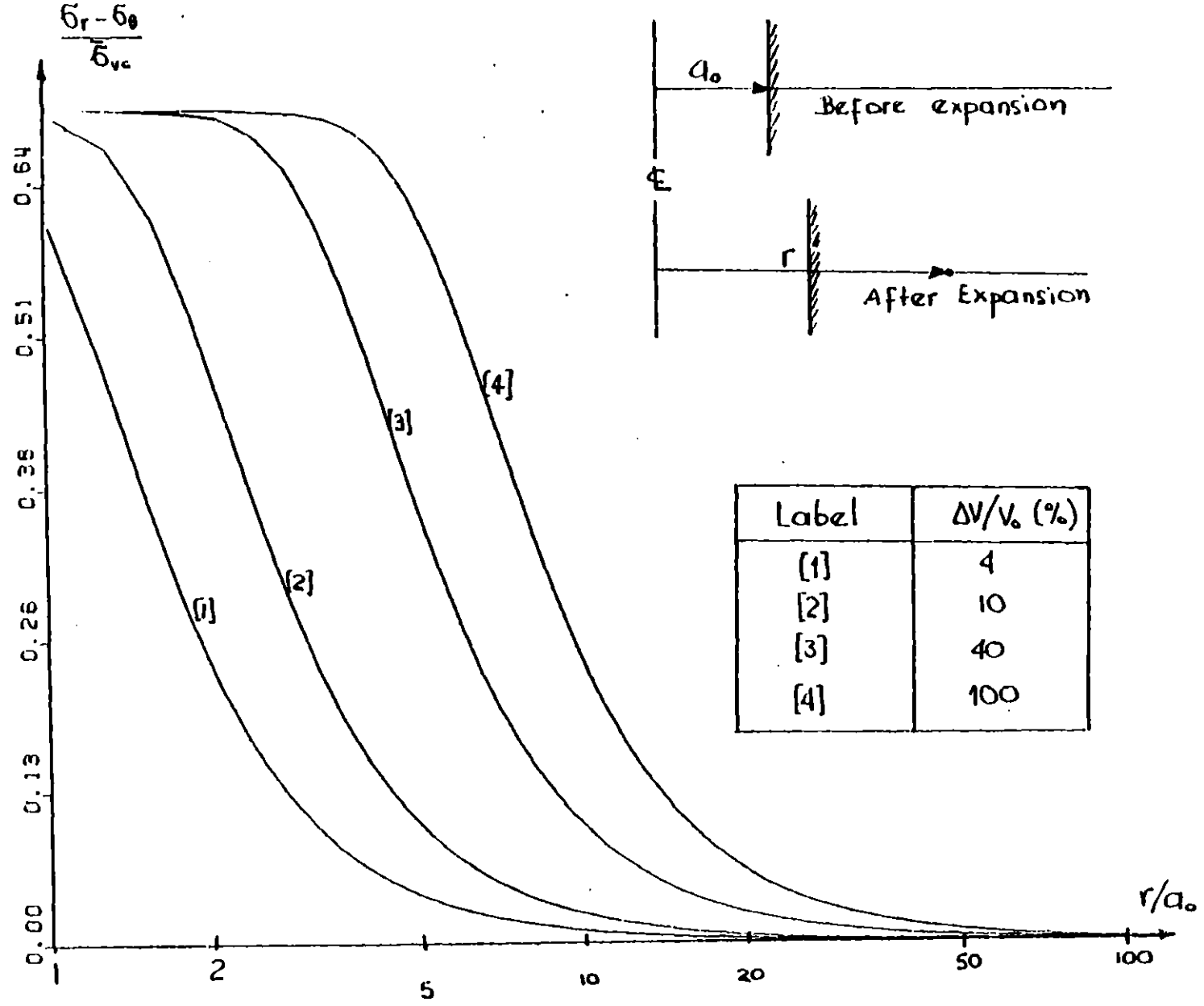

Fig. VI-5: Shear stress vs radial coordinate during the undrained expansion of a cylindrical cavity (Cam-Clay prediction)

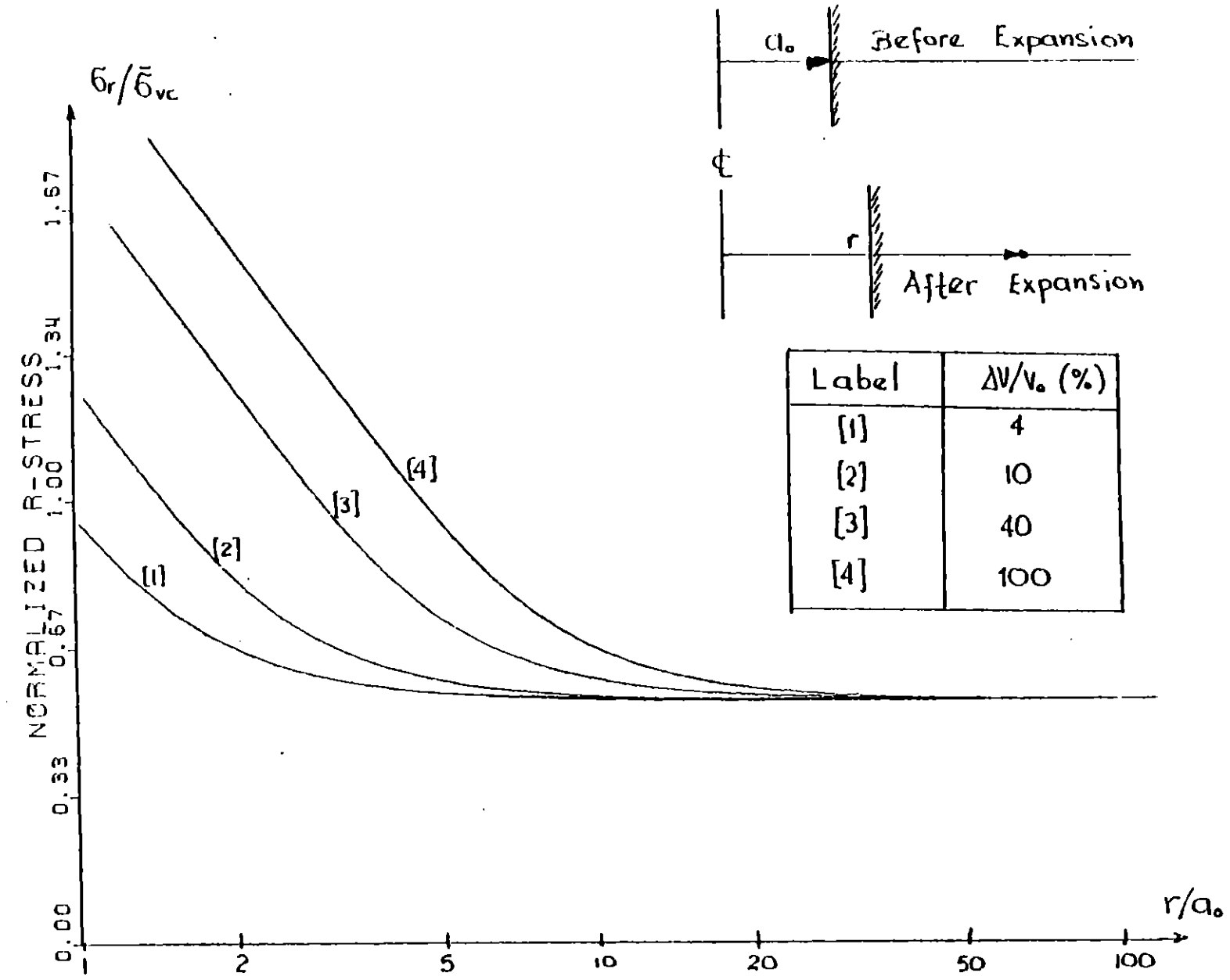

Fig. VI-6: Total radial stress vs radial coordinate during the undrained expansion of a cylindrical cavity. (Cam-Clay prediction).

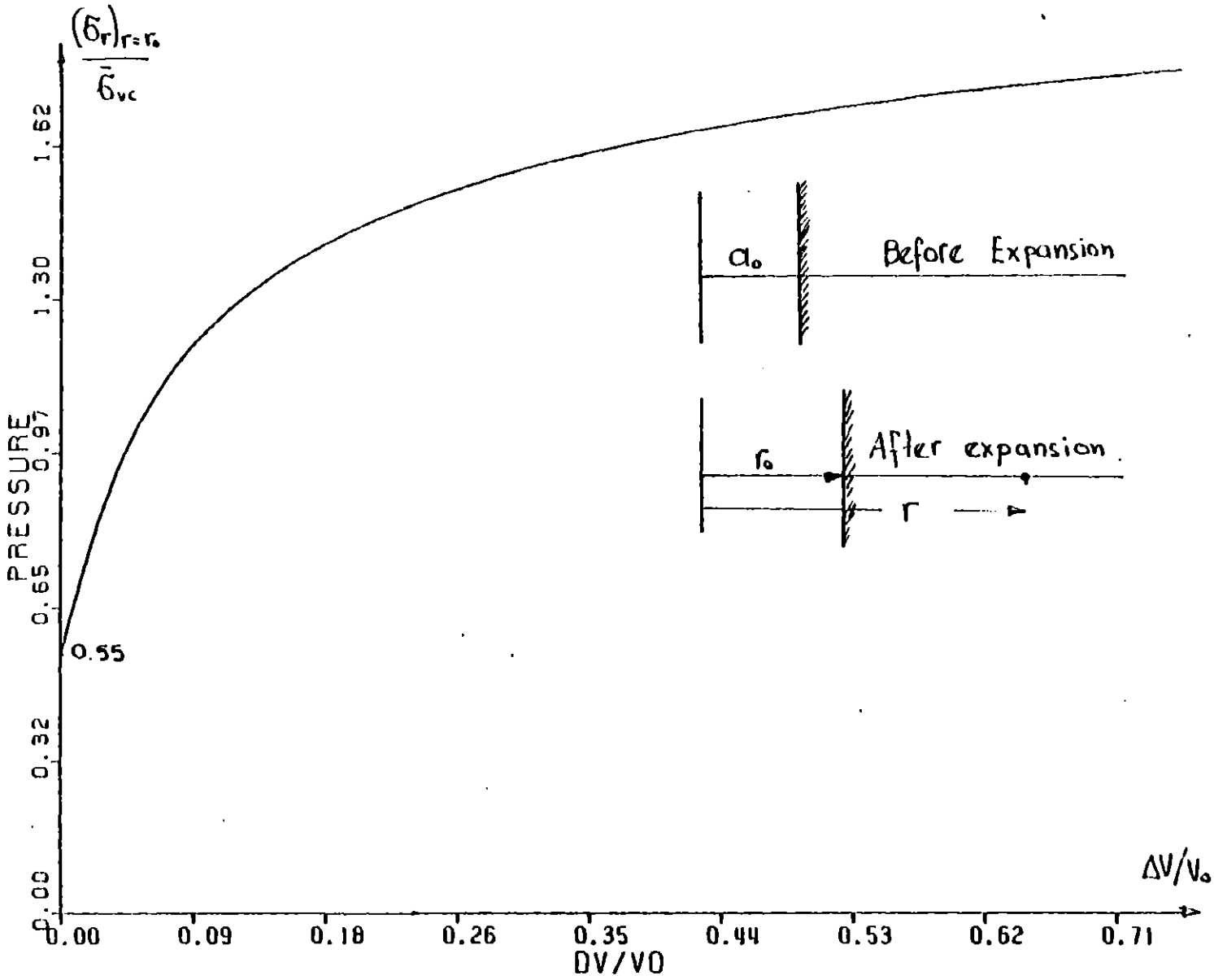

Fig. VI-7: Total radial stress at the Hole boundary vs the expansion ratio. (Cam-Clay prediction)

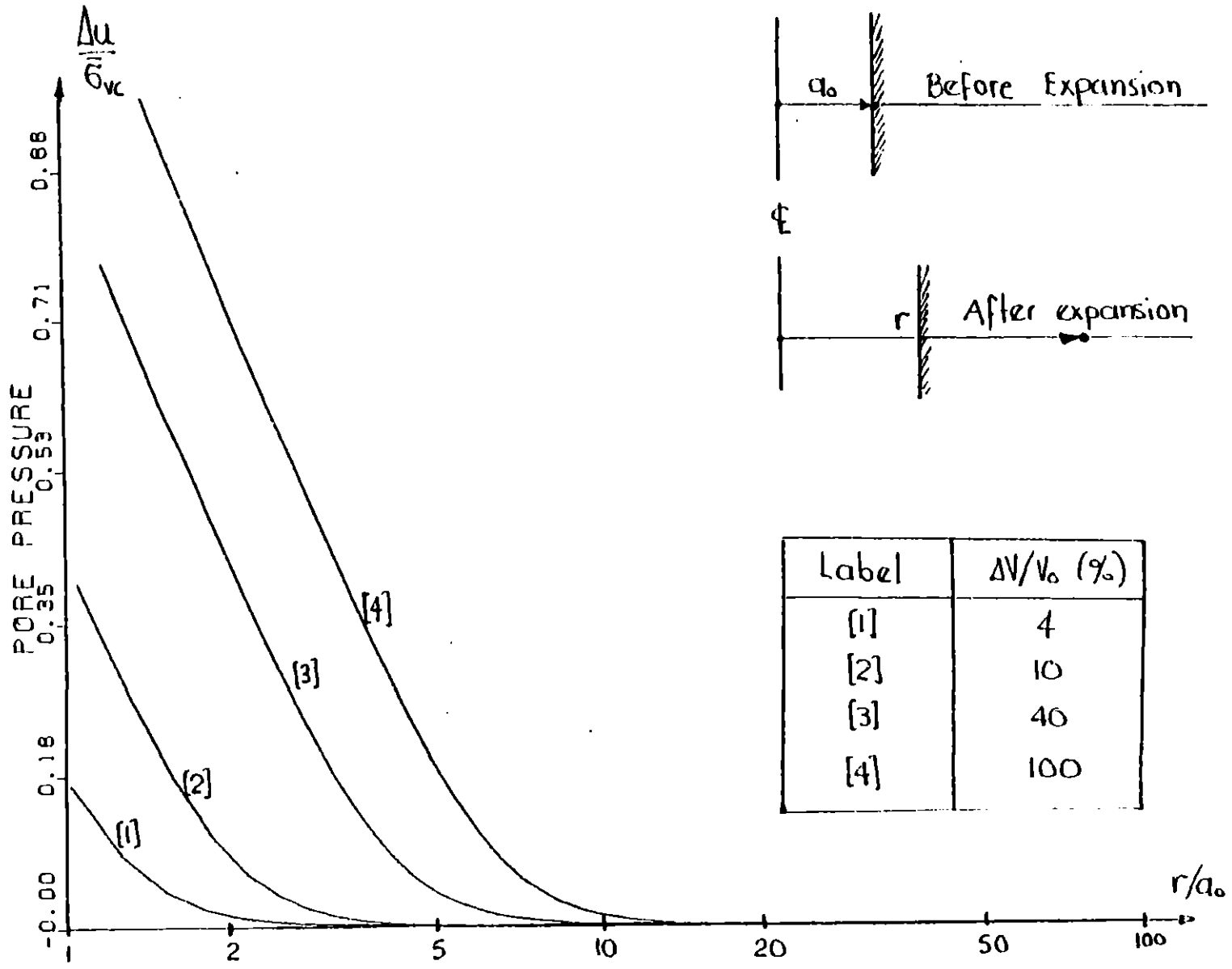

Fig. VI-8: Excess pore pressure vs radial coordinate during of the undrained expansion of a cylindrical cavity. (Cam-Clay prediction).

CONCLUSIONS AND RECOMMENDATIONS

Incremental Plasticity seems to be an efficient tool for the design of rational models of materials with complicated behavior, such as the geologic materials. It can be especially useful for the study of the behavior under general 3-dimensional loading conditions with or without reversals of loading.

In the previous Chapters two such models were evaluated:

A. The Cam-Clay Model

This has the following advantages:

[1] It is based on the Critical State Concept which is a reasonable theory (at least qualitatively) for clys.

[2] It requires few input parameters which can be evaluated from standard routine laboratory tests.

[3] Since it is an effective stress model it can be used for drained, undrained as well as for partially drained loading conditions.

It has the following disadvantages:

[1] It predicts a very extended elastic region during unloading which limits its use for the study of cyclic loading.

[2] It cannot predict strain softening for normally consolidated clays, although most K_o-normally

consolidated clays strain soften during undrained shear in triaxial compression and plane strain compression. This significantly limits its use for K_o-consolidated and sensitive clays.

[3] It predicts too high shear strength in extension tests in general (triaxial and plane strain).

[4] It predicts a too high friction angle for undrained triaxial extension and plane strain tests.

B. The Mroz-Prevost Model.

This has the following advantages:

[1] The concept of the field of Hardening Moduli allows great flexibility in modelling soil behavior accurately.

[2] It gives reasonable predictions of the stress-strain and strength characteristics under undrained conditions.

It has the following disadvantages.

[1] It requires the evaluation of many parameters. This may limit its applications in Numerical Analyses via the Finite Element Method because of storage requirements.

[2] It can only be used for undrained loading.

[3] It does not allow the evaluation of the excess pore pressures and consequently of the effective stresses. Only the total stresses can be evaluated.

Concluding we think that further research should be oriented towards:

(a) Development of more adequate constitutive laws. A combination of the Critical State Concepts with the notion of the field of hardening moduli would be desirable.

(b) Applications of non-linear constitutive laws in practical problems, mainly via the Finite Element Method.

APPENDIX I

STRESS-STRAIN RELATIONS FOR ISOTROPIC SOILS

Assuming that the yield surface is just a function of the two stress invariants, 'p' and 'q', (1) we can write:

$$\frac{\partial f}{\partial \sigma_{ij}} = \frac{\partial f}{\partial p} \cdot \frac{\partial p}{\partial \sigma_{ij}} + \frac{\partial f}{\partial q} \cdot \frac{\partial q}{\partial J_2} \cdot \frac{\partial J_2}{\partial \sigma_{ij}}$$

which gives:

$$\frac{\partial f}{\partial \sigma_{ij}} = \frac{1}{3} \delta_{ij} \frac{\partial f}{\partial p} + \frac{3 s_{ij}}{2q} \frac{\partial f}{\partial q} \qquad (A\text{-}I\text{-}1)$$

In addition since:

$$p = \frac{1}{3} I_1 = \frac{1}{3} \sigma_{ij} \delta_{ij} \qquad (II\text{-}23)$$

---

(1) In Chapter II, Section 2.6 it was defined:

$$p = \frac{1}{3} \sigma_{kk} \quad ; \quad q = \left\{ \frac{3}{2} s_{ij} s_{ij} \right\}^{1/2} = \sqrt{3 J_2}$$

we get:

$$dp = \frac{1}{3}\delta_{ij}\, d\sigma_{ij} \qquad (A\text{-}I\text{-}2)$$

and since:

$$q = \sqrt{3J_2} \qquad (II\text{-}23)$$

we get:

$$dq = \frac{3}{2q}\, s_{ij}\, ds_{ij} = \frac{3}{2q}\, s_{ij}\, d\sigma_{ij} \qquad (A\text{-}I\text{-}3)$$

Then using eq. A-I-1 , A-I-2 and A-I-3 we get:

$$\frac{\partial f}{\partial \sigma_{ij}}\, d\sigma_{ij} = \frac{\partial f}{\partial p}\, dp + \frac{\partial f}{\partial q}\, dq \qquad (A\text{-}I\text{-}4)$$

For the invariant measure of plastic volumetric strain increment we have from eq. II-8 in conjunction with eq. II-15:

$$d\varepsilon_v^p = d\varepsilon_{kk}^p = \alpha \left(\frac{\partial f}{\partial \sigma_{ij}}\, d\sigma_{ij} \right) \frac{\partial f}{\partial \sigma_{kk}}$$

Then using eq. A-I-4 and A-I-1 we get:

$$d\varepsilon_v^p = \alpha \left(\frac{\partial f}{\partial p}\, dp + \frac{\partial f}{\partial q}\, dq \right) \frac{\partial f}{\partial p} \qquad (A\text{-}I\text{-}5)$$

Similarly for the invariant measure of plastic deviatoric strain increment we have:

$$d\bar{\varepsilon}^p = \left\{ \frac{2}{3}\, d\varepsilon_{ij}^p\, d\varepsilon_{ij}^p \right\}^{1/2} = \left\{ \frac{2}{3} \left[d\varepsilon_{ij}^p - \frac{1}{3}\, d\varepsilon_v^p\, \delta_{ij} \right] \left[d\varepsilon_{ij}^p - \frac{1}{3}\, d\varepsilon_v^p\, \delta_{ij} \right] \right\}^{1/2}$$

$$= \left\{ \frac{2}{3} \left[d\varepsilon_{ij}^p \, d\varepsilon_{ij}^p - \frac{1}{3} \left(d\varepsilon_v^p \right)^2 \right] \right\}^{1/2} =$$

$$= \left\{ \frac{2}{3} \left[\alpha^2 \left(\frac{\partial f}{\partial \sigma_{ij}} d\sigma_{ij} \right)^2 \left(\frac{\partial f}{\partial \sigma_{ij}} \frac{\partial f}{\partial \sigma_{ij}} \right) - \frac{1}{3} \alpha^2 \left(\frac{\partial f}{\partial \sigma_{ij}} d\sigma_{ij} \right)^2 \left(\frac{\partial f}{\partial p} \right)^2 \right] \right\}^{1/2} =$$

$$= \alpha \left(\frac{\partial f}{\partial \sigma_{ij}} d\sigma_{ij} \right) \frac{\partial f}{\partial q} \qquad \text{or:}$$

$$d\bar{\varepsilon}^p = \alpha \left(\frac{\partial f}{\partial p} dp + \frac{\partial f}{\partial q} dq \right) \frac{\partial f}{\partial q} \qquad (A\text{-}I\text{-}6)$$

We can now evaluate the parameter α for the case of a yield function, depending on only the stress invariants 'p' and 'q'.

Rewriting eq. II-24:

$$f \equiv f'(p, q) - H(\varepsilon_v^p, \bar{\varepsilon}^p) = 0 \qquad (II\text{-}24)$$

we require the stress point to remain on the yield surface (consistency condition). This means that: $df = 0$ or:

$$\frac{\partial f}{\partial p} dp + \frac{\partial f}{\partial q} dq = \frac{\partial H}{\partial \varepsilon_v^p} d\varepsilon_v^p + \frac{\partial H}{\partial \bar{\varepsilon}^p} d\bar{\varepsilon}^p$$

Using eq. A-I-5 and A-I-6 we end up with:

$$\alpha = \left(\frac{\partial H}{\partial \varepsilon_v^p} \frac{\partial f}{\partial p} + \frac{\partial H}{\partial \bar{\varepsilon}^p} \frac{\partial f}{\partial q} \right)^{-1} \qquad (A-I-7)$$

Eq. A-I-5 , A-I-6 and A-I-7 are very useful and will be used extensively in this Thesis. The first two, express normality rule in a two-dimensional stress subspace. In fact starting from the normality rule in the nine-dimensional stress space (eq. II-15), and by choosing the stress and strain measures appropriately, we deduced normality in a two-dimensional subspace of the stress invariants 'p' and 'q', with associated invariant strain measures ' ε_v^p ' and ' $\bar{\varepsilon}^p$ '.

Finally eq. A-I-7 gives the strain hardening (or softening) parameter. As we have proved in Section 2.5 α is positive in the strain hardening region and negative in the strain softening region.

APPENDIX II

STRESS-STRAIN RELATIONS FOR THE CAM-CLAY MODEL

The equation of the ellipse shown in Fig A-II-1 is:

$$f(p, q, p_c) = M^2 p (p - p_c) + q^2 = 0 \qquad (A\text{-}II\text{-}1)$$

where 'M' is the ratio of the vertical to the horizontal

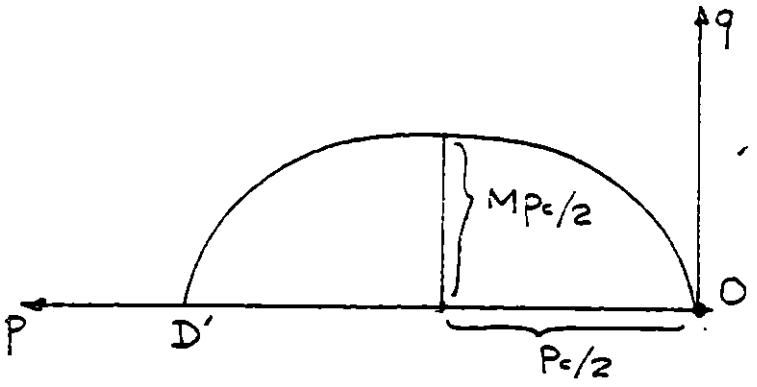

Fig. A-II-1

axis. In Fig A-II-1 point D' is the projection on the p-q plane of a point D which is located on the virgin isotropic consolidation curve (see also Fig 2 in Ch. III), which, according to experiments, is a straight line in a e-lnp plot

with slope λ :

$$e = A - \lambda \ln p_c$$

The isotropic rebound curve is of the form:

$$e^e = B - k \ln p_c$$

Differentiating the last two equations we have for the plastic void ratio changes:

$$de^p = de - de^e = -\lambda \frac{dp_c}{p_c} + k \frac{dp_c}{p_c}$$

or:

$$\frac{dp_c}{de^p} = -\frac{p_c}{\lambda - k} \qquad (A\text{-}II\text{-}2)$$

Using eq. II-24 in conjunction with eq. A-II-1, eq. A-II-2 and eq. III-1 we get:

$$\frac{\partial H}{\partial \varepsilon_v^p} = -\frac{\partial f}{\partial \varepsilon_v^p} = -\frac{\partial f}{\partial p_c} \cdot \frac{\partial p_c}{\partial e^p} \cdot \frac{\partial e^p}{\partial \varepsilon_v^p} =$$

$$= -(-M^2 p)\left(-\frac{p_c}{\lambda - k}\right)\{-(1+e)\}$$

or:

$$\frac{\partial H}{\partial \varepsilon_v^p} = \frac{1+e}{2-k} M^2 p p_c \qquad (A\text{-}II\text{-}3)$$

and :

$$\frac{\partial H}{\partial \bar{\varepsilon}^p} = 0$$

The derivatives of 'f' with respect to 'p' and 'q' have also to be computed. Using eq. A-II-1, we have:

$$\frac{\partial f}{\partial p} = p\left(M^2 - \frac{q^2}{p^2}\right)$$

$$\frac{\partial f}{\partial q} = 2q \qquad (A\text{-}II\text{-}5)$$

Finally substituting from eq. A-II-3, eq. A-II-4 and eqs. A-II-5 into eq. A-I-7, eq. A-I-5 and eq. A-I-6 we have:

$$\alpha = \frac{2-k}{1+e} \cdot \frac{1}{(M^2-\eta^2) M^2 p_c p^2} \qquad (A\text{-}II\text{-}6)$$

and

$$\begin{Bmatrix} d\varepsilon_v^p \\ d\bar{\varepsilon}^p \end{Bmatrix} = \frac{2(2-k)\eta}{p(1+e)(M^2+\eta^2)} \begin{bmatrix} \frac{M^2-\eta^2}{2\eta} & 1 \\ 1 & \frac{2\eta}{M^2-\eta^2} \end{bmatrix} \begin{Bmatrix} dp \\ dq \end{Bmatrix}$$

$$(A\text{-}II\text{-}7)$$

where: $\eta = q/p$.

Eq. A-II-6 gives the value of the hardening parameter, and eq. A-II-7 the incremental stress-strain relations in invariant form. The matrix relating the invariant increments will be noted as $\underset{\sim}{B}$ in the following. Expressing the invariant increments in terms of the principal stress and strain increments we end up with:

$$\underset{\sim}{d\varepsilon}^p = \left(\underset{\sim}{A}^T \underset{\sim}{B} \underset{\sim}{A} \right) \underset{\sim}{d\sigma}$$

where $\underset{\sim}{d\varepsilon}^p$, $\underset{\sim}{d\sigma}$ are the principal plastic strain and stress vectors and matrix $\underset{\sim}{A}$ is given by the form:

$$\underset{\sim}{A} = \frac{1}{3} \begin{bmatrix} 1 & 1 & 1 \\ \frac{2\sigma_1 - \sigma_2 - \sigma_3}{q} & \frac{2\sigma_2 - \sigma_1 - \sigma_3}{q} & \frac{2\sigma_3 - \sigma_1 - \sigma_2}{q} \end{bmatrix}$$

Adding the elastic strain increments from eq. III-7 we get:

$$\underset{\sim}{d\varepsilon} = \underset{\sim}{d\varepsilon}^e + \underset{\sim}{d\varepsilon}^p = \left[\underset{\sim}{\Sigma}^e + \left(\underset{\sim}{A}^T \underset{\sim}{B} \underset{\sim}{A} \right) \right] \underset{\sim}{d\sigma}$$

or:

$$\underset{\sim}{d\varepsilon} = \underset{\sim}{\Sigma} \underset{\sim}{d\sigma} \qquad (A\text{-}II\text{-}8)$$

which are the required incremental stress-strain relations in a principal space.

APPENDIX III

PORE PRESSURE DEVELOPMENT IN SOILS UNDER GENERAL LOADING CONDITIONS

Let's assume that the total stress increment $\Delta\underset{\sim}{\sigma}$ applied on a soil element is specified, and we want to compute the corresponding pore pressure change Δu, resulting from this increment. We will further assume that the soil is fully saturated and that an incremental effective stress-strain law is available (i.e the effective flexibility matrix $\underset{\approx}{S}$ is known as it was discussed in Chapter II). If V_s is the volume of the solids, V_w the volume of the pore water and:

$$V_o = V_s + V_w$$

is the total volume of the soil element (small enough for the assumption of constant stresses to be valid then:

$$\Delta\varepsilon_{vol} = \frac{\Delta V_o}{V_o} = \frac{\Delta V_s}{V_o} + \frac{\Delta V_w}{V_o}$$

or if 'n' is the porosity: (1)

$$\Delta\varepsilon_{vol} = (1-n)\ \frac{\Delta V_s}{V_s} + n\ \frac{\Delta V_w}{V_w}$$

Let's assume for the moment that the compressibility of both the water $1/B^w$ and soil grains $1/B^s$ is constant. Then:

$$\frac{\Delta V_s}{V_s} = \frac{\Delta\bar{\sigma}_{oct}}{B^s}$$

$$\frac{\Delta V_w}{V_w} = \frac{\Delta u}{B^w}$$

where Δu is the pore pressure increment.

This restriction is not significant since in most cases the compressibilities of water and grains are much smaller than the compressibility of the skeleton and they are neglected (i.e the assumption of incompressibility under undrained conditions is done).

Using the last three equations we get:

$$\Delta\varepsilon_{vol} = (1-n)\ \frac{\Delta\bar{\sigma}_{oct}}{B^s} + n\ \frac{\Delta u}{B^w}$$

But: $\Delta\bar{\sigma}_{oct} = \underset{\sim}{m}^T \Delta\underset{\sim}{\bar{\sigma}}$ and $\Delta\varepsilon_{vol} = \underset{\sim}{m}^T \Delta\underset{\sim}{\varepsilon}$.

---

(1) Porosity is defined as: $n = V_w/V_o$

So:

$$\underset{\sim}{m}^T \Delta\underset{\sim}{\varepsilon} = (1-n)\,\frac{\underset{\sim}{m}^T \Delta\bar{\underset{\sim}{\sigma}}}{B^g} + n\,\frac{\Delta u}{B^w}$$

We will then introduce the effective stress increment $\Delta\bar{\underset{\sim}{\sigma}}$ by using the incremental effective stress-strain relationship:

$$\Delta\underset{\sim}{\varepsilon} = \bar{\underset{\sim}{\underset{\sim}{S}}}\,\Delta\bar{\underset{\sim}{\sigma}} \qquad (II-26)$$

and then substitute the effective stress increment with the difference of the total stress $\Delta\underset{\sim}{\sigma}$ and the pore pressure increment Δu, as follows:

$$\underset{\sim}{m}^T \bar{\underset{\sim}{\underset{\sim}{S}}}\,\Delta\bar{\underset{\sim}{\sigma}} = (1-n)\,\frac{\underset{\sim}{m}^T \Delta\bar{\underset{\sim}{\sigma}}}{B^g} + n\,\frac{\Delta u}{B^w}$$

or:

$$\underset{\sim}{m}^T \bar{\underset{\sim}{\underset{\sim}{S}}}\left(\Delta\underset{\sim}{\sigma} - \underset{\sim}{m}\,\Delta u\right) = (1-n)\,\frac{\underset{\sim}{m}^T\left(\Delta\underset{\sim}{\sigma} - \underset{\sim}{m}\,\Delta u\right)}{B^g} + \frac{n\,\Delta u}{B^w}$$

and finally solve for the pore pressure increment:

$$\Delta u = \frac{\underset{\sim}{m}^T\left\{\bar{\underset{\sim}{\underset{\sim}{S}}} - \frac{1-n}{B^g}\,\underset{\sim}{\underset{\sim}{I}}\right\}\Delta\underset{\sim}{\sigma}}{\underset{\sim}{m}^T \bar{\underset{\sim}{\underset{\sim}{S}}}\,\underset{\sim}{m} + \frac{n}{B^w} - \frac{3(1-n)}{B^g}} \qquad (II-28)$$

where $\underset{\sim}{I}$ is a 6x6 unit matrix.

This last equation gives the pore pressure increment as a linear combination of the components of the applied total stress increment $\underset{\sim}{\Delta\sigma}$. The multipliers are functions of the components of the effective flexibility matrix $\underset{\sim}{\Omega}$, which varies along the stress path.

The philosophy underlying the previous procedure is the following:

We need a pore pressure increment with magnitude sufficient to reduce (or increase) the effective stresses to a degree that the corresponding strains (through the incremental stress-strain law) satisfy the incompressibility condition (or limited compressibility depending on its magnitude for the water and grains). The incompressibility condition is one equation which when expressed in terms of the total stress increment and the pore pressure increment, and solved for the pore pressure increment, gives the magnitude of the pore pressure increment in terms of the total stress increment.

The meaning of eq.II-28 will be further explained by applying it to predict the pore pressures developing under some basic loading modes. Specifically the effect of pore pressure generation due to octahedral (i.e hydrostatic) versus shear loading will be studied. In order to separate these two effects, let's assume that we apply a total octahedral stress increment equal to 'Δp' and a shear stress

increment equal to 'Δq', in all directions. Then the vector will be:

$$\underset{\sim}{\Delta\sigma} = \begin{Bmatrix} \Delta p \, \underset{\sim}{J} \\ \Delta q \, \underset{\sim}{J} \end{Bmatrix} \quad ; \quad J = \begin{Bmatrix} 1 \\ 1 \\ 1 \end{Bmatrix} \qquad (A\text{-}III\text{-}1)$$

The Kronecker delta vector $\underset{\sim}{m}$ can be rewritten:

$$\underset{\sim}{m} = \begin{Bmatrix} \underset{\sim}{J} \\ \underset{\sim}{0} \end{Bmatrix} \quad ; \quad \underset{\sim}{0} = \begin{Bmatrix} 0 \\ 0 \\ 0 \end{Bmatrix} \qquad (A\text{-}III\text{-}2)$$

The effective flexibility matrix $\underset{\sim}{\bar{\bar{S}}}$ will also be separated in octahedral and shear components, as follows:

$$\underset{\sim}{\bar{\bar{S}}} = \begin{bmatrix} \underset{\sim}{\bar{\bar{S}}}_{\sigma\sigma} & \underset{\sim}{\bar{\bar{S}}}_{\sigma\tau} \\ \underset{\sim}{\bar{\bar{S}}}_{\sigma\tau}^{T} & \underset{\sim}{\bar{\bar{S}}}_{\tau\tau} \end{bmatrix} \qquad (A\text{-}III\text{-}3)$$

where each submatrix has a dimension 3x3 and superscript T indicates the transpose of a matrix. (1) Submatrix $\underset{\sim}{\bar{\bar{S}}}_{\sigma\sigma}$ represents the relation between normal stresses and normal strains; similarly $\underset{\sim}{\bar{\bar{S}}}_{\tau\tau}$ is the relation of shear stresses with shear strains. Even in Linear Elasticity, these

---

(1) Note that $\underset{\sim}{\bar{\bar{S}}}$ is symmetric and of dimension 6x6. In addition $\underset{\sim}{\bar{\bar{S}}}_{\sigma\sigma}$ and $\underset{\sim}{\bar{\bar{S}}}_{\tau\tau}$ are also symmetric matrices.

matrices are non-zero and positive definite.

Submatrix $\bar{\underset{\sim}{S}}_{\sigma\tau}$ represents the coupling between normal stresses and shear strains (due to symmetricity, it also represents the coupling between shear stresses and normal strains). In Linear Elasticity there is no such coupling and consequently this matrix is identically zero.

Using eq. A-III-3 and eq. A-III-2 we get:

$$\underset{\sim}{m}^T \bar{\underset{\sim}{S}} \underset{\sim}{m} = \underset{\sim}{J}^T \bar{\underset{\sim}{S}}_{\sigma\sigma} \underset{\sim}{J} \qquad (A\text{-}III\text{-}4)$$

which is a scalar quantity.

Using eq. A-III-1, A-III-2, and A-III-3 we get:

$$\underset{\sim}{m}^T \bar{\underset{\sim}{S}} \underset{\sim}{\Delta\sigma} = \Delta p \left(\underset{\sim}{J}^T \bar{\underset{\sim}{S}}_{\sigma\sigma} \underset{\sim}{J} \right) + \Delta q \left(\underset{\sim}{J}^T \bar{\underset{\sim}{S}}_{\sigma\tau} \underset{\sim}{J} \right) \qquad (A\text{-}III\text{-}5)$$

Now we are ready to apply eq. II-28 and compute the pore pressure increments. To simplify the mathematics, incompressible fluid and grains will be assumed (i.e $B^f = B^w = \infty$). Then eq. II-28 rewrites:

$$\Delta u = \frac{\underset{\sim}{m}^T \bar{\underset{\sim}{S}} \underset{\sim}{\Delta\sigma}}{\underset{\sim}{m}^T \bar{\underset{\sim}{S}} \underset{\sim}{m}}$$

and using eq. A-III 4 and eq. A-III-5 we end up with:

$$\Delta u = \Delta p + \frac{\underset{\sim}{J}^T \underset{\sim}{\bar{S}} \underset{\sim}{J}}{\underset{\sim}{J}^T \underset{\sim}{\bar{S}}_{cc} \underset{\sim}{J}} \Delta q \qquad (A\text{-}III\text{-}6)$$

Let's study this equation.

The pore pressure increment due to a hydrostatic and a shear stress increment is given as the sum of two terms.

The first term, gives the pore pressure increment due to the hydrostatic total stress increment 'Δp'. It is equal to the hydrostatic total stress increment which should be expected for a saturated soil (Henkel's b parameter (1) is equal to 1) with incompressible pore fluid.

The second term gives the pore pressure increment due to the applied shear stress increment 'Δq'. The factor by which 'Δq' is multiplied, is equivalent to Henkel's 'a' parameter. Since it depends on the flexibility matrix (which varies with the stress level) this factor also varies with the level of stressing. In linear elasticity this term is zero (since $\underset{\sim}{\bar{S}}_{ct}$ is zero as we have mentioned previously). This result also agrees with the standard Soil Mechanics Literature.

We can also study the sign of this multiplicative factor. (2)

---

(1) Henkel D.J. and Wade N.H. (1966)'Plane Strain Tests on a Saturated Remolded Clay' JSMFD,ASCE Vol 92 No SM6, pp67-80. give the equation:

$$\Delta u = \Delta \sigma_{oct} + a \, \Delta \tau_{oct}$$

for the pore pressure increment in terms of the total stress increment.

(2) A positive sign means that positive pore pressures will be

The denominator (in parentheses) is always positive since $\underset{\sim}{\underset{=}{S}}_{\sigma\sigma}$ is positive definite (for a strain hardening material).

If $\underset{\sim}{\underset{=}{S}}_{\sigma\tau}$ is positive definite (which means that shear stress increments tend to create compressive normal strains),then the numerator is also positive and hence positive pore pressures are generated due to shearing. This is the case of normally consolidated clays.

If $\underset{\sim}{\underset{=}{S}}_{\sigma\tau}$ is negative definite (which means that shear stress increments tend to create dilative normal strains) then negative pore pressures due to shearing are generated, because the nominator will be negative. This is the case of heavily overconsolidated clays.

---

generated with uniform shearing and a negative sign means negative pore pressures.

APPENDIX IV

DERIVATION OF INCREMENTAL STRESS-STRAIN RELATIONS FOR THE MROZ-PREVOST MODEL

The equation of the m^{th} yield surface is:

$$f_m(\sigma_{ij}, \bar{\varepsilon}^p) \equiv \left\{ \frac{3}{2}(s_{ij} - a_{ij}^{(m)})(s_{ij} - a_{ij}^{(m)}) \right\}^{1/2} - k^{(m)}(\bar{\varepsilon}^p) = 0 \qquad (A\text{-}IV\text{-}1)$$

The consistency condition for this surface gives:

$$\frac{\partial f_m}{\partial \sigma_{kl}} d\sigma_{kl} + \frac{\partial f_m}{\partial k^{(m)}} \frac{\partial k^{(m)}}{\partial \bar{\varepsilon}^p} d\bar{\varepsilon}^p = 0 \qquad (A\text{-}IV\text{-}2)$$

Let's study each term separately:

$$\frac{\partial f_m}{\partial \sigma_{kl}} d\sigma_{kl} = \frac{\partial f_m}{\partial (s_{ij} - a_{ij}^{(m)})} \frac{\partial s_{ij}}{\partial \sigma_{kl}} d\sigma_{kl} =$$

$$= \frac{3(s_{ij} - a_{ij}^{(m)})}{2k^{(m)}} (\delta_{ik}\delta_{jl} - \frac{1}{3}\delta_{ij}\delta_{kl}) d\sigma_{kl} =$$

$$= \frac{3}{2k^{(m)}} (s_{kl} - a_{kl}^{(m)}) d\sigma_{kl} \Rightarrow$$

$$\frac{\partial f_m}{\partial \sigma_{kl}} d\sigma_{kl} = \frac{3}{2k^{(m)}} (s_{kl} - a_{kl}^{(m)}) ds_{kl} \qquad (A\text{-}IV\text{-}3)$$

In addition:

$$\frac{\partial f_m}{\partial k^{(m)}} = -1 \qquad (A-IV-4)$$

and:

$$\frac{\partial k^{(m)}}{\partial \bar{\varepsilon}^p} = \frac{3}{2} H'_m \qquad (A-IV-5)$$

where:

$$\frac{2}{3H'_m} = \frac{2}{3H_m} - \frac{1}{3G}$$

and $\frac{2}{3H_m}$ can be obtained from triaxial tests since :

$$\frac{3}{2} H_m = \frac{d(\sigma_1 - \sigma_3)}{d\varepsilon_1}$$

for the triaxial test.

Finally using eqs. II-8 and II-15 we get:

$$d\bar{\varepsilon}^p = \alpha \frac{3}{2k^{(m)}} (s_{kl} - a^{(m)}_{kl}) ds_{kl} \qquad (A-IV-6)$$

Substituting eqs A-IV-3 through A-IV-6 in the consistency condition A-IV-2 we get:

$$\alpha = \frac{2}{3H'_m} \qquad (A-IV-7)$$

Finally eq. II-15 gives:

$$de^p_{ij} = \frac{2}{3H'_m} \left\{ \frac{3}{2k^{(m)}} (s_{kl} - a^{(m)}_{kl}) ds_{kl} \right\} \left\{ \frac{3}{2k^{(m)}} (s_{ij} - a^{(m)}_{ij}) \right\}$$

or:

$$d\varepsilon_{ij}^{p} = \frac{3}{2H'_m} \frac{s_{ij} - a_{ij}^{(m)}}{(k^{(m)})^2} \left(s_{kl} - a_{kl}^{(m)}\right) ds_{kl}$$

Adding the elastic components:

$$d\varepsilon_{ij} = \frac{ds_{ij}}{2G} + \frac{3}{2H'_m} \frac{s_{ij} - a_{ij}^{(m)}}{(k^{(m)})^2} \left(s_{kl} - a_{kl}^{(m)}\right) ds_{kl} \qquad (A\text{-}IV\text{-}8)$$

These are the incremental stress-strain relations which are of the form studied in Chapter II:

$$\underset{\sim}{\Delta\varepsilon} = \underset{\sim}{S}\, \underset{\sim}{\Delta s}$$

Note the similarity of eq A-IV-8 with the incremental stress-strain relations for the Von Mises Hardening model (eq. III-16a) Inverting eq. A-IV-8 we get:

$$ds_{ij} = 2G\, d\varepsilon_{ij} - \frac{3}{2} \cdot \frac{4G^2}{2G + H'_m} \cdot \frac{s_{ij} - a_{ij}^{(m)}}{(k^{(m)})^2} \left(s_{kl} - a_{kl}^{(m)}\right) d\varepsilon_{kl} \qquad (A\text{-}IV\text{-}9)$$

which are of the form:

$$\underset{\sim}{\Delta s} = \underset{\sim}{C}\, \underset{\sim}{\Delta\varepsilon} \qquad (II\text{-}36)$$

Kinematic Hardening

Kinematic hardening is introduced by allowing the yield surfaces to translate in the stress space. If the current position of the stress point is A (see Fig. A-IV-1) then the translation will take place along the vector:

$$\overrightarrow{AB} = \frac{k^{(m+1)}}{k^{(m)}}\left(s_{ij} - a_{ij}^{(m)}\right) - \left(s_{ij} - a_{ij}^{(m+1)}\right) \qquad (A\text{-}IV\text{-}$$

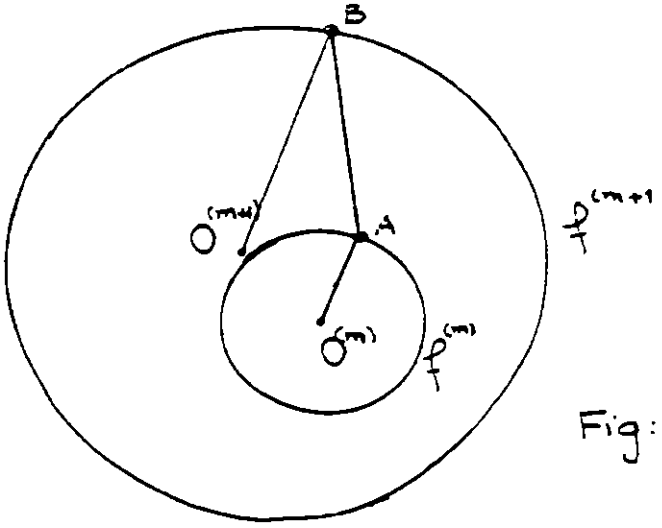

Fig: A-IV-1

where $\overrightarrow{O^{(m+1)}B}$ is parallel to $\overrightarrow{O^{(m)}A}$. This kind of k hardening is generally credited to Ziegler (1959) magnitude of translation of surface f_m will be:

$$da_{ij}^{(m)} = d\mu \ \overrightarrow{AB} \qquad (A\text{-}IV\text{-}11)$$

where:

$$d\mu = \frac{\frac{3}{2}\left(s_{ij} - a_{ij}^{(m)}\right) ds_{ij} \ - \ k^{(m)} dk^{(m)}}{k^{(m+1)} k^{(m)} - \frac{3}{2}\left(s_{ij} - a_{ij}^{(m+1)}\right)\left(s_{ij} - a_{ij}^{(m)}\right)} \qquad (A\text{-}$$

is such that the new position of the stres. continues to be on the yield surface.

---

(1) Ziegler H. (1959) Quarterly of Applied Mathematics 17, 5

Let's study the way that further stress induced anisotropy is taken care of by the model.
Initially due to the method of deposition:

$$s_{ij} = a_{ij}^{(m)} = 0 \qquad ; \quad i \neq j$$

If during subsequent shearing :

$$ds_{ij} = 0 \qquad ; \quad i \neq j$$

(i.e no rotation of the principal stress planes occurs), then eq. A-IV-11 and A-IV-10 result in: $da_{ij}^{(m)} = 0$ for $i \neq j$. i.e the principal axes of anisotropy do not rotate and then equation A-IV-8 gives that:

$$de_{ij} = 0 \qquad ; \quad i \neq j$$

i.e the principal axes of strain do not rotate, too. On the contrary if:

$$ds_{ij} \neq 0 \qquad \text{for} \quad i \neq j$$

i.e the principal stress planes rotate during shearing, then the principal axes of anisotropy and the principal strain axes will rotate, and in general these three sets of axes will not coincide.

Simplification of the model for the case of axisymmetric and plane strain loading.

Axisymmetric and Plane strain loading conditions are very common in practice. Especially for this model due to the large number of parameters involved in the computation it is almost impossible to use the model in general three-dimensional problems because of severe storage restrictions.

Plane strain in the z-direction as well as axisymmetric loading around the y-axis both have $\tau_{yz} = \tau_{xz} = 0$ at all times. Since these components of stress vanish, we can represent the model in the subspace of the three non-vanishing independent components of the deviatoric stress tensor. Mroz (1967) introduced this space for the similar case of plane stress. Prevost (1977) treated the Plane strain and axisymmetric cases.

The following stress components are introduced:

$$S_1 = \sigma_y - \frac{1}{2}(\sigma_x + \sigma_z) = \frac{3}{2} S_{yy}$$

$$S_2 = \frac{\sqrt{3}}{2}(\sigma_z - \sigma_x) \qquad (A\text{-}IV\text{-}13)$$

$$S_3 = \sqrt{3}\ \tau_{xy}$$

The associated kinematic hardening parameters for the m^{th} surface are:

$$\alpha_1^{(m)} = \frac{3}{2} \alpha_y^{(m)}$$

$$a_2^{(m)} = \frac{\sqrt{3}}{2}\left(a_2^{(m)} - a_x^{(m)}\right)$$

$$a_3^{(m)} = \sqrt{3}\ a_{xy}^{(m)} \qquad \text{(A-IV-14)}$$

and the corresponding strain measures are:

$$E_1 = \varepsilon_y$$

$$E_2 = \frac{1}{\sqrt{3}}\left(\varepsilon_z - \varepsilon_x\right) \qquad \text{(A-IV-15)}$$

$$E_3 = \frac{1}{\sqrt{3}}\ \gamma_{xy}$$

Then the yield surfaces are described by equations of the form:

$$f_m \equiv \left\{ \sum_{i=1}^{3} \left(s_{ij} - a_{ij}^{(m)}\right)^2 \right\}^{1/2} - k^{(m)} = 0 \qquad \text{(A-IV-16)}$$

and the incremental stress-strain equations reduce to:

$$dS_i = 3G\,dE_i - \frac{6G^2}{2G + H'_m} \cdot \frac{s_i - a_i^{(m)}}{\left(k^{(m)}\right)^2} \sum_{i=1}^{3} \left(s_i - a_i^{(m)}\right) dE_i \qquad \text{(A-IV-17)}$$

or:

$$dE_i = \frac{dS_i}{3G} + \frac{2}{3H'_m} \cdot \frac{s_i - a_i^{(m)}}{\left(k^{(m)}\right)^2} \sum_{i=1}^{3} \left(s_i - a_i^{(m)}\right) dS_i \qquad \text{(A-IV-18)}$$

and

$$da_i = d\mu \left\{ \frac{k^{(m+1)}}{k^{(m)}} \left(s_i - a_i^{(m)} \right) - \left(s_i - a_i^{(m+1)} \right) \right\} \qquad (A\text{-}IV\text{-}19)$$

where:

$$d\mu = \frac{\frac{3}{2} \sum_{i=1}^{3} \left(s_i - a_i^{(m)} \right) ds_i - k^{(m)} dk^{(m)}}{k^{(m+1)} k^{(m)} - \sum_{i=1}^{3} \left(s_i - a_i^{(m)} \right) \left(s_i - a_i^{(m+1)} \right)} \; ; \qquad (A\text{-}IV\text{-}20)$$

APPENDIX V

APPLICATION OF THE STRESS PATH METHOD IN THE PREDICTION OF THE SETTLEMENT OF A STRIP FOOTING

The undrained loading of a strip footing resting on the surface of a uniform soil deposit is studied, to investigate the effect of choosing various stress paths in the application of the Stress Path Method.

The specific problem was chosen because it is one of the few practical cases, where the stress distributions are independent of the properties of the soil, (1) and consequently the Stress Path Method is particularly suited.
In addition the applied load was chosen small enough to avoid significant local yielding and stress redistributions in which case the stress increments predicted from the Theory of Elasticity would be in error.
The soil was assumed to have properties similar to the normally consolidated Boston Blue Clay.
The geometry chosen is shown in Fig. A-V-1.
The settlement of a point lying at a depth 1.80b under the

---

(1) Assuming Elasticity and uniform deposit.

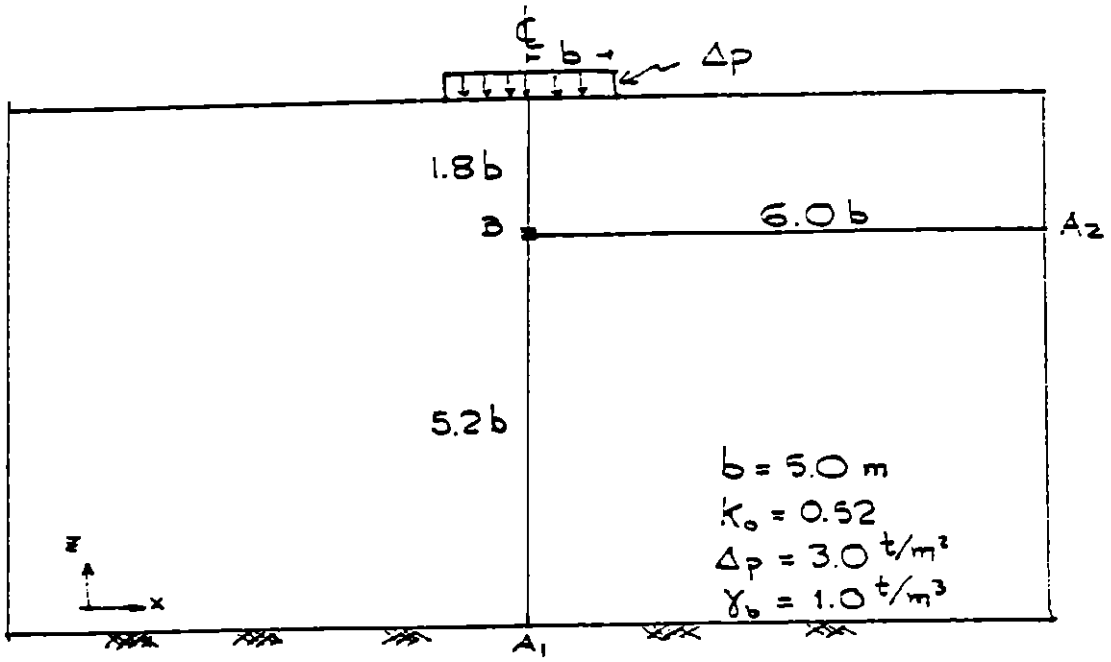

centerline of the footing was studied by choosing two different paths.

1. A Vertical Path A_1B

The stress increments along A_1B correspond to undrained plane strain conditions. Data from $CK_oU(PSC)$ tests on normally consolidated Boston Blue Clay were used. Since the peak in this test is reached at very low strains, (about 0.4%), it is hard to establish the shape of the stress-strain curve in this region accurately. For this reason two possible shapes were used in the analysis.

(a) A straight line between the points:

$$[1]: \left\{ \frac{\sigma_1 - \sigma_3}{2\bar{\sigma}_{vo}} = \frac{1 - k_o}{2} = 0.24 \; ; \qquad \varepsilon_a = 0.0\% \right\}$$

$$[2]: \left\{ \frac{\sigma_1 - \sigma_3}{2\bar{\sigma}_{vo}} = 0.34 \quad ; \quad \varepsilon_a = 0.4\% \right\}$$

(b) A Hyperbola of the form:

$$\frac{\sigma_1 - \sigma_3}{2\bar{\sigma}_{vo}} = \frac{\varepsilon_a}{m + n\,\varepsilon_a} + \frac{1 - k_o}{2}$$

with parameters:

m=0.00469274

n=8.8268

The settlements computed with each of the two shapes were:

From the Straight line: ω_B =26.0 mm

From the Hyperbola : ω_B = 7.6 mm

2. Horizontal Path A_2B

The settlement along this path is mainly governed by the shear strains. In applying the stress path method, shear stresses are computed by using Theory of Elasticity (1) and then the shear strains are obtained by using the test data of a CK_oUDSS test (Direct Simple Shear). However in addition to the shear strains, the vertical settlement depends on the gradient of the horizontal displacements.

In fact since:

$$\gamma = \frac{\partial u}{\partial z} + \frac{\partial w}{\partial x}$$

(1) They are independent of the material properties for uniform deposits

by integration we get:

$$\omega_B = \int_B^{A_2} \frac{\partial u}{\partial z}\, dx - \int_B^{A_2} \gamma\, dx$$

The first term should not be neglected. For this reason it was assumed that the ratio:

$$\int_B^{A_2} \gamma\, dx \Big/ \int_B^{A_2} \frac{\partial u}{\partial z}\, dx$$

is the same in both the elastic solution and in the stress path method. The elastic solution gave the value -4.76 for the above ratio. Using this number in the stress path method, the settlement of point B computed via the path A B was found:

ω_B = 13.3 mm

The following table shows a summary of the results for the two paths:

TABLE A-V-1

Settlement of a point located 1.8b below the centerline of a strip footing

	Vertical Path		Horizontal Path
	straight line	Hyperbolic	
ω_B (mm)	26.0	7.6	13.3

CONCLUSIONS

The computed settlement is greatly integration path dependent. In addition it depends on the stiffness of the stress-strain curve (straight line vs hyperbolic approximation) which is hard to define accurately experimentally.

The above discrepancies are mainly due to strain incompatibilities.

APPENDIX VI

REFERENCES

(1) Baguelin F., Jezequel J.F., Le Mee E., and Le Mehaute A. (1972) 'Expansion of Cylindrical Probes in Cohesive Soils' JSMFD, ASCE, Vol 98, SM11, pp 1129-1142.

(2) Bazant Z. and Krizek R. (1976) 'Endochronic Constitutive Law for Liquefaction of Sand'. JEMD, ASCE, Vol 102, No EM2, pp 225-238.

(3) Bishop A.W and Blight G.E. (1963) 'Some Aspects of Effective Stress in Saturated and Partly Saturated Soils' Geotechnique 13,p 177

(4) Cuellar V. et al (1977) 'Densification and Hysteresis of Sand under Cyclic Shear' JGED, ASCE Vol 103, No GT5, pp 399-416

(5) Drucker D.C (1959) 'Definition of Stable Inelastic Material' J. of Appl. Mechanics 26, pp 101-186

(6) Drucker D.C. and Prager W. (1952) 'Soil Mechanics and Plastic Analysis of Limit design' Q. Appl. Mathematics Vol. 10 pp 157-165.

(7) Gibson R.E and Anderson W.F (1961) 'In situ Measurements of Soil Properties with the Pressuremeter' Civ. Eng. and Public Works Review. 56, 658, pp. 615-618

(8) Hardin B.O. (1972) 'Effects of Strain Amplitude on the

Shear Modulus of Soils' Technical Report No AFWL-TR-72-201 Air Force Base, NM. 63p

(9) Hencky H. (1923) 'Uber einige statisch bestimmte Falle des Gleichwichts in plastichen Korpern' Z. Angew Math. Mech. Vol 3, pp 241-251

(10) Henkel D.J and Wade N.H (1966) 'Plane Strain Tests on a Saturated Remolded Clay' JSMFD, ASCE Vol 92 No SM6 pp 67-80

(11) Hill R. (1950) 'The Mathematical Theory of Plasticity' Clarendon Press Oxford, England.

(12) Hvorslev M.J. (1960) 'Physical Components of the Shear Strength of Saturated Clays' ASCE, RCSSCS pp169-273

(13) Iwan W.D (1967) 'On a Class of Models for the Yielding behavior of Continuous and Composite Systems' J of Appl. Mechanics Vol 34. pp 612-617

(14) Jennings J.E. (1961) 'A Revised Effective Stress Law for use in the Prediction of behavior of Unsaturated Soils'. Pore Pressure and Suction in Soils. London (Butterworth)

(15) Kinner E.B and Ladd C.C (1970) 'Load Deformation Behavior of Saturated Clays during Undrained Shear' Research in Earth Physics, Phase Report No 13, MIT Dept. of Civil Eng. RR70-2,

(16) Ladanyi B.(1963) 'Expansion of a Cavity in a Saturated Clay Medium' JSMFD, ASCE Vol 89, SM4, pp 127-161

(17) Ladanyi B (1972) 'In situ Determination of Undrained stress-strain Behavior of Sensitive Clays with the Pressuremeter' Canadian Geotechnical Journal 9, 3, pp

313-319

(18) Ladd C.C., Bovee R.B., Edgers L., and Rixner J.J. (1971) 'Consolidated Undrained Tests on Boston Blue Clay' Research in Earth Physics, Phase Report No 15 MIT, Dept. of Civ. Eng. RR71-13

(19) Ladd C.C. and Varallyay J. (1966) 'The Influence of Stress System on the Behavior of Saturated Clays during Undrained Shear' Research in Earth Physics. Phase Report No 1, Part II, MIT Dept of Civ Eng. RR65-11.

(20) Lade P.V. and Duncan J.M. (1973) 'Cubical Triaxial Tests on Cohesionless Soil' JSMFD, ASCE, Vol 99, SM10, pp793-812

(21) Lambe T.W. (1967) 'Stress Path Method' JSMFD, ASCE, Vol 93 No SM6 pp309-331

(22) Lambe T.W. and Marr W.A. (1979) 'Stress-Path Method: Second Edition' JGED ASCE Vol 105 No GT6 pp727-738

(23) Martin J.B. (1975) 'Plasticity: Fundamentals and General Results' MIT Press. Cambridge Mass. 931p

(24) Mroz Z. (1967) 'On the Description of Anisotropic Workhardening' J. of the Mech. and Physics of Solids, Vol 15 pp 163-175

(25) Nayak G.C. and Zienkiewicz O.C. (1972) 'Convenient Form of Stress Invariantss of Plasticity' JSD, ASCE Vol 98, No ST4, pp949-954

(26) Palmer A.C. (1972) 'Undrained Expansion of a Cylindrical Cavity in Clay: A simple interpretation of the pressuremeter test' Geotechnique 22,3, pp.451-457

(27) Prevost J.-H. (1977) 'Mathematical Modelling of Monotonic and Cyclic Undrained Clay Behavior' Int. J. for Numer. and Anal. Methods in Geomechanics Vol 1, No 2, pp195-216

(28) Prevost J.-H. (1978) 'Anisotropic Undrained Stress-Strain Behavior of Clays' JGED, ASCE Vol 104, No GT8, pp 1075-1090

(29) Prevost J.-H. and Hoeg K (1975) 'Soil Mechanics and Plasticity Analysis of Strain Softening' Geotechnique 25, 2, pp279-297

(30) Randolph M.F., Carter J.P., Wroth C.P. (1978) 'Driven Piles in Clay: Installation Modelled as the Expansion of a Cylindrical Cavity' Dept. of Civ. Eng. Cambridge U. SOILS/TR-53

(31) Roscoe K.H. and Burland J.B. (1968) 'On the Generalized Stress-Strain Behavior of Wet Clays' Eng. Plasticity. Heyman and Leckie Eds, Cambridge U. Press pp 535-609

(32) Rowe P.W. (1971)' Theoretical Meaning and Observed values of Deformation Parameters for Soil' Proc. Roscoe Memorial Symp., Cambridge U. (Ed. R.H.G. Parry) pp 143-194

(33) Schofield A.N. and Wroth C.P. (1968) 'Critical State Soil Mechanics' McGraw-Hill New-York.

(34) Skempton A.W. (1961) 'Effective Stress in Soils, Concrete and Rocks'. Pore Pressure and Suction in Soils, London (Butterworth).

(35) Skempton A.W. and Sowa V.A. (1963) 'The Behavior of

Saturated Clays During Sampling and Testing' Geotechnique 13, 4, pp 269-290

(36) Terzaghi K.V. (1925) 'Erdbaumechanik auf bodenphysikalischer Grundlage' Vienna.

(37) Timoshenko S.P. and Goodier J.N. (1970) 'Theory of Elasticity' McGraw-Hill pp 269-271